الجمهورية الجزائرية الديمقراطية الشعبية

République Algérienne Démocratique et Populaire

Ministère de L'Enseignement Supérieur et de la Recherche Scientifique

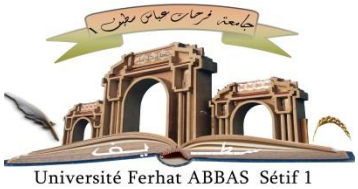

UNIVERSITÉ FERHAT-ABBAS - SETIF 1

FACULTÉ DE TECHNOLOGIE

THESE

Présentée au Département de Génie des Procédés

Pour l'obtention du diplôme de

DOCTORAT EN SCIENCES

Option: Génie des Polymères

Par

BENSEDIRA Abderrahim

THÈME

Study of a cationic dye elimination from water using polyaniline (PANI) and PANI/SiO_2 composite

Soutenue le 18/12/2024 devant le Jury:

M. T. BENANIBA	Professeur	Univ. Ferhat-Abbas Sétif 1	Président
N. HADDAOUI	Professeur	Univ. Ferhat-Abbas Sétif 1	Directeur de thèse
R. DOUFNOUNE	Professeure	Univ. Ferhat-Abbas Sétif 1	Co-directrice de thèse
A. HELLATI	Professeur	Univ. Mohamed. El Bachir El Ibrahimi BBA	Examinateur
A. REFFAS	Professeur	Univ. Mohamed Boudiaf M'sila	Examinateur
D. DADACHE	Professeur	Univ. Mohamed. El Bachir El Ibrahimi BBA	Examinateur

Acknowledgments

Before everything, thanks to Allah Almighty who helped us to achieve this modest work.

First of all, I would like to thank my Professor Nacerddine HADDAOUI (director of the LPCHP and thesis director), for welcoming me into his laboratory and supervising me during these years of thesis, a big thank you also to my professor Rachida DOUFNOUNE (co-thesis director) for her help and very interesting advice.

I sincerely thank the members of the jury, professors Mr. Mohamed Tahar BENANIBA (jury president), Mr. Abdelbaki REFFAS, Mr. Abdelhak HELLATI and Mr. Derradji DADACHE for taking the time to read and judge this work.

I express my sincere gratitude to my colleague Mr. Nouar Sofiane LABIDI (professor at the University of Tamanghasset) who helped me in carrying out this work.

Of course, I thank my family and colleagues for their support. Thank you all !!!

List of Figures and Schemes

Chapter one

Chapter two

Chapter three

List of tables

Chapter one

Chapter two

Table of contents

General Introduction

With the rising awareness of the occurrences of industrial activities and pollution instances of aqueous media, textiles industry is considered as the major source of dye contamination **[1]**. The effective removal of dyes from aqueous wastes is an important issue for many countries **[2]**. This is due to their harmful impact on the environment such as toxic and even carcinogenic as well as mutagenic action towards living organisms. Most dyes have a dangerous effect (directly or indirectly) on fish. Direct activity consist in colouring of water and changing its composition, which significantly deteriorates the living conditions, but indirect activity consist in poisonous properties of many dyes. In this respect, adsorption has gained an important credibility during recent years because of its good performance and low cost **[3]**, much selective, easy to operate and a proven efficient process for the removal of dyes from contaminated aqueous media **[4]**.

Actually, conjugated polymers, particularly those based on polyaniline (PANI), polythiophene (PT) and their derivatives, have gained interesting popularity because of multiple properties such as the low cost synthesis and their numerous applications in rechargeable batteries, display devices and sensors, porous structure, tunable morphology, good electrorheological property, unique redox chemistry, non-toxicity, insolubility in water, environmental stability. In addition, their simple doping and dedoping by acid/base treatment have made them very interesting agents in conducting polymers family. The application of PANI as adsorbent for water purification is due to the large amounts of amine and imine functional groups, which are expected to have interactions with inorganic and organic molecules, such as Hg(II), Cr(VI) and methylene blue **[5-10]**.

Recently, a great work has been made to combine conjugated polyaniline with conventional organic and inorganic adsorbents to form composites or hybrid adsorbents such as PANI-graphene Oxide **[11]**, doped polyaniline-potash alum **[12]**, polyaniline-polystyrene (PANI-PS) **[13]**, PANI-cellulose **[14]**, PANI-cellulose fiber **[15]**, polyaniline-polyethylene glycol (PANI-PEG) **[16]**, polyaniline-magnetite **[17]**, PANI-chitosan **[18]**, PANI-sawdust **[19]**, polyaniline-multiwalled carbon nanotubes (PANI-MWCNT) **[20]**, PANI-chitin**[21]**, PANI-nickel ferrite **[22]**. These functional materials are combined with PANI to generate PANI-related composites to improve its surface area and change its surface morphology and have been studied like adsorbents for removing dyes, heavy metals and ions from aqueous solutions **[23-32]** and demonstrate an important attention because of their excellent adsorption performance **[33-36]**.

The aim of this work is the study of the mechanistic nature of blue methylene removal from aqueous solutions in acidic and basic mediums by adsorption using synthesized polyaniline (PANI) and its silica composite (PANI-SiO_2). For this purpose, a combination of adsorption isotherms, kinetic models are used.

Objectives of the present work:

The overall objective of the thesis is the preparation and characterization of adsorbents for the removal of a dye from aqueous medium under wide range of conditions. The specific objectives of the study are:

• To prepare and characterize of adsorbents.

• To determine the equilibrium time of dye adsorption.

• To determine the optimum concentration of the dye and solution pH at which maximum adsorption occur.

• To study the effect of temperature and determine the values of the thermodynamic parameters.

• To study the kinetics and diffusion rate of dye adsorption.

• To study the adsorption isotherms of dye adsorption.

• To suggest a suitable mechanism of the adsorption for the different cases studied.

Organization of Thesis

The thesis has been organized in three chapters.

Chapter 1: explores the bibliographic studies and contains three parts:

- **Part I:** is about dye pollution, classification of dyes and wastewater treatment technologies.
- **Part II:** explores the conducting polymers and composites, especially polyaniline and polyaniline/SiO_2 composite and their use as adsorbents of methylene blue dye.
- **Part III:** presents the adsorption process for the removal of dyes and study of the different parameters affecting this process.

Chapter 2: contains the experimental section with different results found and discussion.

Chapter 3: explores a modelling approach about the suggested mechanism of adsorption.

A general conclusion will be presented at the end of this work which summarizes the main results obtained.

References:

1. Waheed IF, Al-Janabi OYT and Foot PJS. Novel $MgFe_2O_4$-CuO/GO heterojunction magnetic nanocomposite: Synthesis, characterization, and batch photocatalytic degradation of methylene blue dye. J. Mol. Liq 2022; 357: 119084.
2. Dickcha B and Ackmez M. Adsorption of reactive red 158 dye by chemically treated cocos nucifera L. shell powder. New York: Springer, 2011.
3. Waheed IF, Al-Janabi OYT, Ibrahim AK, et al. $MgFe_2O_4$/CNTs nanocomposite: synthesis, characterization, and photocatalytic activity. Int. J. Ind. Chem 2020; 11: S13-S28.
4. Li J, Wang Q, Bai Y, et al. Preparation of a novel acid doped polyaniline adsorbent for removal of anionic pollutant from wastewater. J Wuhan Univ Technol Mater Sci Ed 2015; 5: 1085-1091.
5. Skotheim TA. Handbook of conducting polymers. New York: Marcel Dekker, 1986.
6. Minisy IM, Salahuddin NA and Ayad MM. Adsorption of methylene blue onto chitosan-montmorillonite/ polyaniline nanocomposite. Appl Clay Sci 2021; 203: 1-10.
7. Bibi A, Shakoor A and Niaz NA. Polyaniline–calcium titanate perovskite hybrid composites: Structural, morphological, dielectric and electric modulus analysis. Polym. Polym. Compos 2022; 30: 1-13.
8. Otero TF. Conducting polymers: bioinspired intelligent materials and devices. United Kingdom: Royal Society of Chemistry, 2016.
9. Li Y, Xing R, Zhang B et al. Fluoro-functionalized graphene oxide/polyaniline composite electrode material for supercapacitors. Polym. Polym. Compos 2019; 27(2): 76-81.
10. Qiu B, Xu C, Sun D, et al. Polyaniline coating with various substrates for hexavalent chromium removal. Appl Surf Sci 2015; 15: 7-14.
11. Huang X, Hu N, Gao R, et al. Reduced graphene oxide-polyaniline hybrid: preparation, characterization and its applications for ammonia gas sensing. J Mater Chem 2012; 22: 22488-22495.
12. Patra BN and Majhi D. Reduced graphene oxide-polyaniline hybrid: preparation, characterization and its applications for ammonia gas sensing. J Phys Chem B 2015; 119: 8154-8164.
13. Alcaraz-Espinoza JJ, Chavez-Guajardo AE, Medina-Llamas JC, et al. Hierarchical composite polyaniline-(electrospun polystyrene) fibers applied to heavy metal remediation. ACS Appl Mater Interfaces 2015; 7: 7231-7240.
14. Qiu B, Guo J, Zhang X, et al. Polyethylenimine facilitated ethyl cellulose for hexavalent chromium removal with a wide pH range. ACS Appl Mater Interfaces 2014; 6: 19816-19824.
15. Liu X, Zhou W, Qian X, et al. Polyaniline/cellulose fiber composite prepared using persulfate as oxidant for Cr(VI)-detoxification. Carbohydr Polym 2013; 92: 659-661.
16. Samani MR, Borghei SM, Olad A, et al. Removal of chromium from aqueous solution using polyaniline-polyethylene glycol composite. J Hazard Mater 2010; 184: 248-254.
17. Gu H, Tadakamalla S, Huang Y, et al. Polyaniline stabilized magnetite nanoparticle reinforced epoxy nanocomposites. ACS Appl Mater Interfaces 2012; 4: 5613-5624.
18. Yavuz AG, Dincturk-Atalay E, Uygun A, et al. A comparison study of adsorption of Cr(VI) from aqueous solutions onto alkyl-substituted polyaniline/chitosan composites. Desalination 2011; 279: 325-331.
19. Mansour MS, Ossman ME and Farag HA. Removal of Cd(II) ion from waste water by adsorption onto polyaniline coated on sawdust. Desalination 2011; 272: 301-305.

20. Hyder MN, Kavian R, Sultana Z, et al. Vacuum-assisted layer-by-layer nanocomposites for self-standing 3D mesoporous electrodes. Chem Mater 2014; 26: 5310-5318.
21. Karthik R and Meenakshi S. Synthesis, characterization and Cr(VI) uptake study of polyaniline coated chitin. Int J Biol Macromol 2015; 72: 235-242.
22. Janaki V, Vijayaraghavan K, Oh BT, et al. Synthesis, characterization and application of cellulose/polyaniline nanocomposite for the treatment of simulated textile effluent. Cellulose 2013; 20: 1153-1166.
23. Patil MR and Shrivastava VS. Adsorptive removal of methylene blue from aqueous solution by polyaniline-nickel ferrite nanocomposite: a kinetic approach. Desalin Water Treat 2015; 57: 1-9.
24. Patil MR, Khairnar SD and Shrivastava VS. Synthesis, characterisation of polyaniline–Fe_3O_4 magnetic nanocomposite and its application for removal of an acid violet 19 dye. Appl Nanosci 2016; 6: 495-502.
25. Ayad MM and Abu El-Nasr A. Adsorption of cationic dye (methylene blue) from water using polyaniline nanotubes base. J Phys Chem C 2010; 114: 14377-14383.
26. Janaki V, Oh BT, Shanthi K, et al. Polyaniline/chitosan composite: an eco-friendly polymer for enhanced removal of dyes from aqueous solution. Synth Met 2012; 162: 974-980.
27. Zheng Y, Liu Y and Wang A. Kapok fiber oriented polyaniline for removal of sulfonated dyes. Ind Eng Chem Res 2012; 51: 10079-10087.
28. Wang L, Wu XL, Xu WH, et al. Stable organic-inorganic hybrid of polyaniline/α-zirconium phosphate for efficient removal of organic pollutants in water environment. ACS Appl Mater Interfaces 2012; 4: 2686-2692.
29. Jayaramudu T, Pyarasani RD, Fakhrabadi AA, et al. Synthesis of Gum Acacia Capped Polyaniline Based Nanocomposite Hydrogel for the Removal of Methylene Blue Dye. J Polym Environ 2021; 29: 2447-2462.
30. Kumar PA and Chakraborty S. Fixed-bed column study for hexavalent chromium removal and recovery by short-chain polyaniline synthesized on jute fiber. J Hazard Mater 2009; 162: 1086-1098.
31. Zhang Y, Li Q, Sun L, et al. High efficient removal of mercury from aqueous solution by polyaniline/humic acid nanocomposite. J Hazard Mater 2010; 175: 404-409.
32. Han J, Fang P, Dai J, et al. One-pot surfactantless route to polyaniline hollow nanospheres with incontinuous multicavities and application for the removal of lead ions from water. Langmuir 2012; 28: 6468-6475.
33. Mahanta D, Madras G, Radhakrishnan S, et al. Adsorption and desorption kinetics of anionic dyes on doped polyaniline. J Phys Chem B 2009; 113: 2293-2299.
34. Mahanta D, Madras G, Radhakrishnan S, et al. Adsorption of sulfonated dyes by polyaniline emeraldine salt and its kinetics. J Phys Chem B 2008; 112: 10153-10157.
35. Qiu B, Xu C, Sun D, et al. Polyaniline coated ethyl cellulose with improved hexavalent chromium removal. ACS Sustain Chem Eng 2014; 2: 2070-2080.
36. Yang J, Wu JX, Lu QF, et al. Facile preparation of lignosulfonate-graphene oxide-polyaniline ternary nanocomposite as an effective adsorbent for Pb(II) ions. ACS Sustainable Chem Eng 2014; 2: 1203-1211.

Chapter one

Bibliographic studies

I. Bibliographic studies

I.1 Dyes

I.1.1 Definition of a dye:

A dye is a coloured compound normally used in solution, which is capable of being fixed to a fabric (substrate). A substrate is the material to which a colourant is applied by one of the various processes of dyeing, printing, surface coating, etc. Generally, the substrate can be textile fibres, polymers, foodstuffs, oils, leather, or many other similar materials.
Visible light consists of electromagnetic radiations of wavelength 400-750 nm. Each wavelength associated with a definite energy and produces a characteristic colour **[1]**.

I.1.2 Chemistry of dyes

Synthetic dyes are aromatic compounds produced by chemical syntheses. Accordingly, aromatic rings in dyes contain delocated electrons (chromophores) and also different functional groups (auxochromes).

a) Chromophore:

The colour of organic compound is due to the presence of certain multiple bonded groups (acceptor of electrons) called chromophores. Chromophores contain double conjugated bonds with delocated electrons. To make substance coloured, the chromophore has to be conjugated with an extensive system of alternate single and double bonds as exists in aromatic rings ("chroma" means colour and "phore" means bearer) **[2]**.

b) Auxochrome:

Certain groups, while not produce colour themselves when present along with chromophores in an organic substance, intensify the colour, such colour assisting groups are called auxochromes. Generally speaking, dyes consist of an assembly of chromophoric groups, auxochromes and conjugated aromatic structures. As the number of aromatic rings increases, the conjugation of double bonds increases and the conjugated system broadens, producing a shift towards long wavelengths. Similarly, when an electron-donating auxochrome group (amino, hydroxy, alkoxy, etc.) is placed on a conjugated aromatic system, this group joins in the conjugation of the π system; the molecule absorbs in the long lengths of waves and gives darker colors **[3-6]**. Some chromophore and auxocrome groups are presented in Table I.1.

Table I.1 Names of chromophore and auxochrome groups of dyes [7].

Chromophore groups	**Auxochrome groups**
Azo (-N=N-)	Amino ($-NH_2$)
Nitroso (-NO or –N-OH)	Methyl amino ($-NHCH_3$)
Carbonyl (=C=O)	Dimethyl amino ($-N(CH_3)_2$)
Vinyl (-C=C-)	Hydroxy (-HO)
Nitro ($-NO_2$ or =NO-OH)	Alkoxy (-OR)
Thio (>C=S)	Electron donor groups

I.1.3 Classification of dyes

Hunger K. **[8]** described that the textile dyes are mainly classified in two different ways, (1) based on the application characteristics (such as acid, basic, direct, disperse, mordant, reactive, sulfur dye, vat dye *etc.*), and (2) based on the chemical structure (such as nitro, azo, carotenoid, diphenylmethane, xanthene, acridine, quinoline, indamine, sulfur, anthraquinone, indigoid, phthalocyanine, *etc.*). The classification of dyes is outlined in Figure I.1.

Considering only the general structure, textile dyes are also classified as anionic, nonionic and cationic dyes. The major anionic dyes are the direct, acid and reactive dyes, and the most problematic ones are the brightly coloured, water soluble reactive and acid dyes because they cannot be removed through conventional treatment systems. The major nonionic dyes are disperse dyes that do not ionise in the aqueous environment, and the major cationic dyes are the azo basic, anthraquinone disperse and reactive dyes, etc. **[9]**.

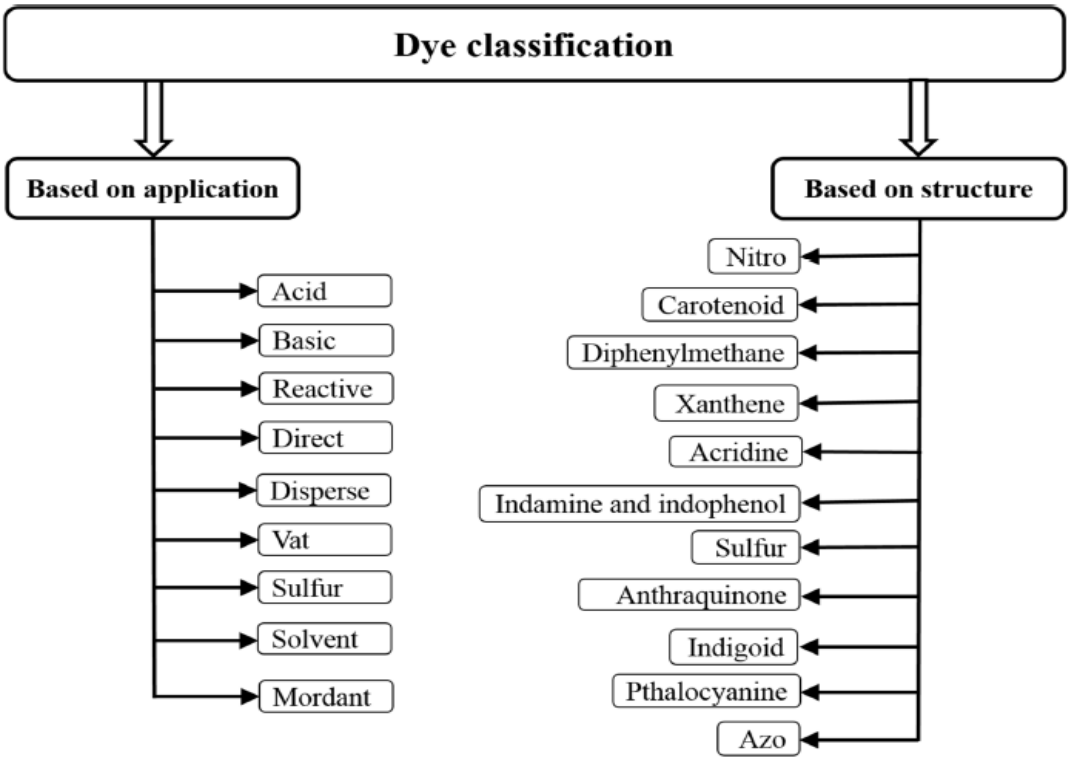

Figure I.1: Classification of dyes [9]

I.1.3.1 Tinctorial classification (based on application)

a) Acid dyes

These compounds are water-soluble thanks to their sulfonate or carboxylate groups. They are applied to animal fibers such as wool and silk and to some modified acrylic fibers. Their interactions with the fiber are based mainly on ionic bonds between the sulfonate anions and the ammonium groups of the fiber. Scheme I.1 shows an example of these dyes. Commonly used acid dyes are the families of Acid Red, Acid Blue, Acid Violet, and Acid Yellow **[10, 11]**.

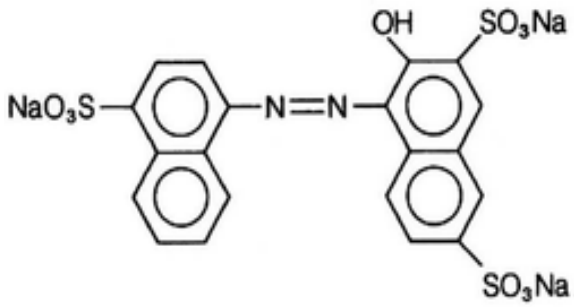

C.I. Acid Red 27

Scheme I.1: Structure of an acid dye

b) Basic dyes

Basic or cationic dyes (Scheme I.2) are salts of organic amines. They are soluble in water and they establish strong bonds with fibers. Many basic dyes have a dangerous impact on the environment. Their handling must be done correctly. This type of dyes can be applied to cotton, certain types of modified polyamides and polyester. Examples of basic dyes are the Basic Blue, Basic Brown, Basic Green, Basic Violet, and Basic Yellow families **[12]**.

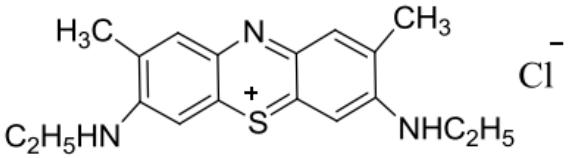

Basic blue 24

Scheme I.2: Structure of a basic dye

c) Reactive dyes

This type of dyes is characterized by the presence of functional groups capable of forming strong covalent bonds with the fibers. They are able to dye cellulosic fibers, fibers of animal origin and polyamide fibers. A representative example of this family is illustrated in Scheme I.3. Most widely used reactive dyes are the Reactive Black, Reactive Red, Reactive orange and Reactive Yellow families **[13-15]**.

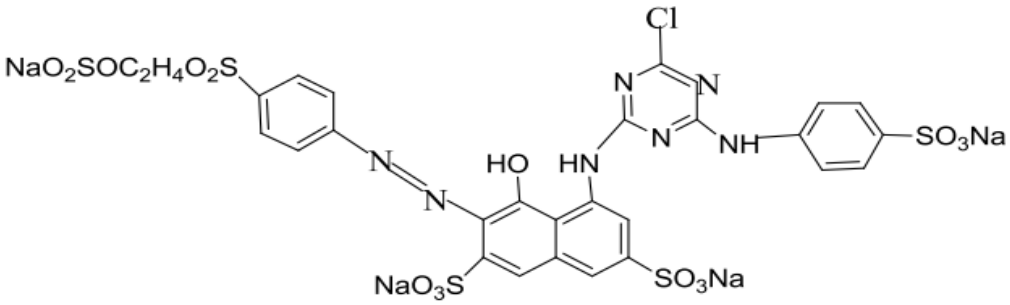

Reactive Red

Scheme I.3: Structure of a reactive dye

d) Direct or substantive dyes

These are water-soluble anionic dyes. They bind to the fibers through weak bonds, which explains their limited resistance to wet tests (water, washing, sweat, etc.). These are the least expensive of the dyes used to dye cellulosic fibers like cotton. Most direct dyes are polyazo compounds, along with some phthalocyanines and oxazines. To improve wash fastness,

frequently chelations with metal (such as copper and chromium) salts are applied to the dyestuff. Commonly used direct dyes in textile industries include the Direct Red, Direct Yellow, Direct Orange, and Direct Green families **[16]**.

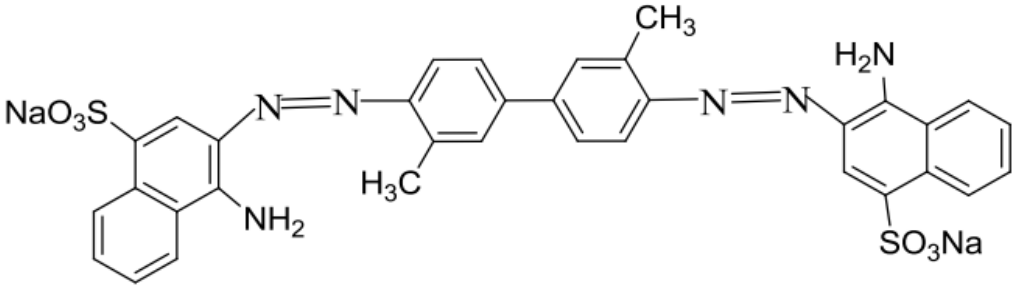

Direct Red

Scheme I.4: Structure of a direct dye

e) Disperse dyes

Chemical structures of these dyes are mainly consisted of azo and anthraquinonoid groups, having low molecular weight which aid in forming stable aqueous dispersions. Disperse dyes are very poorly soluble in water. The fixation of these dyes on the fiber can be the result of either hydrogen interactions, dipole-dipole interactions or Van Der Waals forces. Disperse dyes are predominantly used for acetate, acrylic, nylon, polyester, polyamide, polypropylene and olefin fibers. The Disperse Yellow, Disperse Red, and Disperse Orange families are some of the common disperse dye **[17, 18]**.

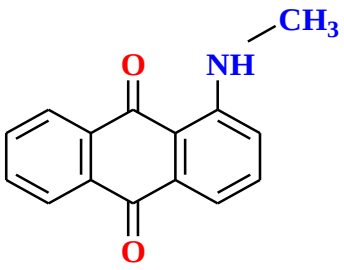

Disperse red

Scheme I.5: Structure of a disperse dye

f) Vat dyes

Vat dyes are water insoluble and can be applied mainly to cellulose fiber by converting them to their leuco compounds. The latter was carried out by reduction and solubilisation with sodium hydrosulfite and sodium hydroxide solution, which is called a "vatting process" **[11]**.

The main structural groups of vat dyes are anthraquinone and indigoid. Most widely used vat dyes are the Vat Black, Vat Blue, Vat Orange, Vat Red and Vat Yellow families **[10]**.

Vat blue

Scheme I.6: Chemical structure of vat dye

g) Mordant dyes

Mordant dyes are characterized by the presence of functional groups capable of reacting with metal salts which have been fixed after prior treatment on the fiber. It results the formation of a stable complex. In industrial dyeing, the most used salts are based on dichromate; this is why we talk about chrome dyes **[14]**. Most commonly used mordant dyes are the Mordant Yellow, Mordant Orange, Mordant Red, Mordant Brown, Mordant Green and Mordant Black families.

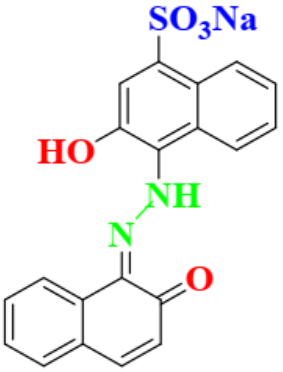

Mordant Black

Scheme I.7: Chemical structure of mordant dye

h) Solvent dyes

Solvent dyes are water insoluble but organic solvent soluble, dyes having deficient polar solubility groups for example, sulfonic acid, carboxylic acid or quaternary ammonium. They are used for colouring plastics, gasoline, oils, and waxes. Solvent dyes that are regularly used in textile industries are the Solvent Yellow, Solvent Red, Solvent Blue, Solvent Orange, Solvent Green, and Solvent Violet families **[19]**.

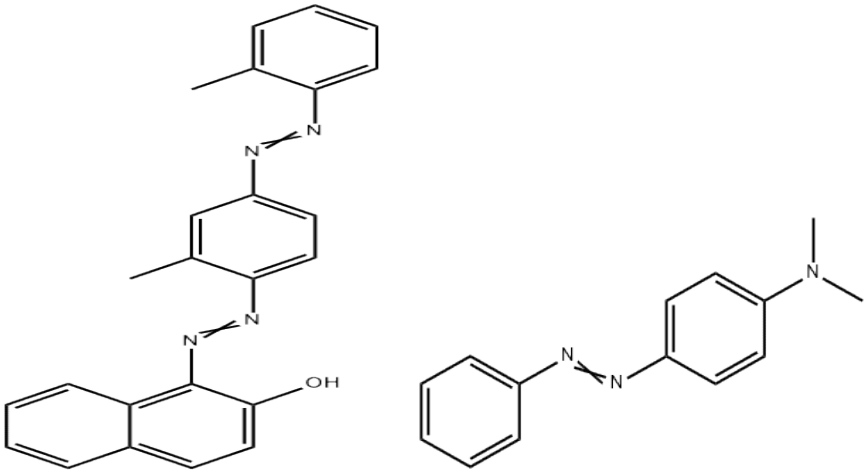

Scheme I.8: Chemical structure of Solvent dyes

i) Sulfur dyes

Sulfur dyes are water insoluble and are applied to cotton in the form of sodium salts by the reduction process using sodium sulfide as the reducing agent under alkaline conditions. The low cost and good wash fastness properties of dyeing make these dyes economic attractive. They have excellent fastness in most areas, but are weak when exposed to chlorine **[20]**. Some sulfur dyes that are most commonly used in textile industries are the Sulfur Black, Sulfur Blue, Sulfur Green, Sulfur Yellow, and Sulfur Red families **[14]**.

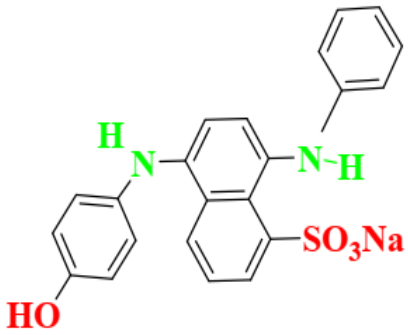

Sulfur green

Scheme I.9: Structure of Sulfur dye

I.1.3.2 Chemical Classification (based on structure)

The classification of dyes according to their chemical structure is based on the nature of the chromophore group (Table 1).

a) Azo dyes

Azo dyes are characterized by the presence within the molecule of an azo group (-N=N-) connecting two benzene nuclei. These structures consists of aromatic or pseudo-aromatic systems linked by an Azo chromophore group (-N=N-). This type of dye is widely used in the textile industry thanks to its resistive property to light, acids, bases and oxygen **[21, 22]**. The

presence of these compounds in industrial effluents presents a dangerous impact on the environment and on human health since they are stable and resistant to biodegradation **[23]**.

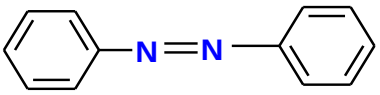

Scheme I.10: Structure of an azo dye

b) Anthraquinone dyes

Anthraquinone dyes are the most important after azo dyes. Their general formula derived from anthracene shows that the chromophore is a quinone nucleus to which hydroxyl or amino groups can attach. This is by far the largest group of carbonyl dyes including hundreds of compounds that are applied to textiles in many ways **[24]**. Anthraquinone chromogens constitute the basis of most natural red dyes, the most famous of which is madder, which after determining the chemical formula (dihydroxy-1,2-anthraquinone), was manufactured synthetically under the name alizarin **[24-26]**.

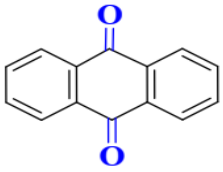

Scheme I.11: The structure of Anthraquinone

c) Indigoid dyes

Similar to the anthraquinone dyes, the indigoid dyes also contain carbonyl groups. They are also vat dyes. Indigoid dyes represent one of the oldest known classes of dyes. For example, 6,6'-dibromoindigo (structure shown in Scheme I.12) is Tyrian Purple **[27]**. Several derivatives of this dye have been synthesized by attaching substituents to the indigo molecule. The selenium, sulphur and oxygen counterparts of indigo blue cause significant hypochromic effects with colours that can range from orange to turquoise. Indigoid dyes are characterized by remarkable resistance to washing treatments, while light fastness is very average. They are used in textiles, the pharmaceutical industry, confectionery and medical diagnostics **[28-32]**.

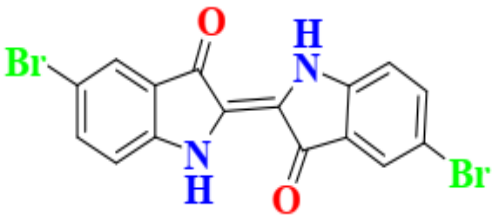

Tyrian purple

Scheme I.12: The structure of indigoid dye

d) Nitro dyes

Nitrated dyes form a class of dyes that are very limited in number and relatively old. The N-O and N=O bonds of the nitro group are equivalent because of resonance, and they are conjugated with the resonating C-C and C=C bonds of the aromatic ring. They are currently still used, due to their very moderate price due to the simplicity of their molecular structure characterized by the presence of a nitro group ($-NO_2$) in the ortho position of an electron donor group (hydroxyl or amino groups) **[16,33]**. Structures of nitro dyes are shown in Scheme I.13.

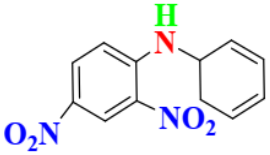

Scheme I.13: Structure of nitro dye

e) Xanthene

The chromophore in xanthene contains the planar skeleton of the oxygen-containing heterocyclic compound xanthene **[34]** as shown in Scheme 1.14.

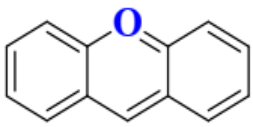

Scheme I.14: Structure of Xanthene

The formula of an aminoxanthene dye is usually shown with a positively charged nitrogen attached to the *p*-quinoid ring, though resonance allows an alternative structure with a positive charge associated with the xanthene oxygen. Xanthene dyes used for biological staining are yellow or red, and many are also fluorescent. There are blue and violet xanthenes that are

used as textile dyes. The pyronines and rhodamines are examples of aminoxanthene dyes; fluorescein and the eosins are well known hydroxyxanthenes **[35]**.

f) Phthalocyanine dyes

Phthalocyanines have a complex structure based on the central copper atom. The dyes in this group are obtained by reaction of dicyanobenzene in the presence of a metal halide (Cu, Ni, Co, Pt, etc.). Phthalocyanine is an intensely blue-green-coloured aromatic macrocyclic compound that is widely used in dyeing. Phthalocyanines form coordination complexes with most elements of the periodic table. These complexes are also intensely coloured and are used as dyes or pigments **[36]**. The structure of copper phthalocyanine (Phthalocyanine Blue BN) is given in Scheme I.15.

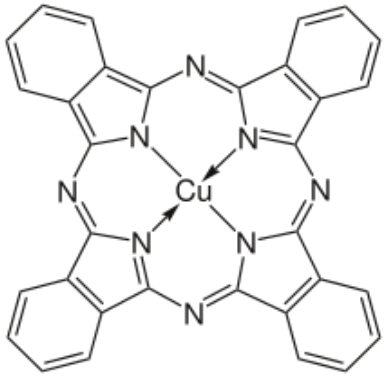

Copper phtalocyanine

Scheme I.15: Structure of phtalocyanine dye

g) Carotenoid

Carotenoids are notable colourants for having no aromatic rings, but contain isoprene units (shown in Scheme I.16) in their molecular structure **[16]**. More than 300 carotenoids occur in plants, and a few are synthesised industrially for colouring foodstuffs. The simplest member of the series is lycopene, named for its presence in *Lycopersicon* (tomato). Structure of lycopene is presented in Scheme I.16.

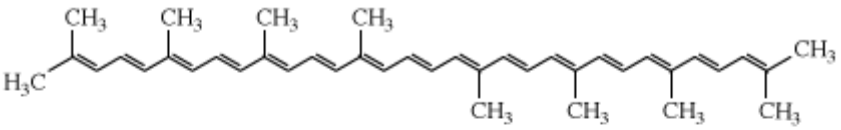

lycopene

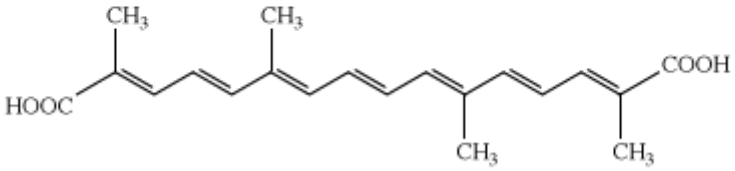

crocetin

Scheme I.16: Structure of carotenoid dye

This formula shows the carotenoid structure comprising eight isoprene units arranged so that there is a long conjugated chain in the middle part of the molecule. In other carotenoids, the ends of the chains are folded into rings, which may be alicyclic or quinonoid, and may bear such substituents as =O, -OH and -$OCOCH_3$ **[37]**.

h) Diphenylmethane

Diarylmethane is a small group of cationic dyes with the general structure shown in Scheme 1.17. Auramine O, is the only diarylmethane commonly used as a biological stain **[38]**.

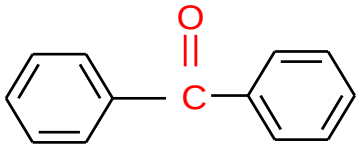

Scheme I.17: Structure of diphenylmethane dye

i) Acridine

The structure of acridine (Scheme 1.18) resembles that of xanthene, except that the heteroatom is nitrogen instead of oxygen **[16]**.

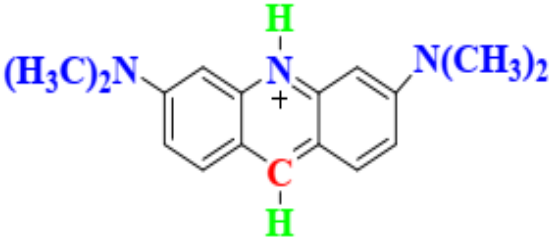

Scheme I.18: Structure of Acridine dye

The acridines are strongly fluorescent yellow cationic dyes. Acridine orange and acriflavine are examples of dyes belonging to this class.

j) Indamine and indophenol dyes

An indamine (-N=) group forms a bridge between an aromatic ring and a quinonoid ring. In indamine dyes, nitrogen atoms terminate the conjugated chain in both ring systems, whereas in an indophenol dye, the chain is terminated by phenolic hydroxyl or a quinonoid carbonyl group at one end **[16]**. These dyes are less important as biological stains **[39]**, but some are used as analytical reagents. Coloured compounds with indamine and indophenol structures are the end products of some histochemical reactions. Example of indamine and indophenol dye is Indophenol Blue.

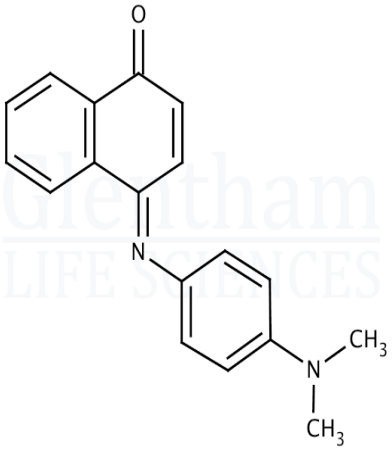

Scheme I.19: Structure of indophenol dye

k) Sulfur dyes

Sulfur dyes are most commonly used dyes manufactured for cotton in terms of volume. They are cheap, generally have good wash-fastness, and are easy to apply. Sulfur dyes are predominantly black, brown, and dark blue. Red sulfur dyes are unknown, although a pink or lighter scarlet colour is available. The most important sulfur dye is Sulfur Black and its structure given in Scheme 1.20 **[16, 40]**.

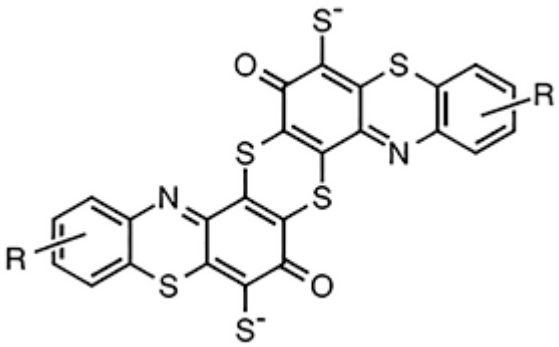

Sulfur black

Scheme I.20: Structure of sulfur dye

I.1.4 Dye containing wastewater

Dye discharged wastewater by some industries under uncontrolled and unsuitable condition causes significant environmental problems. The importance of the environmental pollution control and treatment is undoubtedly the key factor in the human future. If a textile industry discharges the wastewater into the local environment without proper treatment, it will have a serious impact on natural water bodies and land in the surrounding area **[1, 2]**.

The textile dyeing wastewater has a large amount of complex components with high concentrations of organic, inorganic, high-coloured compounds, which has a cumulative effect, and higher possibilities for entering into the food chain. Owing to their high biological oxygen demand/chemical oxygen demand, their colouration and their salt load, the wastewater resulting from dyeing fibres with reactive azo dyes are seriously polluted and dark in colour, which increases the turbidity of water body. As aquatic organisms need light to develop, any deficit in this respect caused by coloured water leads to an imbalance of the ecosystem **[3, 4]**.

Moreover, the water of rivers that is used for drinking water must not be coloured, as otherwise the treatment costs will be increased. The governments of different countries have enacted strict rules controlling the discharge of wastewater into the water system. In order to minimise the pollution, manufacturers and government officials are seeking for solutions to reduce the problem in an efficient way. Thus, studies concerning the feasibility of treating dyeing wastewater are very important.

I.1.5 Wastewater treatment processes

In the past several decades, many techniques have been developed to seek an economical and efficient way for treating the textile dye wastewater, including physico-chemical, chemical,

biological, combined treatment processes. None of the techniques is generally regarded acceptable because all of them offer both advantages and limitations. Because of the high cost and sludge disposal problems, many of these conventional methods for treating dye containing wastewater have not been widely applied at large scale in textile and paper industries **[9]**.

There is no single process capable of adequate treatment, mainly due to the complex nature of the effluents **[6, 7]**. In practice, a combination of different processes is often applied to achieve the desired water quality in the most economical way.

I.1.5.1 Physico-chemical treatment methods

Numerous studies were devoted to remove dyes from textile effluent, and have mainly concentrated on the development of an efficient and cost-effective removal process. These include physico-chemical methods such as adsorption, filtration, specific coagulation, chemical flocculation, *etc*. Dyes can also be removed from an industrial wastewater by other physicochemical treatment technologies such as precipitation, ion exchange, and membrane processes. Some of these methods are simple, cost effective, however, limitations including high cost, low efficiency, labour-intensive operation, lack of selectivity of the process and production of huge toxic solid sludge that required additional treatment before disposal have been encountered **[8, 9]**.

1. Adsorption

2. Membrane filtration

3. Reverse osmosis

4. Filtration

5. Ion exchange

6. Coagulation or flocculation

7. Irradiation

I.1.5.2 Chemical oxidation methods

1. Ozonation

2. Sodium hypochloride (NaOCl)

3. Advanced oxidation process

I.1.5.3 Biological treatments

1. Decolourisation by white-rot fungi

2. Other microbial cultures

3. Adsorption by living / dead microbial biomass **[36]**.

I.1.5.4 Electrochemical techniques

1. Electrocoagulation methods

2. Electrochemical reduction methods

3. Electrochemical oxidation methods

4. Indirect oxidation method

5. Photoassisted methods **[38]**

References:

[1] Ziarani G. M., Moradi R. and Lashgari N., Metal-Free Synthetic Organic Dyes, Hendrik G. Kruger, Elsevier, 2018.

[2] Christie R. Colour chemistry. The Royal Society of Chemistry, Cambridge, United Kingdom, 2001.

[3] Cooper P. Color in dye house effluent. Society of dyes and colourists, United Kingdom, 1995.

[4] Dos Santos A., Cervantes F.J. and Van Lier J.V., (2007). Review paper on current technologies for decolourisation of textile wastewaters: Perspectives for anaerobic biotechnology. Bioresour. Technol., 98: 2369-2385.

[5] Hao O.J., H. Kim et P.C. Chiang. Decolorization of wastewater. Crit. Rev. Environ. Sci. Technol., 2000, 30, 449-505.

[6] Welham A. (2000). The theory of dyeing (and the secret of life). J. Soc. Dyers Colour, 116, 140-143.

[7] Hunger K. Industrial Dyes: Chemistry, Properties, Applications, Edition Dr. Klaus Hunger, Frankfurt, Germany. (2003).

[8] Aksu, Z. Application of biosorption for the removal of organic pollutants: A review. Process Biochemistry, 2005. 40(3): 997-1026.

[9] Sabnis R.W., Handbook of Biological Dyes and Stains: Synthesis and Industrial Applications, John Wiley & Sons, Inc., USA, 2010.

[10] Soldatkina L.M., Zavrichko M.A., Adsorption of anionic dyes on corn stalks modified by polyaniline: kinetics and thermodynamic studies. Chem. Phys. Tech. Surf. 2017. 8: 44-55.

[11] Xiea H., Yana M., Zhanga Q., Qub H., Hem K. J., Desalination and Water Treatment 67, 2017, 346–356.

[12] Sun, Q. and Yang, L. The adsorption of basic dyes from aqueous solution on modified peat-resin particle. Water Research, 2003. 37(7): 1535-1544.

[13] Suteu, D., Zaharia, C. and Malutan, T. Removal of Orange 16 reactive dye from aqueous solutions by waste sunflower seed shells. J Serb Chem Soc., 2011. 76(4): 607-624.

[14] Yu Y, Zhang Y. Controlled synthesis of novel reactive cationic copolymers of 3-chloro-2-hydroxypropylmethyldiallylammonium chloride and dimethyldiallylammonium chloride [P(CMDA-DMDAAC)s]: designed as useful polycationic dye-fixatives on cotton fabric. Res Chem Int 2012; 38(8): 2097–2109.

[15] Yu Y, Zhang Y. Roles of novel reactive cationic copolymers of 3-chloro-2-hydroxypropylmethyldiallylammonium chloride and dimethyldiallylammonium chloride in fixing anionic dyes on cotton fabric. J Chem 2012; 2013: 1–7.

[16] Benkhaya S., Mrabet S., El Harfi A., A Review On Classifications, Recent Synthesis And Applications Of Textile Dyes, Inorganic Chemistry Communications. Journal Pre-proofs (2020).

[17] Umbu zeiro G.A., Freeman H., Warren S.H., Kummrow F and Claxton L.D. (2005). Mutagenicity evaluation of the commercial product CI Disperse Blue 291 using different protocols of the Salmonella assay, Food Chem Toxicol, 43, 49-56.

[18] Sibrian-Vazquez M, Strongin R. Optimising the synthesis and red–green–blue emission of a simple organic dye. Supramol Chem 2009; 21(1–2): 107–110.

[19] Chen B-Y: Toxicity assessment of aromatic amines to pseudomonas luteola: Chemostat pulse technique and dose-response analysis. Process Biochemistry 2006, 41: 1529-1538.

[20] Khan R., Bhawana P., Fulekar M.H. (2013). Microbial decolorization and degradation of synthetic dyes, Review of Environmental Science Biotechnology, 12, 75–97.

[21] Shu H-Y, Chang M-C: Decolorization effects of six azo dyes by O_3, UV/O_3 and uv/H_2O_2 processes. Dyes and Pigments 2005, 65: 25-31.

[22] Saratale, R., Saratale, G., Chang, J. and Govindwar, S. Bacterial decolorization and degradation of azo dyes: A review. J Taiwan Inst Chem Eng., 2011. 42(1): 138-157.

[23] Medvedev Z.A., Crowne H.M and Medvedeva M.N. (1988). Age related variations of hepatocarcinogenic effectof azo dye (3'-MDAB) as linked to the level of hepatocyte polyploidization. Mech. Ageing Develop, 46, 159-174.

[24] Murthy YLN, Kumari BV, Murthy CVVS, Varma KS. Synthesis of 2-methoxy 5-nitro9,10-anthraquinone and study of photophysical properties. Orient J Chem 2009; 25(3): 665–670.

[25] Li Y, Tang Y, Zhang S, Yang J. Synthesis and application of crosslinking blue anthraquinone polyamine dye with high fixation. Text Res J 2007, 77(9): 703–709.

[26] Itoh K., Kitade C., Yatome C. (1996). A pathway for biodegradation of an anthraquinone dye, C.I disperse red 15, by a yeast strain Pichia anomala, Bull. Environ. Contam. Toxicol., 5, 413–418.

[27] Qin Y, Li M, Yan C, Liu S, Dai W, Li M. Simple synthesis regarding novel bianchored metal free organic dyes based on indole for dye sensitized solar cells. J Mater Sci 2016, 27(4): 3974–3981.

[28] Liu X, Cao Z, Huang H, Liu X, Tan Y, Chen H, et al. Novel D–D–π-A organic dyes based on triphenylamine and indole-derivatives for high performance dye-sensitized solar cells. J Power Sources 2014; 248: 400–406.

[29] Ito S, Miura H, Uchida S, Takata M, Sumioka K, Liska P, et al. High-conversion-efficiency organic dye-sensitized solar cells with a novel indoline dye. Chem Commun 2008, 41: 5194–5206.
[30] Liu B, Liu Q, You D, Li X, Naruta Y, Zhu W. Molecular engineering of indoline based organic sensitizers for highly efficient dye-sensitized solar cells. J Mater Chem 2012; 22(26): 13348–13356.
[31] Enoki T, Matsuo K, Ohshita J, Ooyama Y. Synthesis, and optical and electrochemical properties of julolidine-structured pyrido[3,4-b]indole dye. Phys Chem Chem Phys 2017; 19: 3565–3574.
[32] Lévesque É, Bechara WS, Constantineau-Forget L, Pelletier G, Rachel NM, Pelletier JN, et al. General C-H arylation strategy for the synthesis of tunable visible light-emitting benzo[a] imidazo[2,1,5-c,d]indolizine fluorophores. J Org Chem 2017, 82: 5046–5067.
[33] Bei Z, Feng L., Tao W., Dejun S., Yujiang L., (2015), Adsorption of p nitrophenol from aqueous olutions using nanographiteoxide. Colloids and Surfaces A. Phys.chem. Eng. Aspects, 464: 78–88.
[34] Lebkücher A, Rybina A, Herten DP, Hübner O, Wadepohl H, Kaifer E, et al. A fluorescent blue phosphazene dye: synthesis, structure and optical properties of 1,6-bis(dimethylamino)-2,5,7,10-tetraazo-1,6λ5-diphosphapyrene. Z Anorg Allg Chem 2011; 637(5): 547–555.
[35] Gao Z, Zhang X, Zheng M, Chen Y. Synthesis of a water soluble red fluorescent dye and its application to living cells imaging. Dyes Pigm. 2015, 120: 37–43.
[36] Singh L., Sing V.P. Textile Dyes Degradation, A Microbial Approach for Biodegradation of Pollutants, Microbial Degradation of Synthetic Dyes in Wastewaters, Environmental Science and Engineering, Springer International Publishing Switzerland. (2015).
[37] Drumond C.F.M., Anastácio F.E.R., Cardoso J.C., Zanoni M.V.B. Textile Dyes, Dyeing Process and Environmental Impact, Chapter 6. Eco-Friendly Textile Dyeing and Finishing. 2013.
[38] Carmen Z., Daniela S. (2012). Textile Organic Dyes – Characteristics, Polluting Effects and Separation/Elimination Procedures from Industrial Effluents-A Critical Overview, Organic Pollutants Ten Years After the Stockholm Convention-Environmental and Analytical Update, Edition Dr. Tomasz Puzyn, 55-87.
[39] Son Y, Kim H, Kim S-H. Synthesis and chemosensing properties of indole based donor–π–acceptor dye material. J Nanosci Nanotechnol 2014; 14(10): 7976–7980.
[40] T.A. Nguyen and R.-S. Juang, Treatment of waters and wastewaters containing sulfur dyes: A review, Chem. Eng. J. 219 (Supplement C) (2013) 109–117.

I.2 Conducting polymers

Polymers are generally recognized as good insulators. Indeed, conventional polymers such as polyethylene and polystyrene have low electronic conductivities which vary between 10^{-9} and 10^{-18} S/cm. It goes without saying that this insulating property of polymers has been used to coat electronic wires or for the insulation of certain electronic devices **[1]**. Although they are insulating, polymers can, under certain conditions, exhibit remarkable electronic and optical properties. These materials, comprising a system of conjugated double bonds, have the capacity to transport electronic charges: they are called conductive polymers **[2]**.

I.2.1 Properties of conducting polymers

The study of the first conductive polymer began in 1977 with the work of Heeger, MacDiarmid and Shirakawa **[3]**. By treating polyacetylene with iodine vapor, these researchers noticed a considerable increase in the electronic conductivity of the material of up to 10^5 S/cm. From then on, a whole range of conductive polymers were synthesized. Among these, we note polyacetylenes **[4]**, poly(paraphenylenes) **[5]**, poly(phenylenevinylenes) **[6]**, polthiophenes **[7]**, polypyrroles **[8]**, as well as polyanilines **[9]** (figure I.2). Now, these polymers are extensively studied, both in academic and industrial laboratories, in order to develop the most efficient materials.

The main characteristic of these “synthetic metals” is the presence of a π -conjugated system on their main chain. The presence of alternating double bonds and single bonds, in addition to numerous inter-chain interactions, induces great rigidity within these materials, making their characterization difficult. Indeed, most conductive polymers are insoluble and infusible **[10]**.

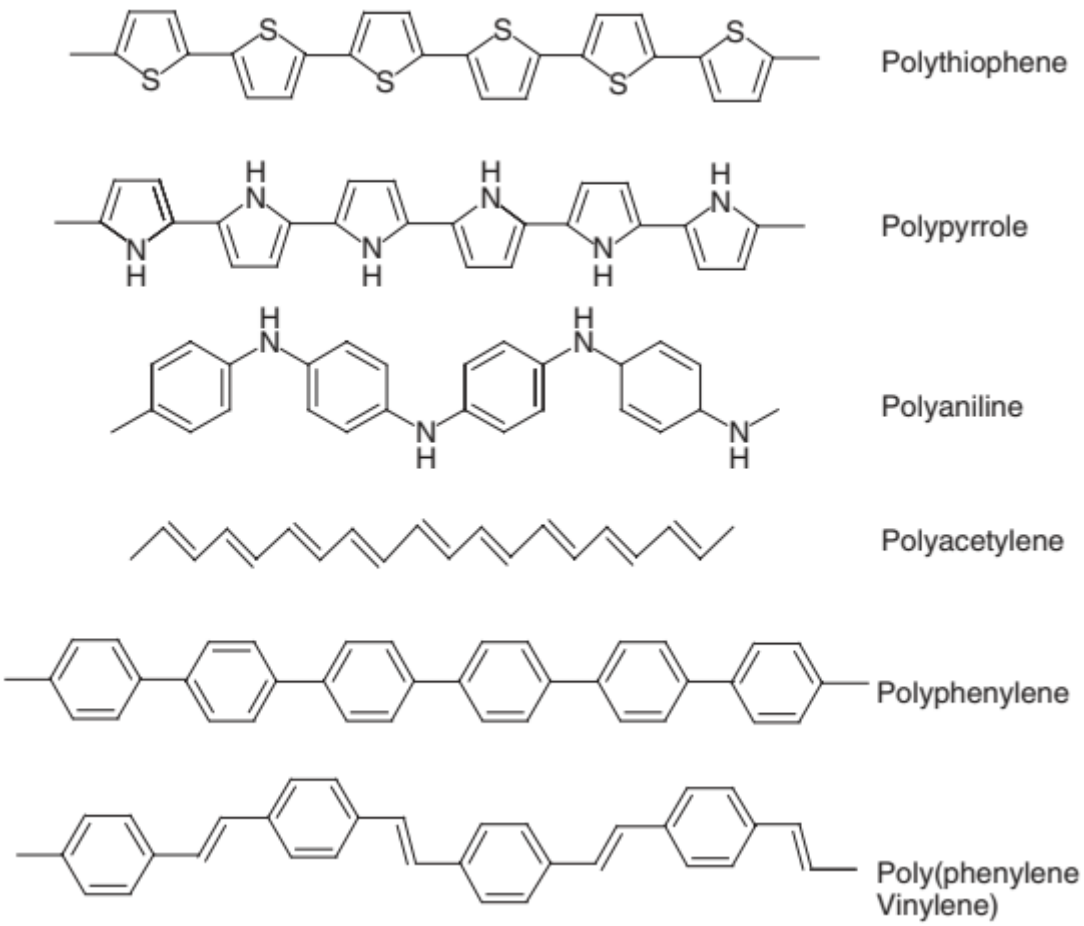

Figure I.2 Chemical structures of some conjugated polymers

I.2.2 Mechanisms of electrical conductivity

The electrical properties of materials are determined by their electronic structure. The theory that helps explain the electronic structure of a material is band theory **[10]** (Figure I.3). In the solid state, electrons are placed in molecular orbitals, which form an energy continuum. The highest energy molecular orbital occupied by electrons (HOMO) is called the valence band, while the unoccupied lowest energy molecular orbital (LUMO) is called the conduction band. The area between the valence band and the conduction band is called the band gap (E_g). Band theory states that the electrical conductivity of a solid depends on how well the valence and conduction bands are filled by electrons. The crucial factor, which determines the filling of the valence and conduction bands, is the band gap width **[11]**.

In the case of an insulator, the band gap is very wide (E_g> 3ev) making it impossible for electrons to pass from the valence band to the conduction band. Thus, the valence band remains completely full and the electrons cannot move under the application of an electric field. In a semiconductor, electrons can move when a field is applied since the valence and conduction bands are not completely full or completely empty. Indeed, the band gap is narrow

(0.5 ev<E_g<3.0 ev) and a certain number of electrons are promoted into the conduction band. Finally, the very high electrical conductivity of metals is explained by the absence of the forbidden band. Thus, the valence and conduction bands form a single band, where electrons can flow freely when an electric field is applied **[12]**.

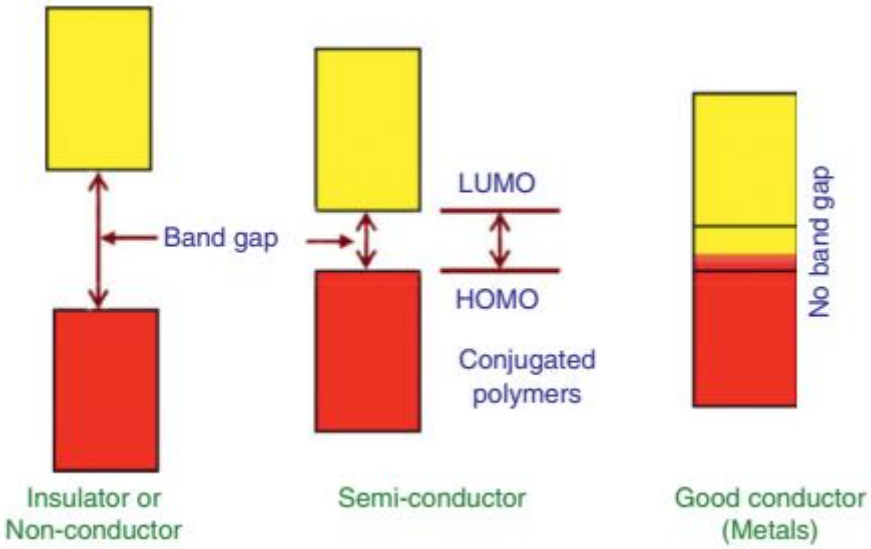

Figure I.3: Band gap structures for insulator, semiconductor and conductor

Although band theory partly explains the principle of electrical conductivity of conductive polymers, it does not reveal all its aspects. To fully understand the electronic phenomena involved in these organic polymers, it is necessary to bring into play the notion of polarons and bipolarons. In the neutral state, polymers that have a double conjugated bond system are insulators. For these materials to become good electrical conductors, they must first undergo a change in their oxidation state. The treatment that a material undergoes to change its oxidation state is commonly called doping. There are mainly two types of doping: “p” type doping, characterized as being oxidation, and “n” type doping, characterized as reduction (figure I-4). During “p” type doping, there is formation of one or two cation radicals per tetramer unit, respectively called positive polaron and positive bipolaron. In “n” type doping, one or two anions are formed per tetramer unit, called negative polaron and negative bipolaron respectively. The formation of a polaron or a bipolaron depends on the degree of doping of the material **[13]**.

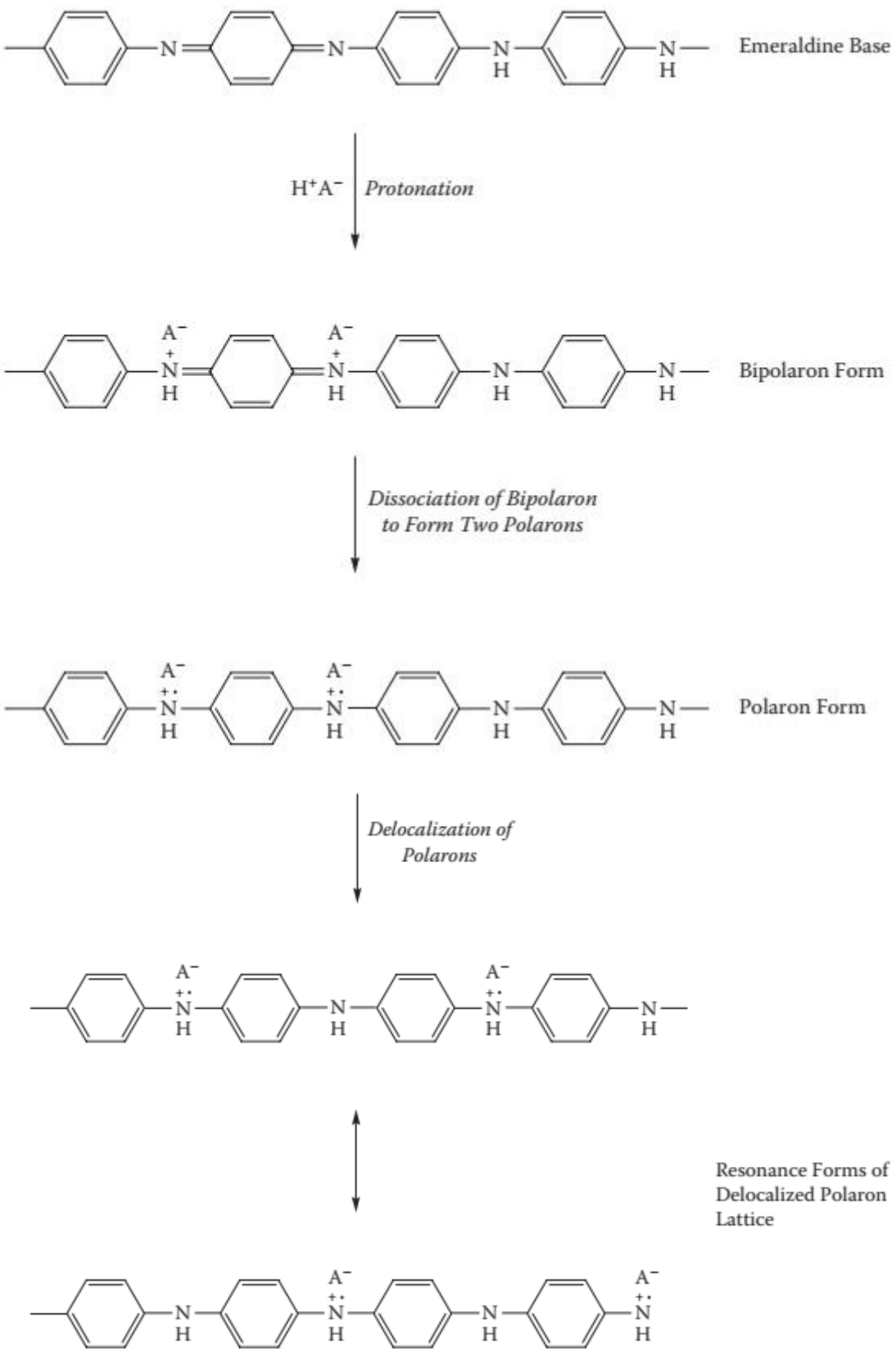

Figure I.4: The doping of emeraldine base with protons to form the conducting emeraldine salt form of polyaniline (a polaron lattice)

Thus, a low degree of doping results in the formation of polarons, while a high degree of doping results in the formation of bipolarons **[14]**.

The association of intermediate energy levels with the different charged species created during doping is very complex, but still possible. During a first oxidation, an electron is removed from the valence band of the conjugated polymer and a positive polaron is created. The energy level associated with this positive polaron, partially delocalized along the polymer chain, is represented by a destabilized bonding orbital whose energy is higher than the energy of the valence band of the material (Figure I.5). In other words, the energy level of this radical cation is in the forbidden band. By carrying out a second oxidation on the polymer, it can produce two different phenomena, either the formation of a second polaron on another tetramer unit, or the formation of a bipolaron. In the second case, an unpaired electron located on the plus high energy level is high, and thus, a bipolaron is formed **[15]**. There are no electrons on the two energy levels between the valence band and the conduction band. The positive bipolaron consists of two electronic holes in the valence band (Figure I-5 and Table I.2). As shown earlier, the electronic holes in the valence band will allow electronic conduction within the material. By carrying out "n" type doping, the polymer is reduced. During a first reduction, a negative polaron is formed. The electrons associated with this excited state are located in the band gap on two distinct energy levels (Figure I-5). If we carry out a second reduction on the polymer, the two energy levels located in the band gap are filled with the electrons generated by the strong reduction. In both cases, these electrons have such energy that they will be able to reach the conduction band and allow high electronic conductivities **[16]**.

The mechanism of electronic conduction within conducting polymers can ultimately be summarized by the formation of polarons and bipolarons during doping. These charged species have the ability to move along the polymer chain by rearrangement of double and single bonds within the conjugated system. Thus, electrons can be transported along and between polymer chains **[17]**.

Table I.2: Chemical term, charge and spin of soliton, polaron and bipolaron in conducting polymers [18]

Carrier nature	Chemical term	Charge	Spin
Positive soliton	Cation	+e	0
Negative soliton	Anion	-e	0
Neutral soliton	Neutral radical	0	1/2

Positive polaron (hole polaron)	Radical cation	+e	1/2
Negative polaron (electron polaron)	Radical anion	-e	1/2
Positive bipolaron	Dication	+2e	0
Negative bipolaron	Dianion	-2e	0

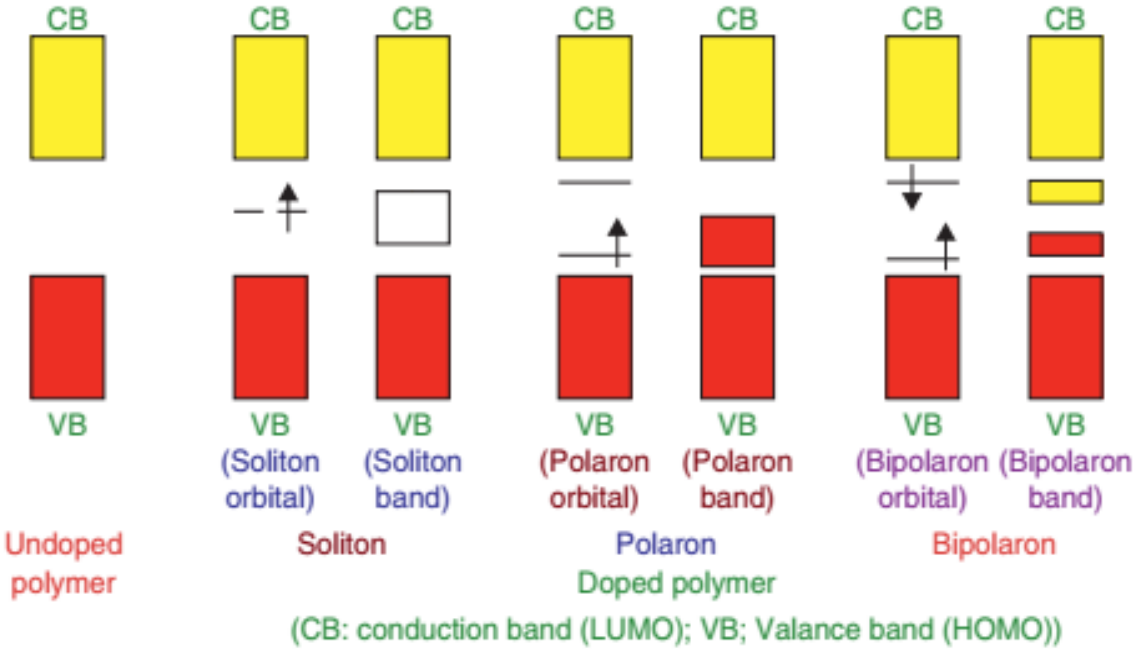

Figure I.5: The orbital and band structures for undoped and doped (soliton, polaron, bipolaron) conjugated polymer [13]

I.2.3 Applications of conductive polymers

I.2.3.1 Batteries

Bridgestone/Seiko used doped polyaniline as a battery constituent for one of the first industrial applications of conductive polymers **[19]**. Partially doped polyaniline was used to make the anode, the cathode is generally made of lithium or a lithium/aluminum alloy. During use (discharge), the polymer anode dedopes and releases anions into the electrolyte. Conversely, lithium atoms are oxidized in the form of cations at the cathode, released into the electrolyte. At the same time, these processes cause electrons to flow through the charge (external circuit) from the cathode to the anode, thereby creating an electric current **[20, 21]**.

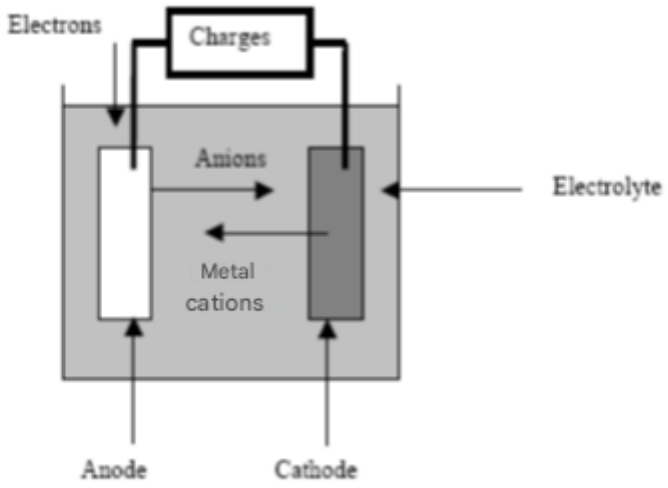

Figure I.6: Schematic diagram of a battery during discharge [22]

I.2.3.2 Electromagnetic shielding

The characteristics of certain conductive polymers, combining good conductivity (greater than 500 S/cm) and a "low" dielectric constant (lower than that of metals), allow them to be used to absorb electromagnetic radiation. Many studies highlighted the effectiveness of doped PANI in use as electromagnetic shielding **[23-26]**.

I.2.3.3 Capacitors

Another application where conductive polymers are increasingly used concerns metal-oxide capacitors. The oxide of the metal constitutes the dielectric, the metal is one electrode and the other electrode is traditionally made from Manganese dioxide (MnO_2). From now on, the conductive polymer replaces manganese dioxide because it has better conductivity, ensures better contacts with the dielectric, which makes it possible to obtain an almost constant capacitance in higher frequency ranges. In addition, implementation by deposition is easily achievable **[27, 28]**.

I.2.4 Polyaniline

I.2.4.1 General information

Polyaniline is a polymer made up of amine and imine units which is mainly studied and used for its qualities as an electronic conductor. This polymer can be prepared using two methods, one chemical and the other electrochemical **[29]**. Each involves oxidizing aniline in an acidic

environment. Although the electrochemical method is useful for obtaining the polymer in film form, a chemical oxidant is generally used to easily produce large quantities of polymer in powder form. In each case, the final product is the result of preferential head–tail coupling between oxidized aniline molecules **[30]**.

Polyaniline was first synthesized in 1862 by electrochemical oxidation of aniline in an acidified aqueous solution, which gave rise to the formation of a very dark green powder. Obviously, the product synthesized at that time was not recognized as a macromolecule but polyaniline was then used as a dye. Green and Woodhead proved, in 1910, the different degrees of oxidation of polyaniline then considered as an octamer **[31]**. In 1968, the monitoring group showed the "redox" properties of polyaniline and the influence of water on its conductivity **[32]**. The discovery of conductive polymers in 1977 created great enthusiasm within the scientific community for polyaniline so that in 1989, Bridgestone-Seiko marketed for the first time an ultra-thin rechargeable battery made with a polyaniline cathode **[19]**. Among the known conductive polymers, polyaniline remains the most interesting polymer due to its low production cost, its particular electrochemical behavior and its good chemical and thermal stability.

I.2.4.2 Different forms and properties

In the neutral state, polyaniline differs from other conductive polymers since it can exist in three distinct forms depending on its degree of oxidation (figure I-7). The different oxidation states of polyaniline are directly linked to the presence of nitrogen atoms on the main chain; they also play a fundamental role in the doping process, and are thus responsible for the different physicochemical properties associated with polyaniline. Polyaniline leucoemeraldine is the completely reduced form of polyaniline and the latter is then only made up of benzenoid units. When polyaniline is partially oxidized (50% oxidized, 50% reduced), we are in the presence of a polymer having as many benzenoid units as quinoid units. In this case, we call the polyaniline emerldine salt and base. Finally, polyaniline pernigraniline is the completely oxidized polymer, possessing only quinoid units throughout the polymer chain **[17]**.

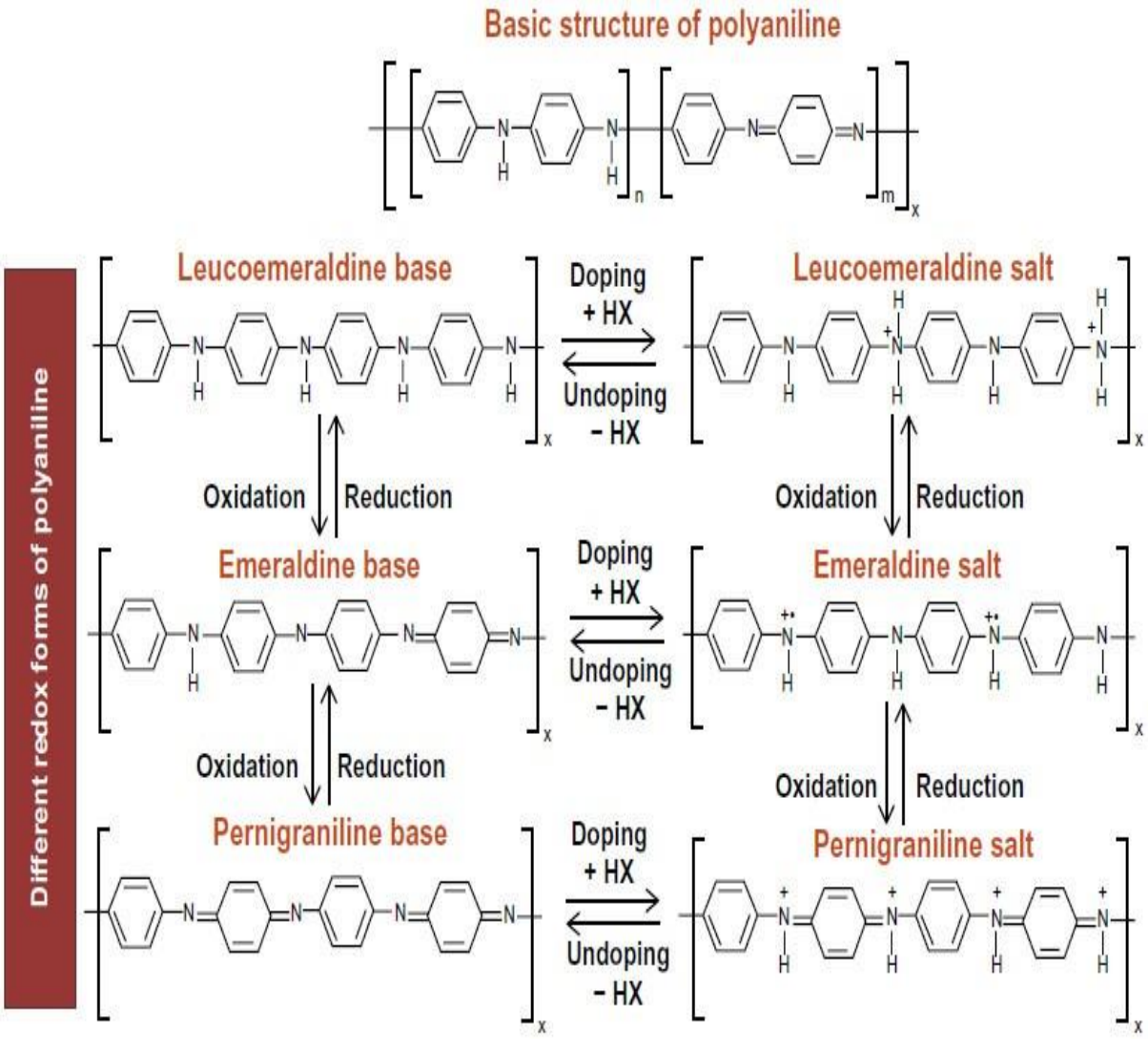

Figure I.7: Proposed chemical structures of PANI in various chemical states

Table I.3: The different forms of PANI [33]

Type of form	Name	Colour	Conductivity ($S.cm^{-1}$)
Reduced form	Polyleucoemeraldine base	Transparent	$< 10^{-5}$
	Polyprotoemeraldine base	Transparent	$< 10^{-5}$
	Polyemeraldine base	Blue	$< 10^{-5}$
	Polynigraniline base	Blue	$< 10^{-5}$
Oxidized form	Polypernigraniline base	Purple	$< 10^{-5}$
	Polyemeraldine salt	Green	~ 15

Although each of these three non-conductive forms of polyaniline are well known in the literature, it is polyaniline emerldine base (PANI-EB) that is attracting the greatest interest. Indeed, it is from PANI-EB that it is possible to dope the polymer and obtain an electroconductive polymer. The doping of polyaniline is very particular. Generally, doping of conductive polymers is carried out by oxidation or reduction of the polymer, involving a change in the number of electrons **[12]**. However, polyaniline doping is an acid type doping in which the number of electrons remains the same. Therefore, when PANI-EB is treated with an acid capable of prototonating the imine sites of the polymer, partial charges are formed (figure II-6). The positive bipolaron then created generates an electronic reorganization within the material and thus allows the delocalization of electrons throughout the polymer chain. The presence of positive polarons, following the rearrangement of the electrons, ensures the ionic complexation between the positively charged polymer and the counterion of the negatively charged acid. Once doped, polyaniline is called emerldine salt (PANI-ES) **[13]**.

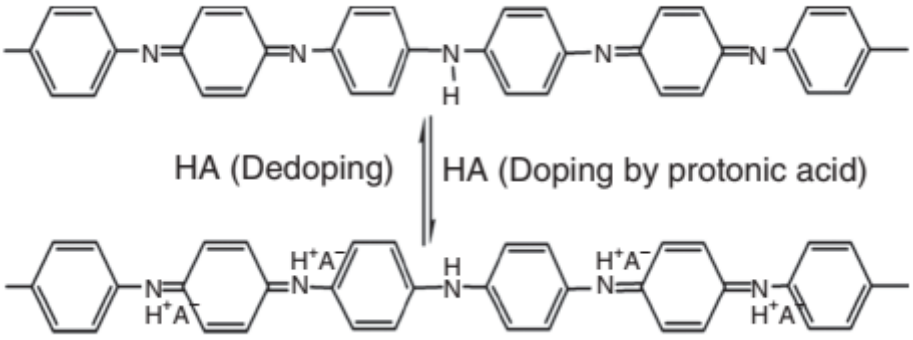

Figure I.8: Protonic acid doping in polyaniline

When doping conductive polymers, their electrical and optical properties are altered. Indeed, the transition from the insulating form to the conductive form is accompanied by the change in the color of the polymer, which can easily be characterized by UV/visible spectroscopy. In the case of polyaniline, the insulating emeraldine base form (10^{-10} S/cm) appears as a dark blue powder, while the conductive emeraldine salt form is forest green and can conduct electricity up to values of 100 S/cm **[14]**.

As described previously, electrical conductivity in conductive polymers is a process of charge diffusion between free sites and occupied sites on the polymer.

In the case of polyaniline, electrical conductivity is a function of two closely related factors: the degree of oxidation and the degree of protonation of the polymer. To obtain maximum electrical conductivity, polyaniline must first be 50% oxidized, so that it contains an equal

number of quinoid and benzenoid units. This principle is well known in the field of conducting polymers **[15]**. If the polymer is too oxidized, the charge density is too high, which prevents the electrons from moving to the few free sites. Otherwise, where the polymer is too weakly oxidized, there is little charge carrier and the system will not be perfectly delocalized. In each of these two cases, a decrease in conductivity results. The degree of protonation also plays an important role in the process of electrical conductivity of polyaniline since it determines the quantity of charges formed. Indeed, it is necessary to protonate each of the imine sites, which functionalize the quinoid units of the polyaniline to obtain maximum conduction. The imine groups are preferentially protonated during doping, since their basicity is stronger than that of the amine groups. Therefore, the degree of oxidation of the polyaniline, which must be 50%, determines the number of imine groups on the polymer. If each of the imine groups is then protonated, all the necessary characteristics are combined to obtain maximum electrical conductivity **[33]**.

Obviously, there are other factors that can influence electrical conductivity, including the type of acid used, the crystallinity rate, as well as the percentage of humidity present in the polymer. Acid type doping is inherent to polymers with acid-base properties. It is the presence of nitrogen atoms on the polyaniline chain that allows this property. This particularity of being able to conduct electrons by a simple acid treatment is a marked advantage of polyaniline compared to other conductive polymers. In this way, we can go from an insulating polyaniline to a conductive polyaniline, and return to an insulating polyaniline by a simple reversible and controlled acid-base process. Moreover, this property was studied several times in the literature and used to develop interesting analysis methods **[34]** based on the color change of the polymer.

As described above, polyaniline can exist in three different oxidation states. Whether chemically or electrochemically, it is possible to easily obtain polyaniline in the completely reduced (leucoemeraldine), semi-oxidized (emerldine base or salt) and completely oxidized (pernigraniline) form (Figure II-6). Although polyaniline leucoemerldine and polyaniline pernigraniline are very stable polymers, both chemically and thermally **[35]**, it is possible to stabilize each of these forms by the application of a suitable electrical potential. Therefore, the transition between the different forms of polaniline is possible by varying the potential applied to the system. Thus, if it is placed in an acidic environment, polyaniline exhibits two reversible redox processes. The first corresponds to the leucoemerldine – emerldine salt transition, while the second is the result of the emerldine salt – pernigraniline transition. Each of these redox reactions is accompanied by a change in the optical properties of the polymer,

since polyaniline is electrochromic – changing color under the application of a varying electronic potential. The electrochromic behavior of polyaniline is unique among conductive polymers since it is manifested by the passage of three distinct colors, namely blue, green and yellow **[36]**.

I.2.4.3 Synthesis of polyaniline

All conducting polymers are generally prepared in solution, by the action of an oxidizing or reducing reagent on the monomer unit. The polymer formed may be soluble in the synthesis medium, or will appear in the form of a precipitate. In the case of polyaniline, it is an oxidative polymerization in an aqueous medium, giving a precipitate. It can also be obtained by another synthesis route: the electrochemical route **[37]**.

The radical oxidative polymerization of aniline is a reaction in a homogeneous medium, meaning that the monomer, the oxidant and the solvent of these first two reagents constitute a single phase. The most widely used method is the oxidation of the aniline monomer with ammonium persulfate, in an acidic aqueous H_2SO_4 medium, for a pH of 1 to 3. A priori, this oxidative polymerization requires 2 electrons per aniline molecule. The oxidant/monomer ratio should therefore be 1:1. But a lower quantity of oxidant will often be used; to avoid oxidative degradation of the polymer formed (overoxidation).

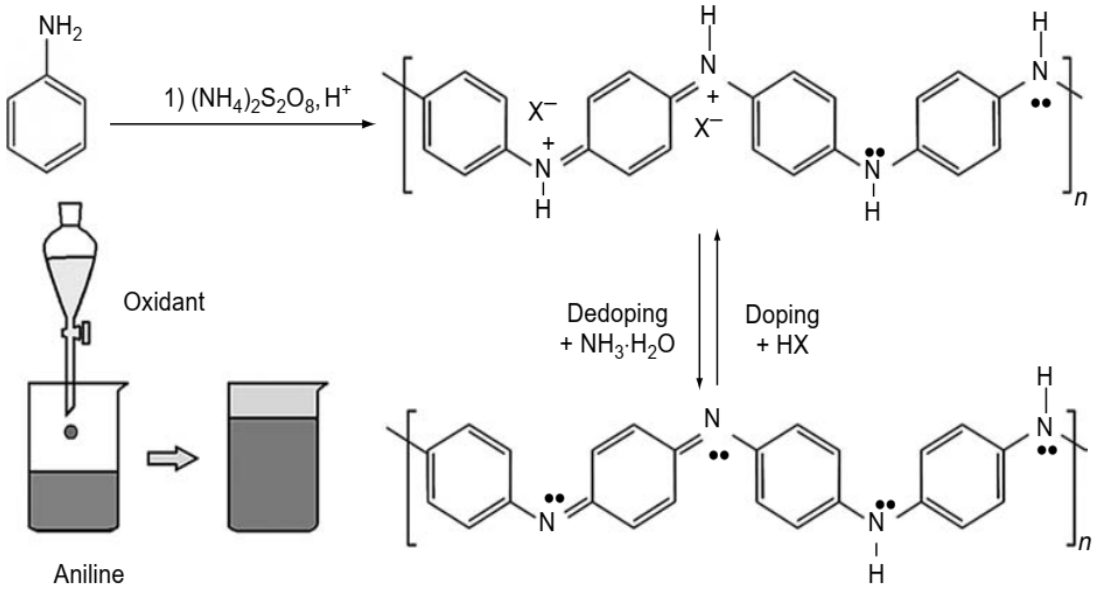

Figure I.9: The oxidative polymerization of aniline in an acidic solution. The synthesized polyaniline forms in its doped emeraldine salt state that then can be dedoped by a base to its emeraldine base form [37]

I.2.5 Conducting polymer composites

Conducting polymer composites, particularly PANI/inorganic have attracted increasing attention in recent years due to the fact they can combine the properties of each constituent usually with a synergistic effect, have interesting physical and chemical properties and many potential applications. Among various inorganic particles, SiO_2 particles have attracted attention due to their excellent reinforcing properties for polymer materials. However, SiO_2 is an insulator and a lot of work has been done to expand the applications of insulator SiO_2 as a filler to improve the processability of PANI.

I.2.5.1 Silica surface chemical properties

Silica is a mineral made up of silicon and oxygen, two of the most common elements on the planet. It comes in several forms, although by far the most common is crystalline silica. Crystalline silica is so abundant that it makes up over 12% of the earth's crust, making it the second-most common mineral on the planet.

Hydrous silica is the most important when adsorption is considered, since these surface hydroxyls represent the key of activity of silica in any process taking place at the surface. The least important property of silica as a desiccant relies completely upon silica hydroxylation.

The surface of hydrous silica can be visualized an extending domain of Si-O-Si bonds and the relatively high polarizability of the large oxygen ion compared with the small silicon ion makes it imperative that the surface is formed by oxygen ion alone. The implication is that at the uppermost layer of the extending joined tetrahedra, the oxygen atoms reside at a higher level than that accommodating the surface silicon atoms. When these oxygens attach to protons to form hydroxyls on the surface the latter are therefore at higher positions than the linked silicons. Brunauer et al. **[38]** reported value of 129 ± 8 ergs/cm^2 at 23°C for the total energy of the silanol surface of silica which is only slightly higher than the total surface energy of liquid water, 118.5 ergs/cm^2 **[6]**. This slight difference in surface energies made Brunauer et al. suggest that the chemical composition of the surfaces, H_2O and SiO_2 should show considerable similarity if the hydroxyls on silica are on top and the silicon atoms are below the OH groups. An atom or molecule physically adsorbed (via H-bonding for example) near a surface group perturbs motions of atoms of the group **[39, 40]**.

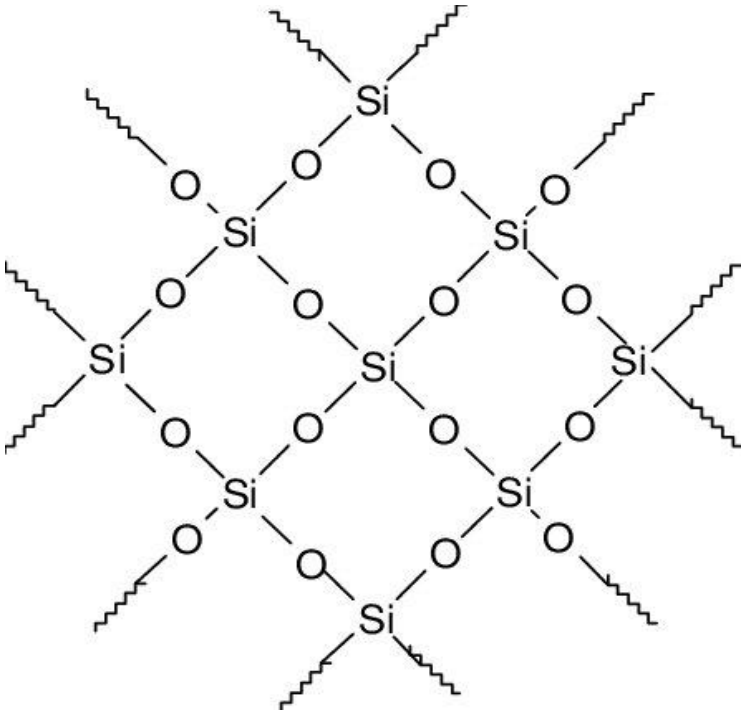

Scheme I.21: Chemical structure of SiO_2

The summary silica formula (SiO_2) does not do a good job of representing its factual chemical structure (Figure 1). In reality, it creates an expanded special structure in which almost every silicon atom is connected to four oxygen atoms, whereas almost every oxygen atom connects itself with two silica atoms, where the chemical structure of silica (SiO_2) providing negative surface charges **[41]**. However, many defects appear in this network. Additionally, the surface of the silica can contain many hydrogen, alkaline metals or hydroxyl group atoms, depending on their origins.

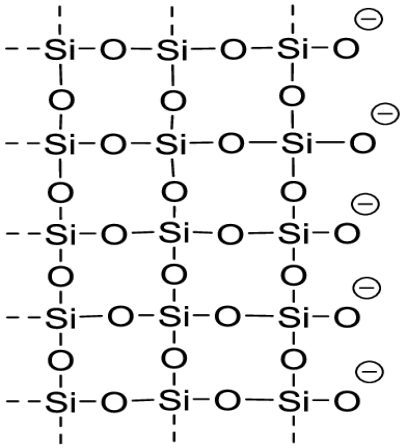

Scheme I.22: Idealized diagram of a realistic silica structure [42]

I.2.5.2 Polyaniline/silica composites

In the design of polyaniline/silica composites, a number of composites with silica sol, fumed silica, nano-silica, porous and spherical nano-SiO_2, mesoporous and colloidal silica particles have been developed and characterized for their electrical conductivity. In addition, the conductive properties of polyaniline/silica hybrid composites, polyaniline/silica nancomposites (NPs) and PANI/SiO_2 composite films have also been investigated **[43]**.

Also, polyaniline nanotube-based silica composite was used as an adsorbent for the adsorption of cationic methylene blue dye (Ayad et al. 2012) **[44]** and acid green (Ayad and El-Nasr 2012) **[45]**. The researchers carried out the adsorption of dyes onto the polyaniline nanotube-based silica composite in a batch system concerning the initial concentration of dyes and contact time. In both the studies, the pseudo-second-order kinetics model was best described the adsorption process. The adsorptions of methylene blue and acid green onto the polyaniline nanotube-based silica composite found to followed Langmuir adsorption isotherm with maximum monolayer adsorption capacity were 10.31 and 6.896 mg/g respectively. In both research articles, it was observed that amount of methylene blue and acid green onto the convention polyaniline and polyaniline nanotubes was found to follow the order polyaniline nanotubes base/ silica composite > polyaniline nanotubes base > conventional polyaniline base/silica composite > conventional polyaniline base.

I.2.5.3 The use of PANI and PANI composites in adsorption process

The application of PANI as adsorbents for water purification is due to the large amounts of amine and imine functional groups, which are expected to have interactions with inorganic and organic molecules, such as Hg(II), Cr(VI), methylene blue and antibiotic drugs. However, bare PANI particles can easily aggregate due to the inter- and intra-molecular interactions, which significantly reduce the surface area, resulting lower adsorption abilities. Other functional materials, including silica, sawdust, carbon nanotubes, graphene/GO, cellulose acetates, inorganic salts, and organic molecules, are combined with PANI to generate PANI-related composites to improve its surface area and change its surface morphology. A selective summary of adsorption capacities of PANI-based materials is provided in Table I.4.

Table I.4: A selective summary of adsorption capacities of PANI-based materials for dye removal [46]

Material	Dye	Maximum adsorption capacity (mg g^{-1})
PANI-EB		
PANI nanoparticle	MB	6.1
PANI nanotube	MB	9.2
PANI nanotube/silica composite	MB	10.3
Nanostructured crosslinked	MB	13.8
PANI **PANI-ES**		
PANI-HCl	PR	18.4
PANI-HCl	MO	154.6
PANI-HCl	MB	192.3
PANI-HCl	OG, CBB, RBBR, AG	175, 129, 100, 56
PANI-HCl/chitosan composite	OG, CBB, RBBR	322, 357, 303
PANI-HCl/TMP nanocomposite	MG	78.9
PANI-HCl/ZSP nanocomposite	MB	12
PANI-H_2SO_4	MO	75.9

References

[1] Waheed IF, Al-Janabi OYT and Foot PJS. Novel $MgFe_2O_4$-CuO/GO heterojunction magnetic nanocomposite: Synthesis, characterization, and batch photocatalytic degradation of methylene blue dye. J. Mol. Liq 2022; 357: 119084.

[2] Dickcha B and Ackmez M. Adsorption of reactive red 158 dye by chemically treated cocos nucifera L. shell powder. New York: Springer, 2011, p.1-3.

[3] Waheed IF, Al-Janabi OYT, Ibrahim AK, et al. $MgFe_2O_4$/CNTs nanocomposite: synthesis, characterization, and photocatalytic activity. Int. J. Ind. Chem 2020; 11: S13-S28.

[4] Li J, Wang Q, Bai Y, et al. Preparation of a novel acid doped polyaniline adsorbent for removal of anionic pollutant from wastewater. J Wuhan Univ Technol Mater Sci Ed 2015; 5: 1085-1091.

[5] Skotheim TA. Handbook of conducting polymers. New York: Marcel Dekker, 1986, p.32-45.

[6] Minisy IM, Salahuddin NA and Ayad MM. Adsorption of methylene blue onto chitosan-montmorillonite/ polyaniline nanocomposite. Appl Clay Sci 2021; 203: 1-10.

[7] Bibi A, Shakoor A and Niaz NA. Polyaniline–calcium titanate perovskite hybrid composites: Structural, morphological, dielectric and electric modulus analysis. Polym. Polym. Compos 2022; 30: 1-13.

[8] Otero TF. Conducting polymers: bioinspired intelligent materials and devices. United Kingdom: Royal Society of Chemistry, 2016, p.202-206.

[9] Li Y, Xing R, Zhang B et al. Fluoro-functionalized graphene oxide/polyaniline composite electrode material for supercapacitors. Polym. Polym. Compos 2019; 27(2): 76-81.

[10] Freund M. S. and Deore B. A. Self doped conducting polymers, John Wiley & Sons Ltd, England. 2007.

[11] Sanjoy Mukherjee Bryan W. Boudouris, Organic Radical Polymers New Avenues in Organic Electronics, Springer, 2017.

[12] Conjugated Microporous Polymers R. Dawson and A. Trewin, **In**: Porous Polymers Design, Synthesis and Applications Shilun Qiu, Teng Ben. The Royal Society of Chemistry, 2016.

[13] Kar P. Doping in Conjugated Polymers. Scrivener Publishing LLC. 2013.

[14] Corrosion Protection of Metals by Intrinsically Conducting Polymers, Pravin P. Deshpande Dimitra Sazou. Taylor & Francis Group. 2016.

[15] Wallace G. G., Spinks G. M., Kane-Maguire L. A. P. and Teasdale. Conductive electroactive polymers: Intelligent Polymer Systems. Taylor & Francis Group, LLC. 2009

[16] Conducting Polymers, Fundamentals and Applications Including Carbon Nanotubes and Graphene: Prasanna Chandrasekhar, Springer, 2018.

[17] Wan M. Conducting polymers with micro and nanometer structure. Springer. 2008.

[18] Conducting polymers: Bioinspired Intelligent Materials and Devices: Toribio Fernández Otero

[19] M. Deka, A. K. Nath, and A. Kumar, Effect of dedoped (insulating) polyaniline nanofibers on the ionic transport and interfacial stability of poly(vinylidene fluoride-hexafluoropropylene) based composite polymer electrolyte membranes, J. Membrane Sci., 327, 188–194 (2009).

[20] F. Cheng, W. Tang, C. Li, J. Chen, H. Liu, P. Shen, and S. Dou, Conducting poly(aniline) nanotubes and nanofibers: Controlled synthesis and application in lithium/poly(aniline) rechargeable batteries, Chem. Eur. J., 12, 3082–3088 (2006).

[21] Wessling, B. Dispersion as the link between basic research and commercial applications of conductive polymers (polyaniline). Synth. Met. 1998, 93, 143 – 154.

[22] J. Chen and F. Cheng, Combination of lightweight elements and nanostructured materials for batteries, Acc. Chem. Res., 42, 713–723, 2009.

[23] Jonas, F.; Heywang, G. Technical applications for conductive polymers. Electrochim. Acta. 1994, 39, 1345 – 1347.

[24] Kuhn, H.H.; Child, A.D.; Kimbrell, W.C. Toward real applications of conductive polymers. Synth. Met. 1995, 71, 2139 – 2142.

[25] Wang, Y.; Jing, X. intrinsically conducting polymers for electromagnetic interference shielding. Polym. Adv. Technol. 2005, 16, 344 – 351.

[26] Poddar, A.K.; Patel, S.S.; Patel, H.D. Synthesis, characterization and applications of conductive polymers: A brief review. Polym. Adv. Technol. 2021, 32, 4616 – 4641.

[27] Tseng R. J., Huang J., Ouyang J., Kaner R. B., and Yang Y., Polyaniline nanofiber/gold nanoparticle nonvolatile memory, Nano Lett., 2005, 5, 1077-1080.

[28] Tseng R. J., Baker C. O., and Shedd B., Charge transfer effect in the polyaniline-gold nanoparticle memory system, Appl. Phys. Lett., 2007, 90, 053-101.

[29] Motheo A. J., Aspects on fundaments and applications of conducting polymers. InTech, Croatia, 2011.

[30] Michaelson L., Advances in conducting polymers research. Nova Science Publishers, New York, 2015.

[31] Green, A. G. & Woodhead, A. E. CXVII.-Aniline-black and allied compounds. Part II. *J. Chem. Soc., Trans.* 1912, 101, 1117-1123.

[32] Materials, C. Flexible and Stretchable Electronic Composites; Kalia, S., Ed.; Springer: Berlin/Heidelberg, Germany, 2016.

[33] Lux, F. Properties of electronically conductive polyaniline: a comparison between wellknown literature data and some recent experimental findings. *Polymer* 35**,** 2915–2936 (1994).

[34] Kang, E. T. *et al.* Polyaniline: A polymer with many interesting intrinsic redox states. *Prog. Polym. Sci.* 1998, 23**,** 277-324.

[35] Jamadade, V. S. *et al.* Studies on electrosynthesized leucoemeraldine, emeraldine and pernigraniline forms of polyaniline films and their supercapacitive behavior. *Synth. Met.* 2010, 160**,** 955–960.

[36] Tran, H. D. *et al.* The oxidation of aniline to produce 'polyaniline': a process yielding many different nanoscale structures. *J. Mater. Chem.* 2011, **21,** 3534–3550.

[37] Handbook of Conducting Polymers Third Edition: Conjugated polymers. Terje A. Skotheim and John R. Reynolds, Taylor & Francis Group, 2007.

[38] Brunauer, S., Kantro, D. L., & Weise, C. H. The surface energies of amorphous silica and hydrous amorphous silica. Can. J. Chem., 1956, 34, 1483–1496.

[39] Gill M., Baines F.L. and Armes S.P., Some Observations on the Preparation of Colloidal Polyaniline-Silica Composites, *Synth. Met.*, 1993, 1029, 55-57.

[40] Panaitescu D. M., Vuluga Z., Radovici C. et al., "Morphological investigation of PP/nanosilica composites containing SEBS," Polymer Testing, 2012, 31, 355-365.

[41] Katarzyna Kupiec, Piotr Konieczka, and Jacek Namiesnik, Characteristics, Chemical Modification Processes as well as the Application of Silica and its Modified Forms, Critical Reviews in Analytical Chemistry, 2009, 39, 60-69.

[42] Roshchina T. M., Shonia N. K., Lagutova M. S., Borovkov V. Y., Kustov L. M. and Fadeev A. Y., Properties of the surface of silicas modified with bi-and trifunctional perfluorohexylsilanes: Adsorption of benzene. Russ. J. Phys. Chem. A, 2007, 81, 1128–1135.

[43] Riaz T., Kanwal F., Siddiqi S. A., Gull N., Jamil T., Ali A., Batool A., Phulpoto S. N., and Thebo K. H. Study of Conducting Properties of Chemically Synthesized Polyaniline/crystalline Silica Composites. IJSER, 2016, 7, 513-519.

[44] Ayad MM and Abu El-Nasr A. Adsorption of cationic dye (methylene blue) from water using polyaniline nanotubes base. J Phys Chem C. 2010, 114, 14377-14383.

[45] Ayad MM, Abu El-Nasr A and Stejskal J. Kinetics and isotherm studies of methylene blue adsorption onto polyaniline nanotubes base/silica composite. J Ind Eng Chem 2012, 18, 1964-1969.
[46] Shen J., Shahid S., Amura I., Sarihan A., Tian M., Emanuelsson E. AC. Enhanced adsorption of cationic and anionic dyes from aqueous solutions by polyacid doped polyaniline. Synth. Met, 2018, 245, 151-159.

I.3 Adsorption

Adsorption produces high quality product water by adsorbing the cationic, mordant and acid dyes from the textile wastewater. Adsorption techniques have gained favour recently due to their efficiency in the removal of pollutants that are too stable for conventional methods. This process is also economically feasible **[1]**. Decolourisation by adsorption is a result of two mechanisms, surface adsorption and ion exchange **[2]**, and is influenced by many physiochemical factors, such as dye / sorbent interaction, sorbent surface area, particle size, temperature, pH, and contact time **[3]**. In addition to activated carbon, a number of low-cost adsorbent materials, for example, peat, fly ash, wood chips, bentonite clay and fly ash have been investigated for colour removal **[4]**.

I.3.1 Definition of adsorption

The adsorption separation process constitutes one of the most important technologies today; it is widely used for depollution and purification in a wide variety of fields, such as the petroleum, petrochemical and chemical industries, environmental and pharmaceutical applications **[1]**.

Batch adsorption technology is used to study the effects of various important parameters such as adsorbent quantity, pH values, and contact time between adsorbents and absorption **[2, 3]**.

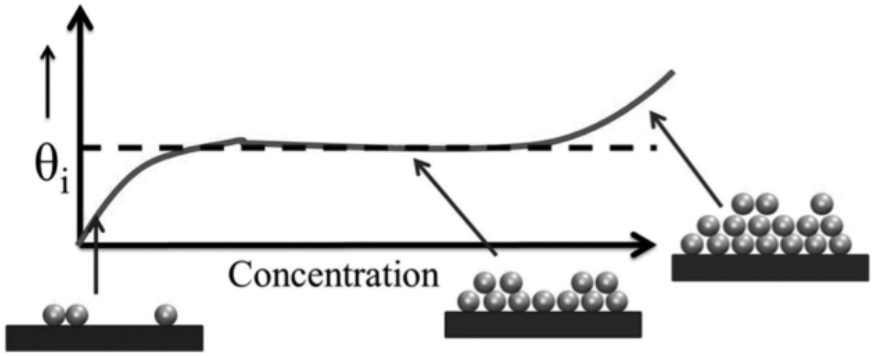

Figure I.10: Representation of the adsorption process, where symbol (θi) is the fraction of the surface sites occupied [5]

I.3.2 Types of adsorption

Depending on the types and nature of adsorbate-adsorbent interactions or the forces that hold the adsorbates on the solid surface, two types of adsorption are distinguished: physical adsorption (physisorption) and chemical adsorption (chemisorption).

I.3.2.1 Physical adsorption

This type of adsorption results from the establishment of an exchange of low energy forces between the surface of a solid and molecules near this surface. In this case, the retention is the result of electrostatic bonds of the Van Der Walls type. From an energetic point of view, physisorption occurs at low temperatures with energies of the order of 10 kcal.mol^{-1} at most. It corresponds to a reversible process and does not lead to a modification of the chemical identity of the adsorbed molecule.

Physically adsorbed molecules can diffuse along the surface of the adsorbent and are generally not bound to a specific location on the surface. Being only weakly bound, physical adsorption is easily reversed **[6]**.

I.3.2.2 Chemical adsorption

Chemical adsorption results from a chemical interaction between adsorbent and adsorbate. Molecules cannot move freely on the surface. It generates high adsorption energies thus favored by high temperatures **[7]**. It involves one or more covalent or ionic chemical bonds between the adsorbate and the adsorbent. Chemisorption is generally irreversible, producing a modification of the adsorbed molecules **[1]**.

This type of adsorption is involved in the mechanism of heterogeneous catalytic reactions. The following table summarizes the main differences between physical adsorption and chemical adsorption **[5]**.

Table I.5 : The main differences between physical adsorption and chemical adsorption [5]

Parameters	**Physical adsorption**	**Chemical adsorption**
Bonding type adsorbent – adsorbate	Van der Waals or hydrogen bridge	Covalent or ionic
Temperature range	Relatively low	Higher
Specificity	Non-specific process	Depends on the nature of the adsorbent and the adsorbate
Desorption	Easy	Difficult
Kinetics of adsorption	Fast	Very slow, especially below the activation temperature
	Low heat of adsorption (<2 or 3	High heat of adsorption

	times heat of evaporation).	(>2 or 3 times latent heat of evaporation).
	Non specific	Highly specific
	Monolayer or multilayer no dissociation of adsorbed species. only significant at relatively low temperatures	Monolayer only. May involve dissociation possible over a wide range of temperature.
	Rapid, non-activated reversible	Activated, may be slow and irreversible
	No electron transfer although polarization of sorbate may occur	Electron transfer leading to bond formation between sorbate and surface
Heat of adsorption	Lower than 10 Kcal/mole	Upper than 10 Kcal/mole

I.3.3 Adsorption mechanisms

The mechanism of adsorption of a solute on the surface of a solid can be broken down into several successive elementary steps, each of which can control the overall phenomenon under given conditions **[8]**.

1- External mass transfer (external diffusion) which corresponds to the transfer of the solute from the solution to the external surface of the particles.

2- Internal mass transfer in the pores (internal diffusion) which takes place in the fluid filling the pores. Indeed, the molecules propagate from the surface of the grains towards their center through the pores.

3- Surface diffusion: for certain adsorbents, there may also be a contribution from the diffusion of the adsorbed molecules along the surfaces of the pores on the scale of an adsorbent grain.

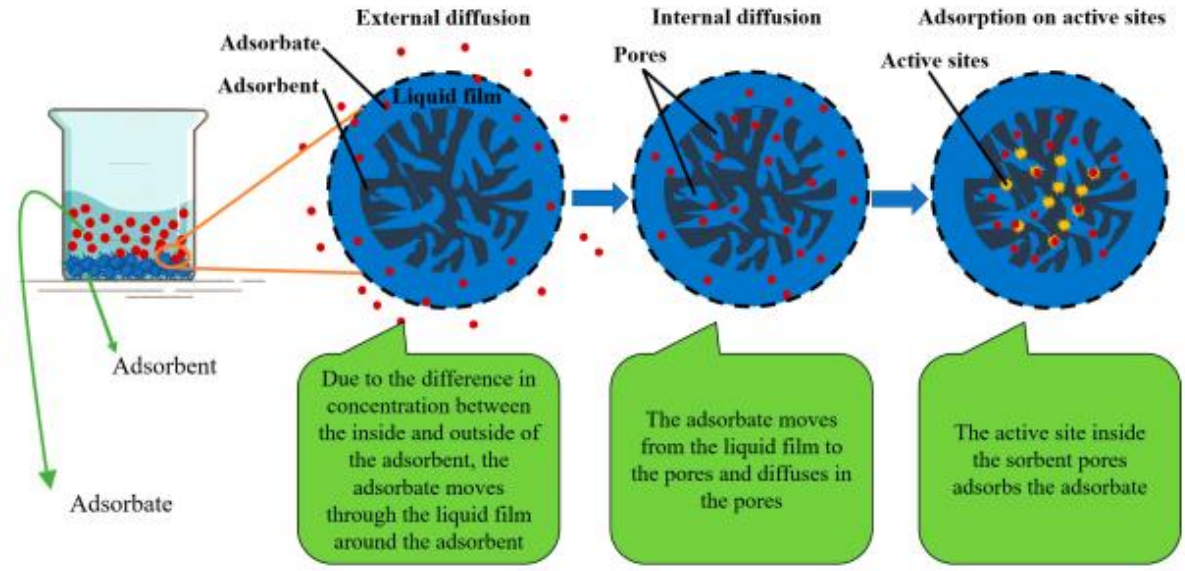

Figure I.11: Adsorption and mass transfer diagram [8]

I.3.4 Factors influencing adsorption

The adsorption capacity of a material is influenced by the physicochemical properties of the adsorbent. When a solid is brought into contact with a solution, each constituent of the latter, the solvent and the solute, shows a tendency to adsorption on the surface of the solid. There is therefore a competition on the surface between two adsorptions which are competitive **[1, 7]**. Therefore the quantity adsorbed depends on numerous factors, the main ones of which are:

I.3.4.1 Influence of temperature

The adsorption process which is not affected by chemical reactions is always accompanied by a release of heat (exotherm), so that when the temperature increases, the desorption phenomenon will dominate. On the other hand, for activated adsorption (chemical adsorption), the adsorption equilibrium cannot be reached quickly and the increase in temperature promotes adsorption. Some adsorption studies have shown that adsorption increases with increasing temperature. This increase in adsorption is mainly due to the increase in the number of adsorption sites caused by the breakage of some internal bonds near the edges of the active surface of the adsorbent **[6]**.

I.3.4.2 Influence of pH

The change in pH affects the adsorption process through the dissociation of functional groups on the adsorbing surfactant sites. This subsequently leads to a change in the reaction kinetics and equilibrium characteristics of the adsorption process **[6]**. For solutes that are not found in

ionized forms at the pH studied, the effect of pH will be negligible. And the pH sometimes has a significant effect on the adsorption characteristics; for compounds whose pK_a is close to the pH studied, this parameter will have an effect on the adsorption capacity of these solutes. In most cases, the best results are achieved at the lowest pH. This property particularly applies to the adsorption of acidic substances **[8]**.

I.3.4.3 Influence of initial concentration

Parameter seems to have an impact on the adsorption process such that with higher initial concentration of dye solution, the absorption of dye is higher.
This is because at lower initial concentration, the ratio of the initial number of moles of dyes to the available surface area is low. Therefore, it is important to determine the maximum adsorption capacity of the adsorbent for which experiments should be conducted at the highest possible initial dye concentration **[5, 7]**.

I.3.4.4 Influence of the nature of the adsorbent

The adsorption of a given substance increases with the decrease in the particle size of the adsorbent, which allows the compounds of the solution to penetrate into the capillaries of the substance, therefore the subdivision of the particle of the solid directly influences the pores of the latter as well as its specific surface which will be developed. However, if the dimensions of the pores are smaller than the diameters of the molecules of one of the components of the solution, the adsorption of this compound does not take place, even if the surface of the adsorbent has a high affinity for this compound **[1, 5]**.

- Specific surface area

Adsorption is a surface phenomenon and as such the extent of adsorption is proportional to the specific surface area. The specific surface area is essential data for the characterization of solids and porous materials. It is very important to give adsorbents a large specific surface area, this quantity refers to the accessible surface area relative to the unit weight of adsorbent **[9]**.

- Porosity

The porous distribution or porosity is related to the pore size distribution. It reflects the internal structure of microporous adsorbents **[7]**.

I.3.4.5 Influence of the nature of the adsorbate

1) Solubility

The solubility of an adsorbate plays an important role during its adsorption. The greater the solubility, the lower the adsorption will be **[7]**.

2) Polarity

Polar solids preferentially adsorb polar bodies, and apolar solids adsorb apolar bodies. The affinity for the substrates increases with the molecular mass of the adsorbate.
Adsorption is more intense for bodies which have relatively more affinity for the solute than for the solvent **[1]**.

3) The size of the molecule

The size of the molecule also has a direct influence on adsorption, molecules whose size is appropriate for that of the pores will be adsorbed more favorably, because they have more points of contact with the surface of the molecule. On the contrary, the molecule moves with difficulty inside the pores because of its relatively large size **[7]**.

I.3.5 Adsorption kinetic models

The kinetic parameters are used for prediction of the adsorption rate, which provides information for modelling the process. Generally, three models are used for the analysis of adsorption kinetics **[2]**.

I.3.5.1 First order kinetic model (Lagergren equation)

Lagergren (1998), proposed the pseudo-first order kinetic model:

$$\frac{dq_t}{dt} = K_1 (q_e - q_t) \qquad \textbf{(I.1)}$$

The integration of this equation gives us [1]:

$$\ln (q_e - q_t) = \ln q_e - K_1 t \qquad \textbf{(I.2)}$$

With:

q_e: The adsorption capacity at equilibrium (mg/g)
q_t: The adsorption capacity at time t (mg/g)

K_1 : First order rate constant (min^{-1})

I.3.5.2 Second-order model

The differential equation of the second-order adsorption model is given in the form **[2]**:

$$\frac{dq_t}{dt} = k_2 (q_e - q_t)^2 \qquad \textbf{(I.3)}$$

Its linear form is written:

$$\frac{1}{q_t} = \frac{1}{K_2 . q_e^2} + \frac{1}{q_e}.t \qquad \textbf{(I.4)}$$

K_2: Second order rate constant ($g. mg^{-1}. min^{-1}$).

Note that k_2 and q_e are determined by plotting $1/(q_e - q_t)$ as a function of t.

I.3.5.3 Intraparticle diffusion model

Weller and Morris proposed a theoretical model based on intra-particle diffusion. Described by the following equation **[2]**:

$$q_t = K_D . t^{1/2} + C \qquad \textbf{(I.5)}$$

K_D: Intraparticle diffusion rate constant ($g.mg^{-1}.min^{-1/2}$)

C: Observation linked to the thickness of the boundary layer (mg. g)

The representation of q_t as a function of $t^{1/2}$ allows the speed constant K_D to be calculated.

The transfer of an adsorbate from the liquid phase to an adsorption site, represented by the figure (1.12), involves the following steps **[5]**:

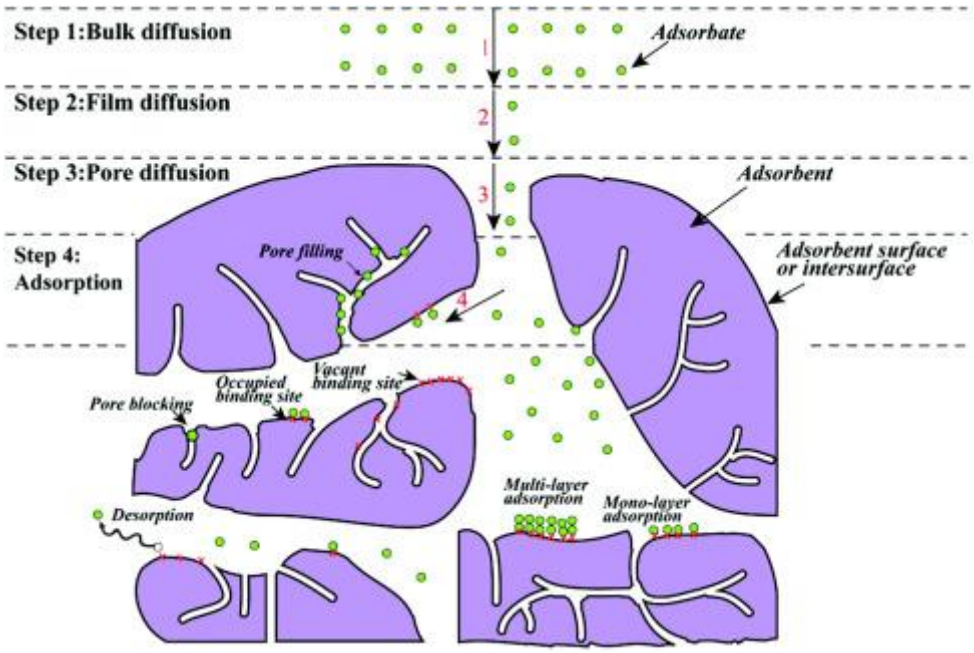

Figure I.12: The stages of adsorption kinetics [5]

1st step: transfer of the adsorbate from the liquid phase to the boundary layer of the liquid film linked to the solid particle (by convection or diffusion). Very fast stage.

2nd step: Transfer of the adsorbate through the liquid film to the external surface of the adsorbent. Quick step.

3rd stag: Diffusion inside the adsorbent particle in two ways, under the influence of the concentration gradient. Slow step.

3a: Under the adsorbed state, by surface diffusion.

3b: In the free state, by pore diffusion.

4th stag: Adsorption in a micropore. Very fast stage.

I.3.6 Adsorption isotherms

Not all adsorbent/adsorbate systems behave the same way. Adsorption phenomena are often approached by their isothermal behavior. Isothermal curves describe the existing relationship at adsorption equilibrium between the quantity adsorbed and the solute concentration in a given solvent at a constant temperature **[7]**.

I.3.6.1 IUPAC classification

According to the UPAC classification, adsorption-desorption isotherms can be grouped into six classes (Figure I.13) **[1, 10]**:

- **Type I**

The type I adsorption equilibrium isotherm is characteristic of an adsorbent whose microporous volume is particularly high. The saturation of the adsorption sites occurs gradually from low concentrations and the shape of the isotherm is characterized by a long plateau indicating weak formation of multilayers.

- **Type II**

The type II isotherm is observed in the case of adsorbents having a large macroporous volume with a diameter greater than 500 Å. Adsorption takes place first in a monolayer then in multilayers until capillary condensation, which reflects the existence of strong intermolecular interactions compared to the interactions between the molecules and the solid.

- **Type III**

It indicates the formation of poly-molecular layers, from the start of adsorption and before the surface is completely covered with a mono-molecular layer. Additional adsorption is facilitated because the interaction of the adsorbate with the layer formed is greater than the interaction between the adsorbate and the adsorbent **[10]**.

- **Type IV**

The type IV adsorption equilibrium isotherm is associated with rather mesoporous adsorbents. The presence of two levels can result from the formation of two successive layers of adsorbate on the surface of the solid. When the interactions between the adsorbate molecules and the adsorbent surface are stronger than those of the adsorbate molecules with each other, the adsorption sites of the second layer only begin to be occupied when the first layer is totally saturated.

- **Type V**

Type V adsorption equilibrium isotherms are characteristic of microporous adsorbents with the formation of multilayers at low concentrations. As for the type III isotherm, this behavior is representative of stronger interactions between adsorbate molecules than between adsorbate and adsorbent molecules.

➢ **Type VI**

The type VI is associated with layer-by-layer adsorption on a highly uniform surface **[10]**.

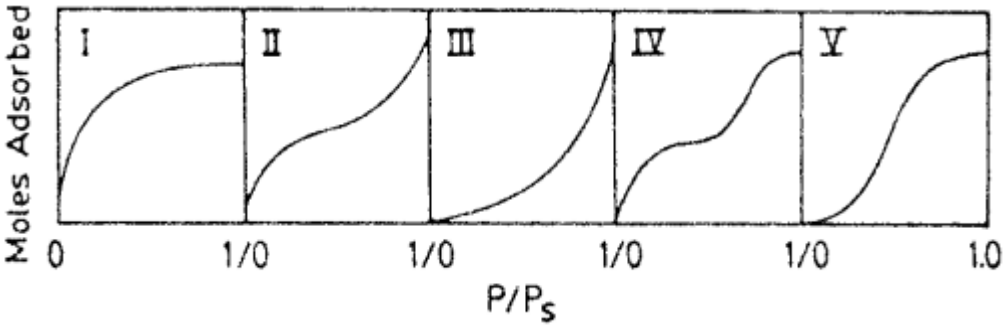

Figure I.13: Classification of isotherms according to Brunauer et al. [1]

I.3.6.2 Mathematical models of adsorption isotherms

Experimentally, it is very common in sorption reaction studies to relate the surface concentration of the complex formed to equilibrium (amount of solute retained by the solid, q_e, in $mol.g^{-1}$ or $mg.g^{-1}$ or derived units) at the equilibrium concentration of the solute in the liquid or gas phase (C_e, in $mol.L^{-1}$ or $g.L^{-1}$ or derived units). The relationship obtained is called equilibrium isotherm provided that the experiment is carried out at constant temperature **[11]**:

$$\mathbf{q_e = (C_0 - C_t).} \left(\frac{V}{m}\right) \qquad \textbf{(I.6)}$$

V: Volume of solution (L)

m: mass of adsorbent solid (g)

C_0 and C_t: Initial concentration and at time t of solute in liquid or gas phase (mg/L) respectively.

1) Langmuir models (Langmuir, 1916)

The assumptions of this model are as follows **[1]**:

- The adsorption sites on the solid surface are homogeneous from an energetic point of view: we speak of a "homogeneous adsorption surface".

- Each of these sites can adsorb a single molecule, and a single layer of molecules can form.

- Each of the sites has the same affinity for the molecules in solution.

- There are no interactions between the adsorbed molecules.

The Langmuir model assumes that adsorption takes place on sites of the same energy and that there is no interaction between the adsorbed molecules.

The Langmuir isotherm is represented by the following equation **[7]**:

$$\mathbf{q_e = \frac{X}{m} = q_m \times \frac{b\,.Ce}{1+b.Ce}} \qquad \textbf{(I.7)}$$

b: thermodynamic equilibrium constant in relation to the adsorption energy.

C_e: equilibrium concentration in the gas or liquid phase. The representation

graph of this equation gives: $1/qe = f(1/C_e)$ which is a line with slope $1/b.q_0$ and of intercept $1/q_0$.

The Langmuir isotherm can be rearranged into the following linear forms **[12, 13]**:

$$\mathbf{\frac{1}{q_e} = \frac{1}{q_m} + \frac{1}{k.q_m.C_e}} \qquad \textbf{(I.8)}$$

$$\mathbf{\frac{C_e}{q_e} = \frac{1}{K.q_m} + \frac{C_e}{q_m}} \qquad \textbf{(I.9)}$$

$$\mathbf{qe = -\frac{qe}{K.Ce} + q_m} \qquad \textbf{(I.10)}$$

$$\mathbf{\frac{Ce}{qe} = -k.qe + k\,q_m} \qquad \textbf{(I.11)}$$

$$\mathbf{\frac{1}{C_e} = \frac{k.q_m}{qe} - k} \qquad \textbf{(I.12)}$$

q_e: The adsorption capacity at equilibrium (mg/g)

q_m: Maximum adsorption capacity (mg/g)

C_e: equilibrium concentration in the gas or liquid phase (mg/L)

By putting the previous equation in linear form **[10-13]**:

$$\mathbf{\frac{Ce}{qe} = \frac{1}{K.q_m} + \frac{Ce}{q_m}} \qquad \textbf{(I.13)}$$

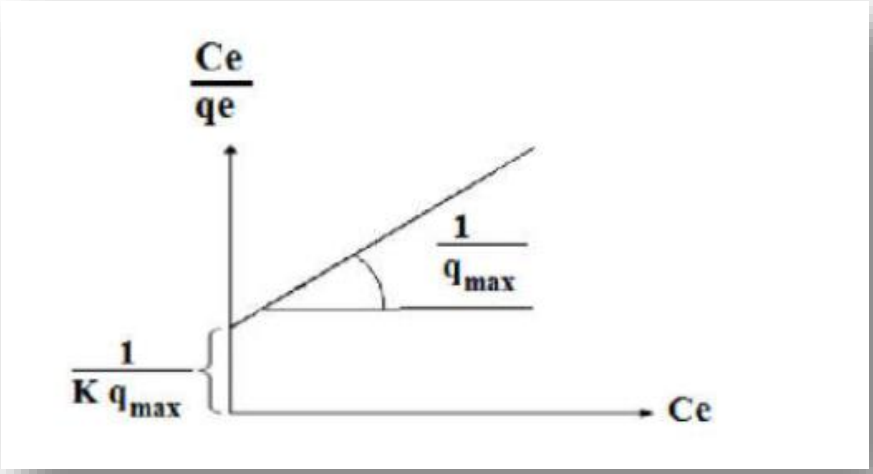

Figure I.14: Application of the Langmuir model [10]

2) Freundlich isotherm

The Freundlich model is a semi-empirical model which makes it possible to model adsorption isotherms on heterogeneous surfaces (where the adsorption sites are not all equivalent). This model can only be used in the domain of low concentrations because it has no upper limit for high concentrations, which is contradictory with the experience used to describe heterogeneous systems characterized by the heterogeneity factor (n) **[1, 11]**.

The Freundlich Isotherm can be described by the following equation **[7]**:

$$q_e = k_f \cdot Ce^{1/n} \qquad \textbf{(I.14)}$$

Q_e: Quantity of adsorbate adsorbed per gram of adsorbent at equilibrium (mg/g)

C_e: Concentration of the adsorbate in the solution at equilibrium (mg/L)

k_f: is the Freundlich constant (1/g) which indicates the sorption capacity of the sorbent

n: is the heterogeneity factor.

The linearization of this equation gives the following equation **[13]**:

$$\ln q_e = \ln K_f + \frac{1}{n} \ln Ce \qquad \textbf{(I.15)}$$

Theoretically, it is a line with slope 1/n and ordinate at the origin Ln K. Extrapolation of this line for $C_e = C_o$ gives the maximum adsorption capacity or saturation capacity q_{max}

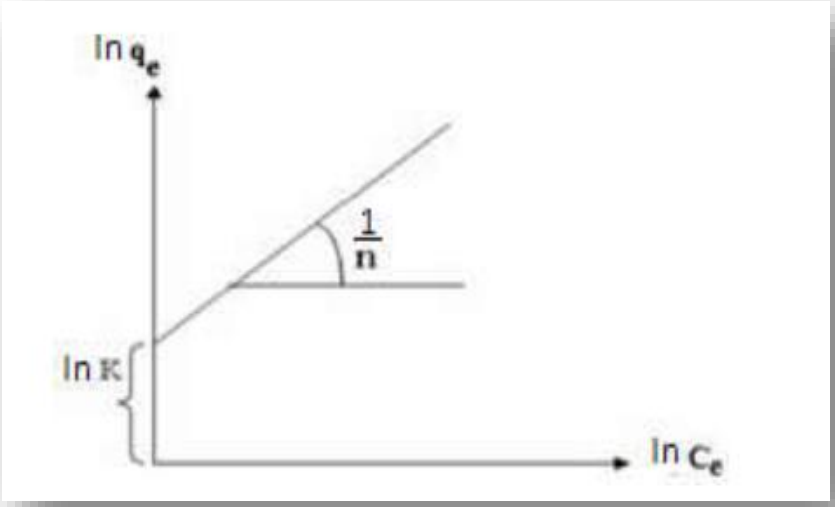

Figure I.15: Application of the Freundlich model [10]

3) Temkin isotherm

Temkin's model is based on the assumption that the heat of adsorption due to interactions with the adsorbate decreases linearly with the recovery rate during gas-phase adsorption. It is an application of the Gibbs relation for adsorbents whose surface is considered energetically homogeneous. Several authors have proposed using this model in the liquid phase, by plotting qe or q as a function of ln Ce according to the following expression **[14]**:

$$q_e = \left(\frac{RT}{b_T}\right). Ln\ (A_T.\ Ce) \qquad \textbf{(I.16)}$$

$$q_e = B\ Ln\ A_T + B\ Ln\ Ce \qquad \textbf{(I.17)}$$

C_e (mg.L^{-1}): equilibrium concentration and T (K): absolute temperature.

4) Elovich isotherm

The equation is based on the principle of kinetics which assumes that the number of adsorption sites increases exponentially with adsorption, implying multilayer adsorption **[15]**. Described by the relationship:

$$q_t = \frac{1}{\beta}\ln(\alpha\beta) + \frac{1}{\beta}\ln(t) \qquad \textbf{(I.18)}$$

K_e ($L.mg^{-1}$): Elovich equilibrium constant. If adsorption is described by the Elovich equation, the equilibrium constant and the maximum capacity; can be calculated from the plot of ln (q_e/C_e) versus (q_e).

5) BET (Brunauer-Emmett-Teller) isotherm

The Brunauer Emmett Teller (BET) isotherm, proposed in 1938, was designed as an extension of the Langmuir adsorption mechanism to a number of layers that can go up to infinity. It is represented by the following equation **[16, 17]**:

$$q/q_m = (K\,(\,C/(C_0)\,))/(1-C/(C_0)\,)[1+(K-1)C/(C_0)] \qquad \textbf{(I.19)}$$

q: the retention capacity at time t

q_m: monomolecular retention capacity

C: concentration at time t

C_0: the initial concentration

K: The adsorption constant

The linear form of this equation is given by the equation below:

$$C/(q(C_0-C)) = 1/(q_m\,.\,K)+ (K-1)/(q_m\,.\,K\,)\,(C/(C_0)) \qquad \textbf{(I.20)}$$

I.3.7 Use of adsorption

Adsorption has many practical applications. We understand that the phenomena causing a modification of the composition of a gas mixture, of a liquid mixture, can have industrial developments; however, the adsorption of pure gases and vapors is of less practical interest **[10]**.

a. Application of gas phase adsorption

In the practical use of adsorption phenomena of gas mixtures with a view to their fractionation, it must not be forgotten that the operation of an adsorption column or adsorber is by nature intermittent and must comprise two phases.

- An adsorption phase, which must be stopped when the mass transfer zone reaches the desired purity, at the outlet of the column: breaking point or leak point.

- A consecutive phase of desorption or regeneration of the adsorbent to make it suitable for a new adsorption phase and to possibly recover the adsorbate **[4]**.

b. Application of liquid phase adsorption

The applications of liquid phase adsorption can be classified into two areas: that of the treatment of dilute solutions and that of the fractionation of liquid mixtures, although, in both cases, it is always a question of separation of chemical compounds. Industrial applications concerning the treatment of diluted solutions (purification and extraction) are extremely numerous **[8]**. The most important treatments:

- Discoloration of sweet juices;
- The purification of various petroleum products and animal and vegetable fats;
- Water treatment (elimination of heavy metals, odors, and organic matter).
- Desiccation of industrial organic products.

I.3.8 Areas of application of adsorption

The numerous applications of adsorption are cited **[5, 10]**:

- Refining of petroleum products;
- Drying, purification, dehumidification and deodorization of the air;
- Catalysis;
- Recovery of solvents and alcohol in the fermentation process;
- Discoloration of liquids;
- Gas chromatography (fractionation method based on differences in adsorption speed of different substances, on a given adsorbent.

References

[1] Douglas M. Ruthven, principles of adsorption and adsorption processes, John Wiley and sons, Canada, 1984.

[2] Faust S. D., Aly O. M., Adsorption Processes for Water Treatment, Butterworth Publishers, USA, 1987.

[3] Schweitzer P. A., Handbook of separation techniques for chemical engineers, McGraw Hill, New York, 1997.

[4] Iqbal J.. Adsorption of acid yellow dye on flakes of chitosan prepared from fishery wastes. Arab. J. Chem. 4, 2011. 389-395.

[5] Theory, Molecular, Mesoscopic Simulations, and Experimental Techniques of Aqueous Phase Adsorption Singh J. K. and Verma N. **In:** Aqueous Phase Adsorption Theory, Simulations and Experiments: Singh J. K. and Verma N., Taylor & Francis Group, USA, 2019.

[6] Gusain D. and Bux F., Batch Adsorption Process of Metals and Anions for Remediation of Contaminated Water. Taylor & Francis Group, USA, 2021.

[7] Worch E. Adsorption technology in water treatment fundamentals, processes and modeling. Berlin: Walter de Gruyter, 2012.

[8] Li, T.; Xin, R.; Wang, D.; Yuan, L.; Wu, D.; Wu, X. Research Progress on the Applications of Seashell Adsorption Behaviors in Cement-Based Materials. Buildings. 2023, *13*, 1-16.

[9] V. J. Inglezakis and S. G. Poulopoulos, adsorption, ion exchange, and heterogeneous catalysis: Design of operations and environmental applications. Elsevier, 2006

[10] Mohammad A. Al-Ghouti, Dana A. Da'ana, Guidelines for the use and interpretation of adsorption isotherm models: A review. J. Hazard. Mater., 2020, 393, 1-100.

[11] Humelnicu D, Soroaga LV, Arsene C, et al. Adsorptive performance of soy bran and mustard husk towards arsenic (V) ions from synthetic aqueous solutions. Acta Chim Slov 2019; 66: 326-336.

[12] Dada AO, Adekola FA and Odebunmi EO. Kinetics, mechanism, isotherm and thermodynamic studies of liquid-phase adsorption of Pb^{2+} onto wood activated carbon supported zerovalent iron (WAC-ZVI) nanocomposite. Cogent Chem 2017; 3: 1-20.

[13] Maruthapandi M, Kumar VB, Luong JHT, et al. Kinetics, isotherm, and thermodynamic studies of methylene blue adsorption on polyaniline and polypyrrole macro-nanoparticles synthesized by C-Dot-initiated polymerization. ACS Omega 2018; 3: 7196-7203.

[14] Allen, S., Mckay, G. and Porter, J. Adsorption isotherm models for basic dye adsorption by peat in single and binary component systems. J. Colloid Interface Sci., 2004, 280(2): 322-333.

[15] Almalike, L. Equations Adsorption Isotherms for Biuret on Soils, Paper and Cortex Plant Application of the Freundlich, Langmuir, Temkin, Elovich, Flory-Huggins, Halsey, and Harkins-Jura. Int. j. adv. res. chem. sci., 2017, 4(5): 9-20.

[16] Aremu, J., Lay, M., & Glasgow, G. Kinetic and isotherm studies on adsorption of arsenic using silica based catalytic media. J. Water Proc.engineering, 2019, *32*: 1-13.

[17] Chen, X. Modeling of Experimental Adsorption Isotherm Data. *Information*, 2015. 6(1): 14-22.

Chapter two

Experimental section

II. Experimental section

II.1 Synthesis of polyaniline emeraldine salt (PANI-ES)

PANI-ES can be synthesized from monomeric aniline (99.5%, Biochem) by oxidative chemical polymerization **[1, 2]**. In summary, PANI was prepared as follows: the first solution was prepared with 0.5 M of aniline dissolved in 100 ml of 1M HCl (32%, VWR) and the second solution with 0.25 M of $(NH_4)_2S_2O_8$ (98%, VWR) in 100 ml of distilled water. The latter was added slightly to the first solution with continuous stirring. The mixture was placed under stirring for one hour at 0-5 °C. The greenish black precipitate resulting from this solution was passed to filtration and washing repeatedly with water first, diluted HCl solution and methanol until the wash liquid was colorless to remove oligomers and other non-polymeric impurities. Then, the collected polymer was dried for 48 hours in a 40 °C oven, grinded and stored for processing **[3-11]**.

II.2 Synthesis of PANI/Silica (SiO_2) composite:

Determined amount of silica suspension (including 0.23 g of silica / 10 ml), aniline (9.313 g, 0.10 mol) and 10 ml of conc. HCl in 200 ml of distilled water was added by mixing in the ice water bath. The mixture was stirred for a further 30 minutes. Then, a volume of 100 ml of aqueous APS solution (containing 22.820 g, 0.10 mol of APS) was dropped into the emulsions in 60 minutes. The mixture was placed under stirring for another 4 hours in a cooled water bath. The PANI/silica composite was filtered and washed with water three times. Finally, it was dried in the oven at 40 °C for 48 hours **[12-16]**.

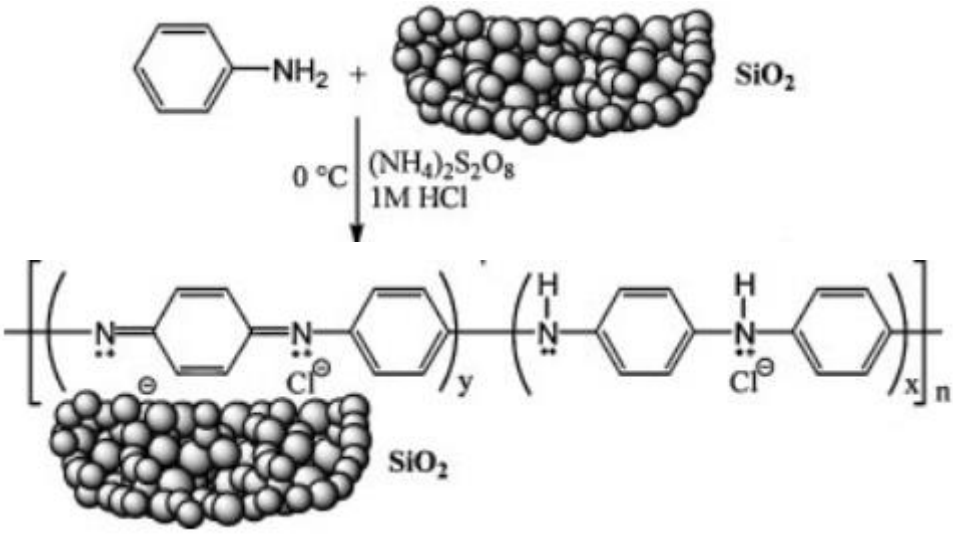

Figure II.1: Polymerization of PANI/SiO_2 composite **[13]**.

II.3 Sorbate dye (Methylene Blue)

To prepare the MB solution 1g of MB was dissolved in 1L of distilled water. It has a molecular formula $C_{16}H_{18}N_3ClS$ with molecular weight 319.85 $g.mol^{-1}$. It is a non-toxic water soluble dye, blue in color (λ_{max} 661 nm) **[14, 17]**. Initial and final concentrations of MB solutions were determined by measuring absorbance at 661 nm using UV visible absorption spectroscopy.

II.4 Adsorption experiments

The adsorption study was performed using an aqueous MB dye solution for the determination of adsorption capacity of the synthetic PANI and PANI/SiO_2 composite. Sample concentrations were determined in the UV-visible apparatus at λ= 661 nm. The effect of different parameters was carried out from this study such as the adsorption time (0-120 min), the initial concentration in MB (4 - 21 mg/L) and the mass of the adsorbents (0.05 - 1.0 g).

The q_e (equilibrium adsorption amount) was calculated as follows:

$$q_e = \frac{(C_i - C_e).V}{m} \qquad (II.1)$$

where C_i and C_e are the initial concentration (before adsorption) and concentration at equilibrium (after adsorption) in mg/L of MB, respectively; V and m are the volume (L) of the MB solution and the weight (g) of the used material (adsorbent) **[18-22]**.

II.5 Results and discussion

II.5.1 Study of adsorption of the dye (MB)

II.5.1.1 Effect of adsorbent dosing:

With increasing the adsorbent mass, the number of adsorption sites increases, which consequently increases the adsorption of more dye molecules. By checking the Figure II.2, it was seen a decrease in the values of q_e ($mg.g^{-1}$) with increasing the mass of PANI and PANI/SiO_2 composite from 0.05 to 1 g. The marginal improvement in the adsorption of the dye can be explained by the reason that a fixed volume of dye solution with a known C_o of dye has a defined number of total dye molecules and in this condition, the dose of adsorbent becomes very important. Therefore, many adsorbent adsorption sites remain empty, resulting in a decrease in q_e **[23]**. Consequently, selecting the appropriate dose becomes a very important factor for an effective, efficient treatment process. In this case, the 0.133 g adsorbent mass was selected for all adsorption studies.

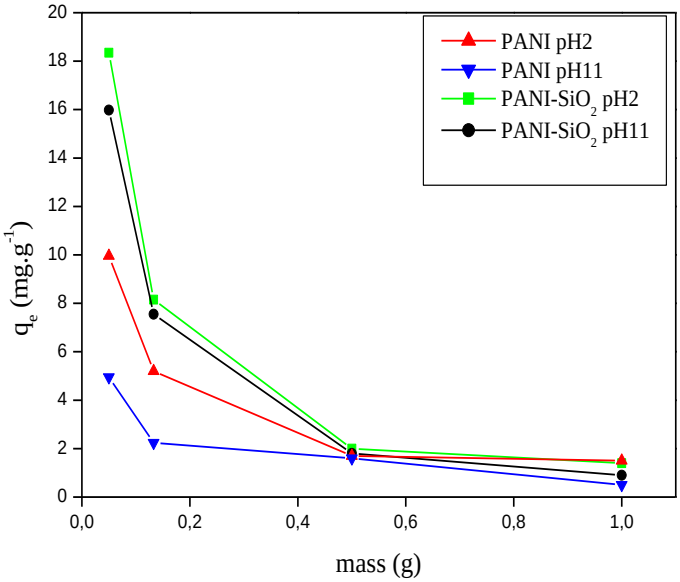

Figure II.2: Effect of the mass of PANI and PANI-SiO_2 composite on the removal of MB in acidic and alkaline mediums (T=25°C, C_o= 3.10^{-5} mol/l)

Of the two adsorbents used in the study, the PANI/SiO_2 composite exhibits greater elimination at all levels of the adsorbent dosing than pure PANI because the specific surface area of PANI/SiO_2 (43.7 $m^2.g^{-1}$) is higher than that of pure PANI (30.3 $m^2.g^{-1}$).

II.5.1.2 Effect of the dye initial concentration:

It was seen from the figure II.3 that the dye adsorption increases almost linearly with the increase in C_o of the dye (from 4 to 21 $mg.L^{-1}$) in both cases of PANI and PANI/SiO_2 composite. At higher concentrations, a large number of dye molecules completely occupy the binding sites of adsorbent materials that were not possible at low dye concentration. Therefore, the C_o equal to 3. 10^{-5} $mol.L^{-1}$ was chosen as the ideal adsorbate concentration for further studies.

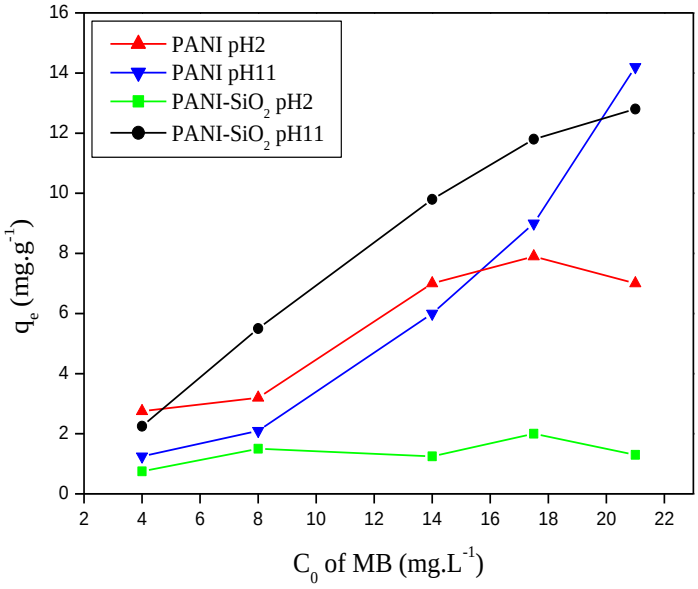

Figure II.3: Effect of the initial concentration of MB on the removal of MB by PANI and PANI/SiO_2 composite in acidic and alkaline mediums (T=25°C, m=0.133 g)

II.5.1.3 The influence of the contact time

The contact time effect on the quantity of adsorbed methylene blue dye is shown in Figure II.4 (a, b). First, it was seen that the MB concentration after adsorption decreases continuously when the contact time increases with the two adsorbents PANI and PANI/SiO_2 composite.

Also, the dye removal rate is faster in the first 25 minutes, which is due to the large number of free sites for adsorption of MB; therefore, it reaches equilibrium in the 60^{th} minutes and subsequently remains constant. The quantity of MB adsorbed q_t increases from 3.53 $mg.g^{-1}$ in the acidic medium to 5.2 $mg.g^{-1}$ in the alkaline medium when the PANI homopolymer is used. With the PANI/SiO_2 composite, the amount of adsorbed dye q_t increases from 2.23 $mg.g^{-1}$ in acidic medium to 6.97 $mg.g^{-1}$ in alkaline medium.

By comparing the effect of the medium (acidic or alkaline), the PANI homopolymer and the PANI/SiO_2 composite exhibit high adsorption efficiencies in the alkaline medium compared to those in the acidic medium, this can be explained for PANI/SiO_2 by the fact that the particles are more and more negatively charged as the pH becomes more and more basic. This is due to the deprotonation of surface silanols (Si-OH) by OH^- hydroxyls in solution to form silanolates (SiO^-). For the PANI, the ES form transforms into the EB form at higher pH. The negative charged surface revealed and the negative charge density increased with the increasing pH value. Therefore, the adsorption capacity increased with the increasing pH value.

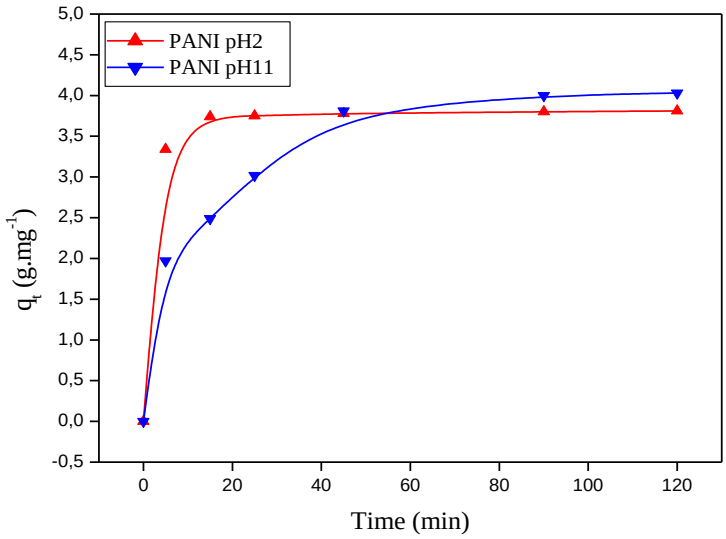

a)

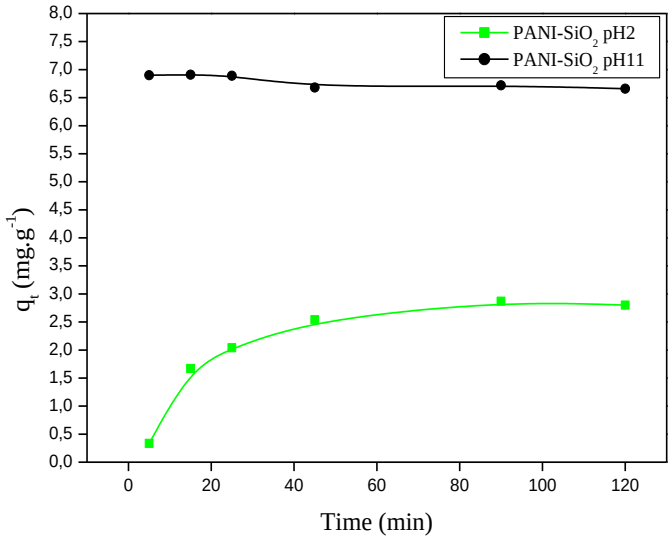

b)

Figure II.4: Effect of contact time on the removal of MB by (a) PANI and (b) PANI/SiO_2 composite in acidic and alkaline mediums (T=25°C, C_o= 3.10^{-5} mol.L^{-1}, m=0.133 g)

II.5.2 Adsorption kinetics

Two kinetic models have been studied in this part, those of pseudo first and second order. The kinetic curves are shown in Figures II.5 and II.6.

The Lagergren's first order pseudo kinetic model (linear form) is expressed by:

$$\ln (q_e - q_t) = \ln q_e - K_1 t \qquad (II.2)$$

where K_1 is the adsorption rate constant (min^{-1}), q_e and q_t are the adsorbed amount of dye in equilibrium and at time t (in mg.g^{-1}), respectively **[18, 24]**. K_1, q_e and R^2 (correlation coefficient) were obtained graphically and are illustrated in table 1.

As evident in Table II.1, R^2 values varies from 0.92 to 0.98 for PANI and from 0.80 to 0.85 for PANI/SiO_2 in acid and basic medium respectively. As you can see, the (cal. q_e) estimated by the velocity equation is significantly different from the experimental value of q_e (exp. q_e). Also, R^2 value was not very nearby to 1. Therefore, the pseudo first-order model does not fit our experimental data.

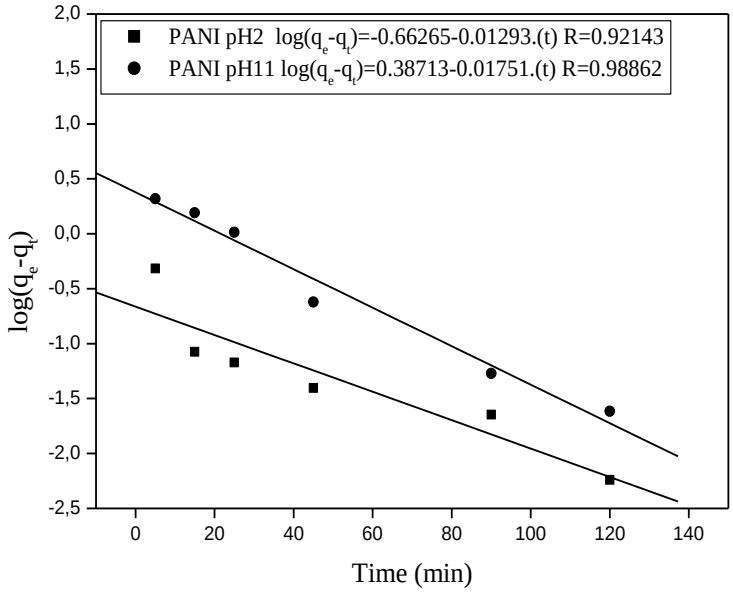

a)

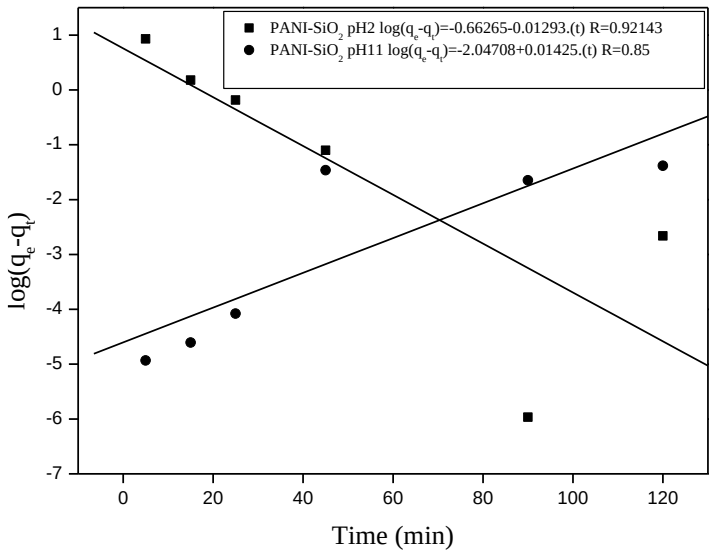

b)

Figure II.5: (a) (b) Pseudo first-order model of PANI and PANI/SiO_2 kinetic plot for adsorption of MB in acidic and basic mediums.

In addition, the second order pseudo kinetic model (linear form) is expressed by:

$$t/q_t = (1 / K_2 q_e^2) + (t / q_e) \qquad \text{(II.3)}$$

where K_2 is the adsorption rate constant for the pseudo-second order (in g. mg^{-1}. min^{-1}), q_t and q_e were described before. K_2, q_e and R^2 were obtained graphically **[25]** and are illustrated also in Table II.1. The correlation coefficients (R^2) of the graphs for various adsorbents vary from 0.99 to 1.00 for PANI in acidic and basic medium and from 0.965 to 0.999 for PANI/SiO_2 in acidic and basic medium, which suggests that adsorption of MB on PANI homopolymer and PANI/SiO_2 composite follows the pseudo-second order model. In addition, (q_e, exp) are very close to the (q_e, cal).

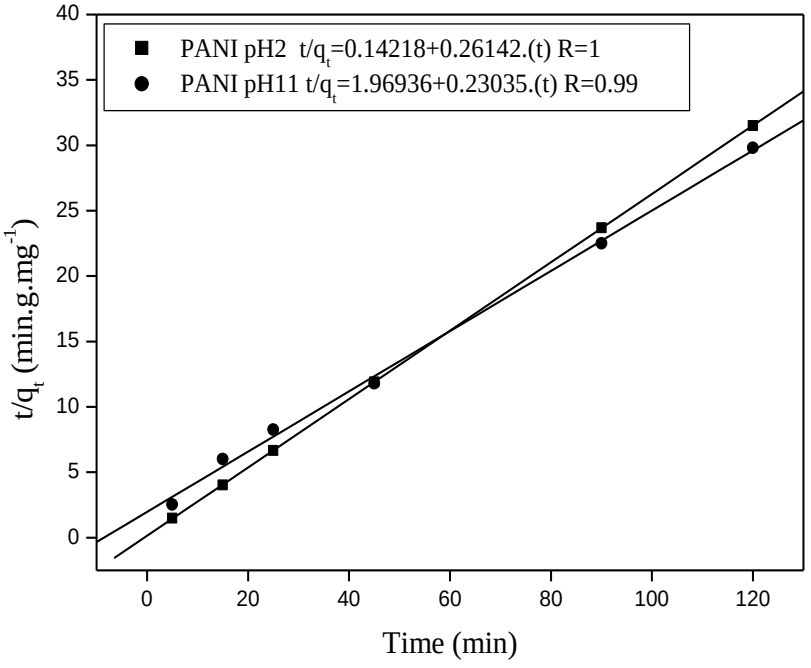

a)

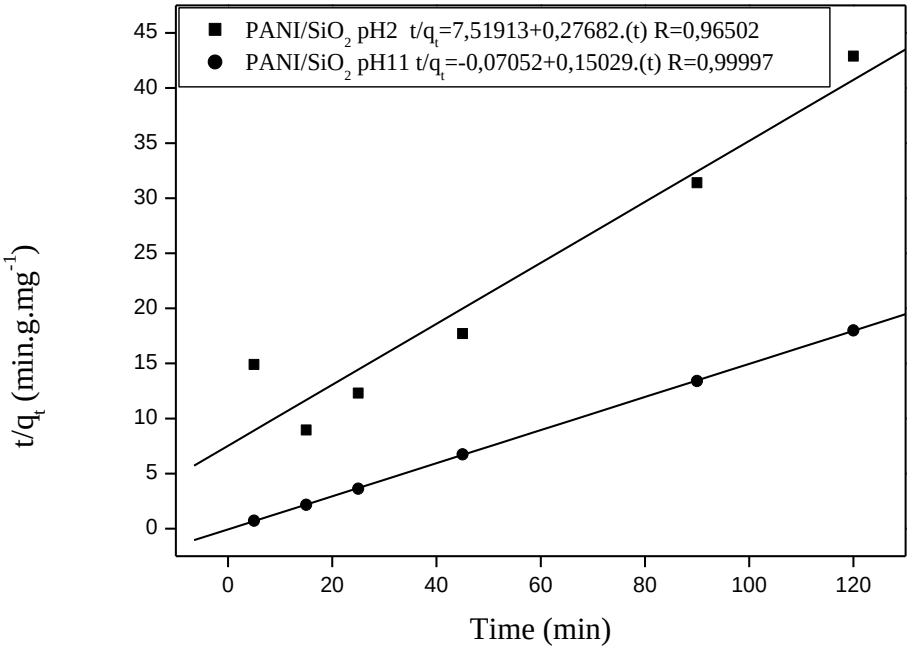

b)

Figure II.6: (a) (b) Pseudo second-order model of PANI and PANI/SiO_2 kinetic plot for adsorption of MB in acidic and basic mediums

II.5.3 The intraparticle diffusion

The intraparticle diffusion model was used to analyze kinetic data of the MB adsorption process, this kinetic model is given by the following equation:

$$q_t = K_{id} (t)^{0.5} + C \qquad (II.4)$$

where, K_{id} and C are the intraparticle diffusion rate constant and a constant related to the thickness of the boundary layer, these constants are obtained graphically **[21, 26, 27]**. If the plot is a line, the adsorption of MB is controlled by diffusion resistance. Intraparticle diffusion plots for the adsorption of MB on pure PANI and PANI/SiO_2 composite are illustrated in Figure II.7.

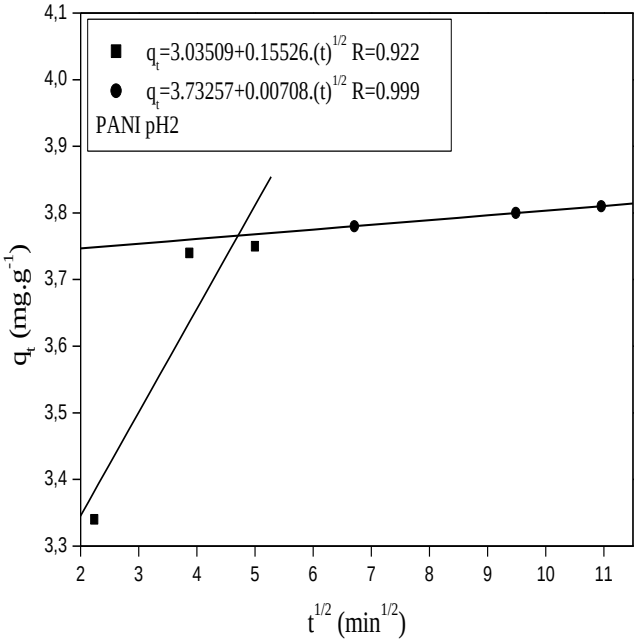
q_t=3.03509+0.15526.(t)^1/2 R=0.922
q_t=3.73257+0.00708.(t)^1/2 R=0.999
PANI pH2
q_t (mg.g^-1)
t^1/2 (min^1/2)

a)

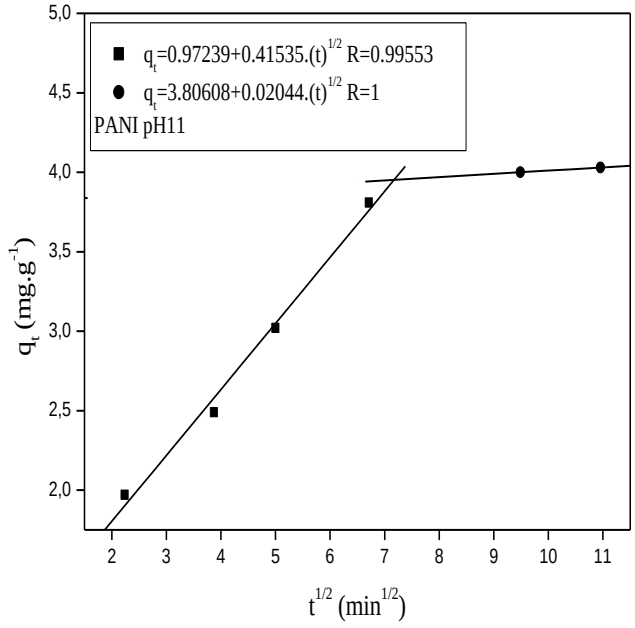
q_t=0.97239+0.41535.(t)^1/2 R=0.99553
q_t=3.80608+0.02044.(t)^1/2 R=1
PANI pH11
q_t (mg.g^-1)
t^1/2 (min^1/2)

b)

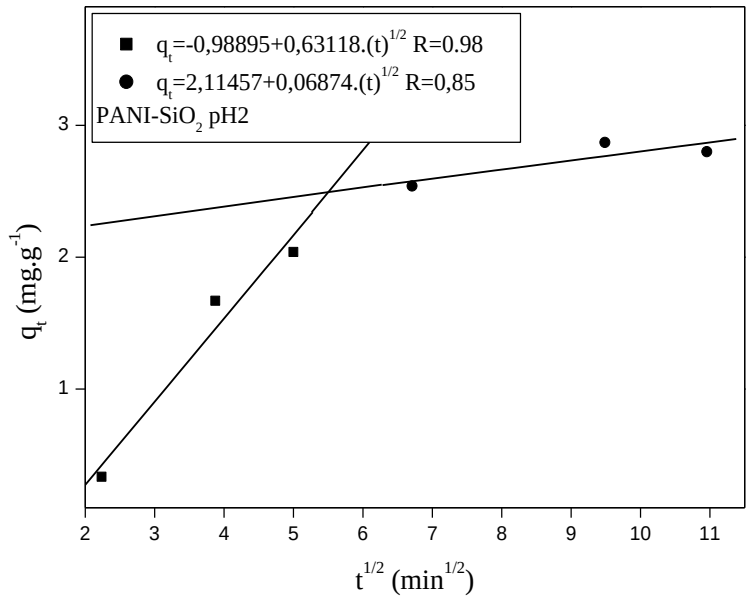

c)

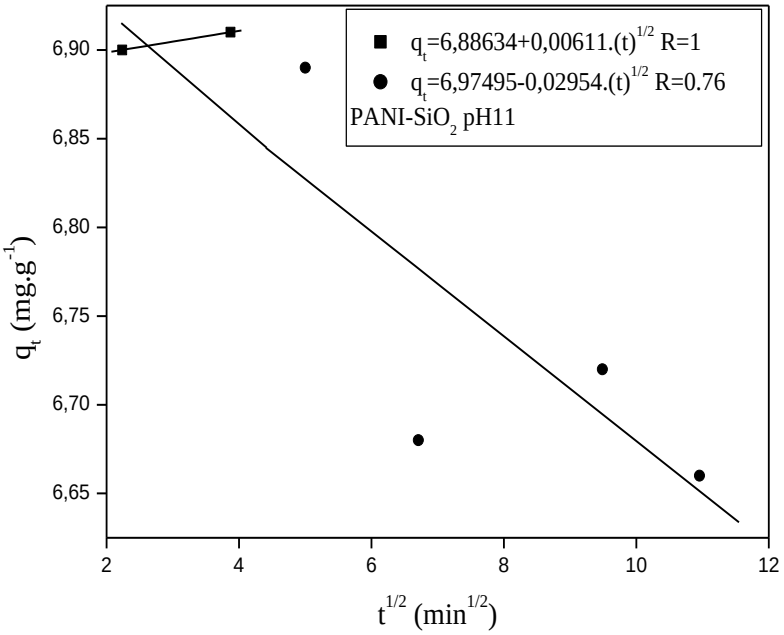

d)

Figure II.7: Intraparticle diffusion plots for MB adsorption onto (a) (b) PANI and (c) (d) PANi/SiO_2 in acidic and basic mediums

The Figure II.7 show two stages with different slopes for the polyaniline/SiO_2 composite and for pure polyaniline. The intraparticle diffusion constants (K_{id} and C) for all steps are given in

Table II.1. As evident from the PANI plot, the MB molecules are scattered in adsorbent particles and then spread in their macropores at the beginning of the adsorption process. Subsequently, MB molecules are propagated in polymeric micropores then the equilibrium take place. However, the PANI/SiO_2 plot also involves two steps. This can be explained by the presence of silica nanoparticles and, consequently, to the raise in surface area of the composite. As well illustrated in the first three figures, the intraparticle diffusion stage is a gradual process. High C values show that the transfer of additional mass of MB molecules on PANI is significant and take place in the beginning of the adsorption process.

Table II.1: Kinetic parameters of adsorption of MB on PANI and PANI/SiO_2 in acidic and alkaline mediums

Model	**Parameters**	**PANI**		**PANI/SiO_2**	
		pH=2	**pH=11**	**pH=2**	**pH=11**
Pseudo-first order	K_1 (min^{-1})	0.03	0.04	0.04	-0.03
	q_e (mg/g)	0.22	2.43	2.13	0.009
	R^2	0.921	0.988	0.80	0.85
Pseudo-second order	K_2 (min^{-1})	0.48	0.027	0.01	-0.32
	q_e (mg/g)	3.83	4.34	3.61	6.66
	R^2	1.000	0.990	0.965	0.999
Intraparticle diffusion	K_{id1}	0.15	0.41	0.63	0.006
	C_1	3.03	0.97	-0.98	6.88
	R^2	0.922	0.99	0.98	1.00
	K_{id2}	0.007	0.02	0.068	-0.029
	C_2	3.73	3.80	2.11	6.97
	R^2	0.999	1.00	0.85	0.76

II.5.4 Adsorption isotherms

Adsorption isothermal studies are required to apply the adsorption technique for practical purposes. The adsorption mechanism could be determined by evaluating the equilibrium data also known as adsorption data obtained from the experiments. An equilibrium relationship could be established between the amounts of dye adsorbed on the surface of an adsorbent through the adsorption isotherms. In this study, several isothermal models (Langmuir, Freundlich and Dubinin-Radushkevich) were used to examine the adsorption data.

1) Langmuir isotherm

The basic assumption of this isotherm is that monolayer formation occurs so that only one dye molecule could be absorbed at an adsorption site and that intermolecular forces decrease with distance. It is also assumed that the surface of the adsorbent has a homogeneous character and has identical and energy equivalent adsorption sites. The Langmuir model is given by the equation below;

$$\frac{C_e}{q_e} = \frac{C_e}{q_m} + \frac{1}{K_L q_m} \qquad \text{(II.5)}$$

Where q_m is the maximum adsorption amount with full monolayer coverage on the surface of the adsorbent ($mg.g^{-1}$) and K_L is the Langmuir adsorption constant for adsorption energy ($L.g^{-1}$) **[28]**.

The values of q_m and K_L can be determined from the slopes and the interception of the linear curve of C_e/q_e in function of C_e (Figure II.8) and are represented in Table II.2 together with R^2 (correlation coefficient).

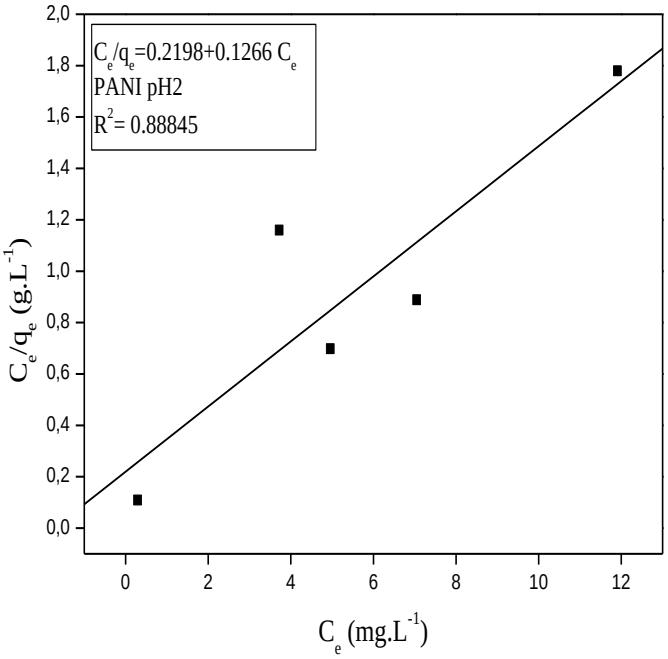
Ce/qe =0.2198+0.1266 Ce
PANI pH2
R2= 0.88845
Ce /qe (g.L-1)
Ce (mg.L-1)

a)

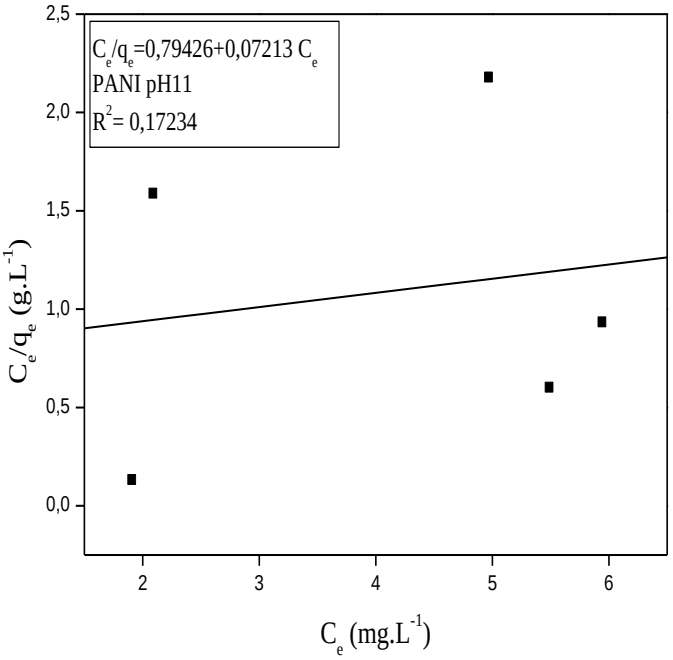
Ce/qe =0,79426+0,07213 Ce
PANI pH11
R2= 0,17234
Ce /qe (g.L-1)
Ce (mg.L-1)

b)

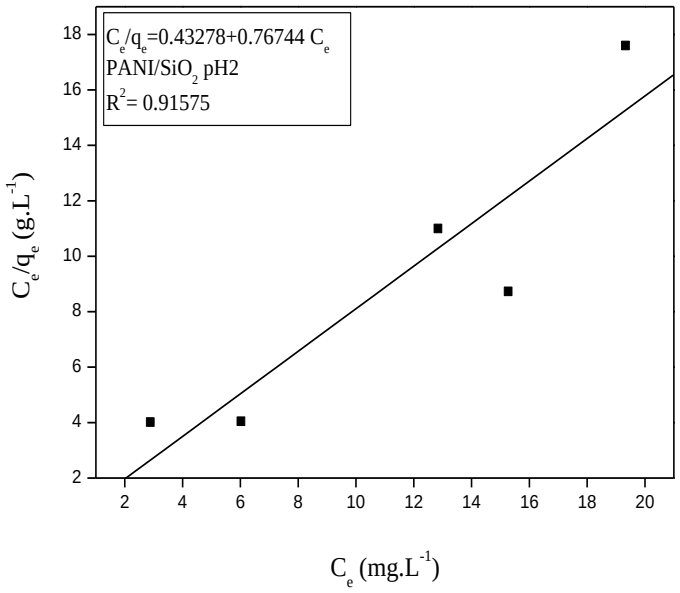

c)

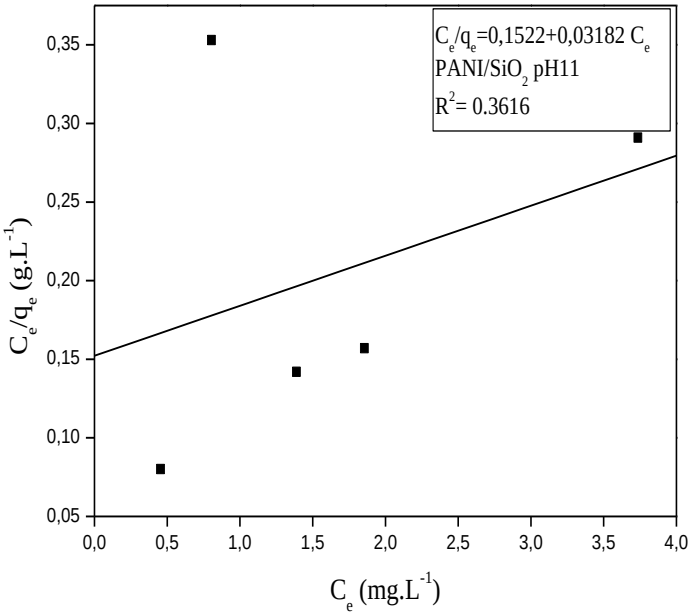

d)

Figure II.8: Langmuir isotherm plot for MB adsorption by (a) (b) PANI and (c) (d) PANI/SiO_2 composite in acidic and basic mediums

The isotherm is linear for all concentrations range and shows a reasonable adaptation to the adsorption data.

The preference and viability of the adsorption process can be determined by the separation factor R_L in the data analysis using the Langmuir isotherm. It is given by the equation below:

$$R_L = \frac{1}{1+ K_L C_0} \qquad \text{(II.6)}$$

If: $0<R_L<1$ adsorption is favorable, but if $1 < R_L$ adsorption is unfavorable. If $R_L=0$: adsorption is irreversible and if $R_L=1$: adsorption is reversible **[29]**. In this case study, in all the cases: $0<R_L<1$ indicating that MB adsorption on PANI and PANI/SiO_2 composite is favorable.

2) Freundlich isotherm

Freundlich's model is applicable to heterogeneous systems and involves the formation of multilayers. This adsorption isotherm is given by:

$$\log q_e = \log k_f + \frac{1}{n} \log C_e \qquad \text{(II.7)}$$

where k_f and n are the Freundlich constants and represent, respectively, the adsorption capacity and the measure of heterogeneity **[30]**. The values of k_f and n were determined from the linear diagram of ln q_e in function of ln C_e (Figure II.9) and the values are represented in Table II 2.

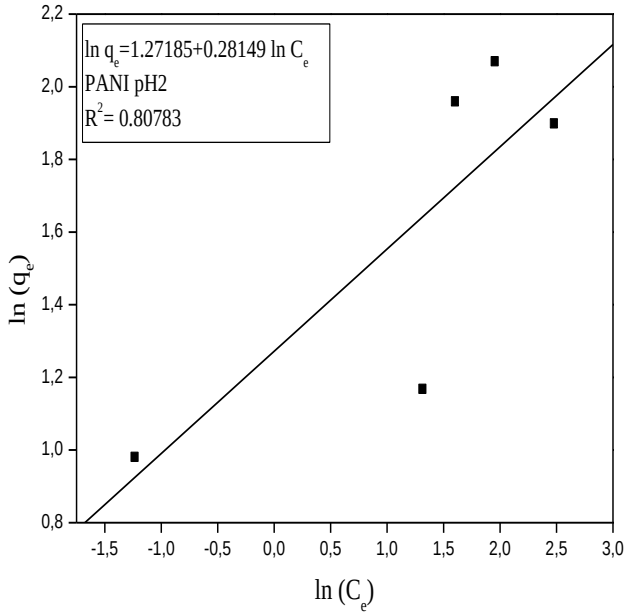
ln q_e =1.27185+0.28149 ln C_e
PANI pH2
R^2= 0.80783
ln (q_e)
ln (C_e)
2,2
2,0
1,8
1,6
1,4
1,2
1,0
0,8
-1,5
-1,0
-0,5
0,0
0,5
1,0
1,5
2,0
2,5
3,0

a)

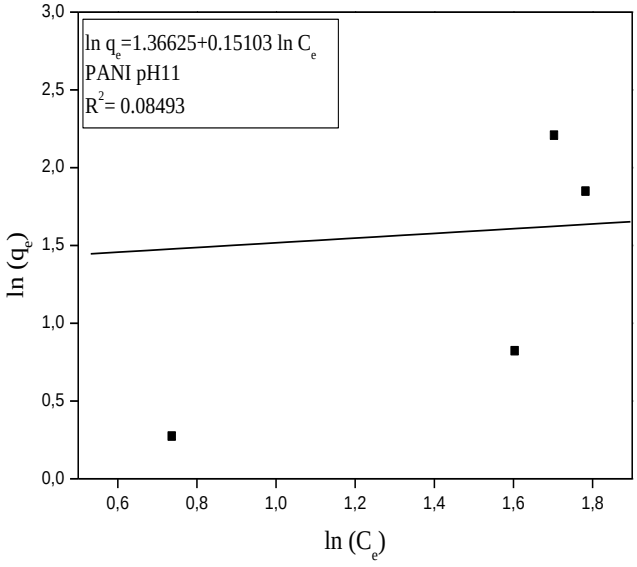
ln q_e =1.36625+0.15103 ln C_e
PANI pH11
R^2= 0.08493
ln (q_e)
ln (C_e)
3,0
2,5
2,0
1,5
1,0
0,5
0,0
0,6
0,8
1,0
1,2
1,4
1,6
1,8

b)

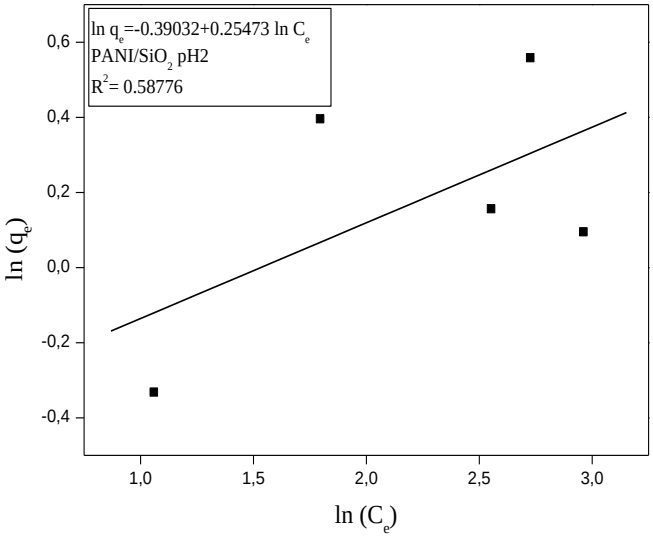

c)

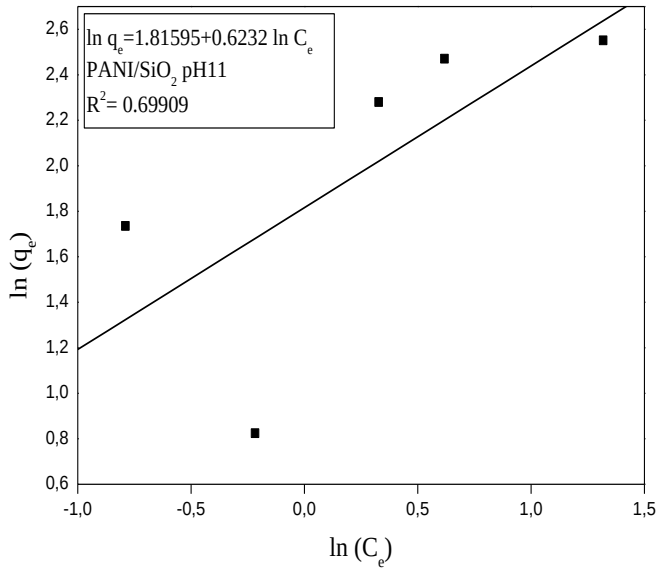

d)

Figure II.9: Freundlich isotherm plot for MB adsorption by (a) (b) PANI and (c) (d) PANI/SiO_2 composite in acidic and basic mediums

The linear plot of ln q_e vs. ln C_e shows Freundlich adsorption. In adsorption, if k_f value increases, the quantity of dye adsorbed onto the surface of PANI and PANI/SiO_2 will increase (Figure II.9 and Table II.2). The results in table 2 demonstrate that Freundlich isotherm have low agreement with the experimental data (low R^2 values). However, k_f values increase and the quantity of dye adsorbed onto the surface of PANI and PANI/SiO_2 increase (best values at pH 11).

In this study, n > 1 in all cases, which indicate the favorability of the adsorption process **[31]**. The data evaluation of the linearly calculated model above sometimes does not provide satisfactory results since linear equations can provide multilinear graphs.

3) Dubinin - Kaganer - Radushkevich (DKR) isotherm

In adsorption studies, the different isotherms studied before are generally used to describe single layer adsorption and cannot determine the mechanisms and energy of adsorption. It is the Dubinin - Kaganer - Radushkevich (DKR) isotherm that can provide the adsorption mechanism and the energy of the adsorption process, which is expressed linearly:

$$\ln q_e = \ln q_m - B\varepsilon^2 \qquad \text{(II.8)}$$

where q_m is the theoretical monolayer saturation capacity ($mg.g^{-1}$), B is the constant, called D-R model constant, and ε^2 is the Polanyi potential **[32]**, which is determined by the equation:

$$\varepsilon = RT \log (1+1/C_e) \qquad \text{(II.9)}$$

where R is the general gas constant and T is the absolute temperature **[33]**.

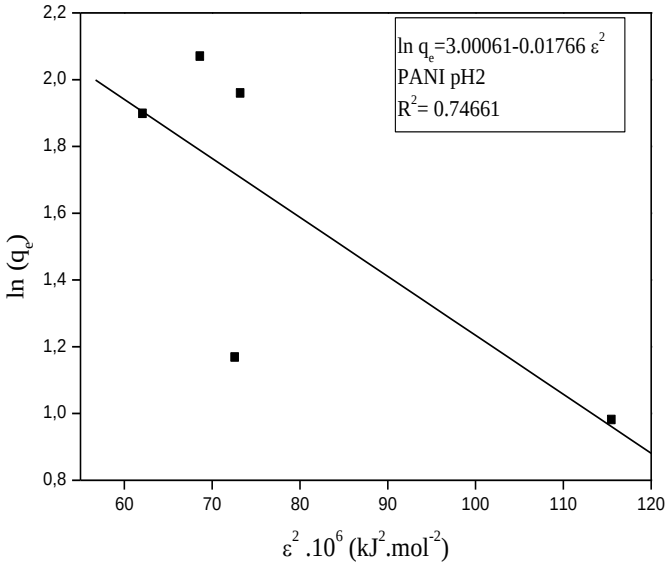
ln q_e=3.00061-0.01766 ε^2
PANI pH2
R^2= 0.74661
ln (q_e)
ε^2 .10^6 ($kJ^2.mol^{-2}$)

a)

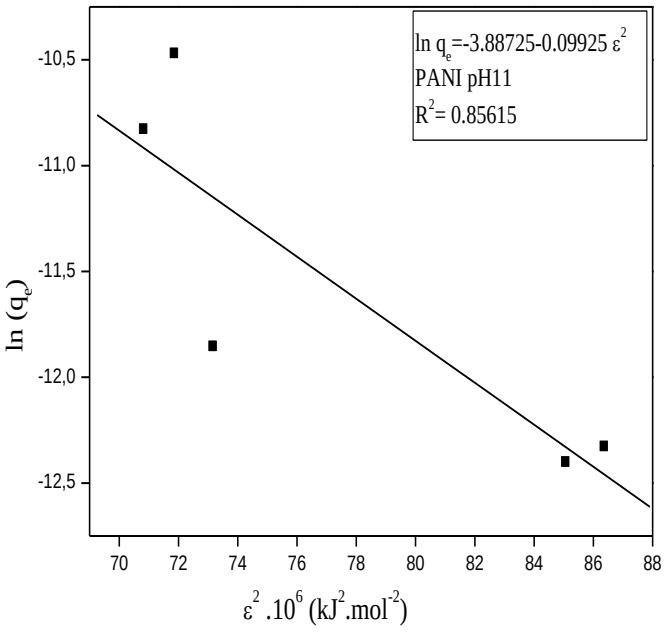
ln q_e=-3.88725-0.09925 ε^2
PANI pH11
R^2= 0.85615
ln (q_e)
ε^2 .10^6 ($kJ^2.mol^{-2}$)

b)

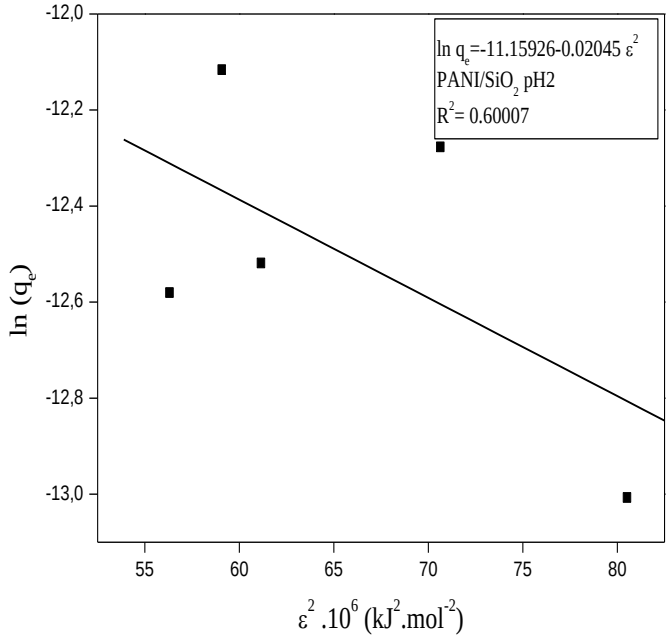

c)

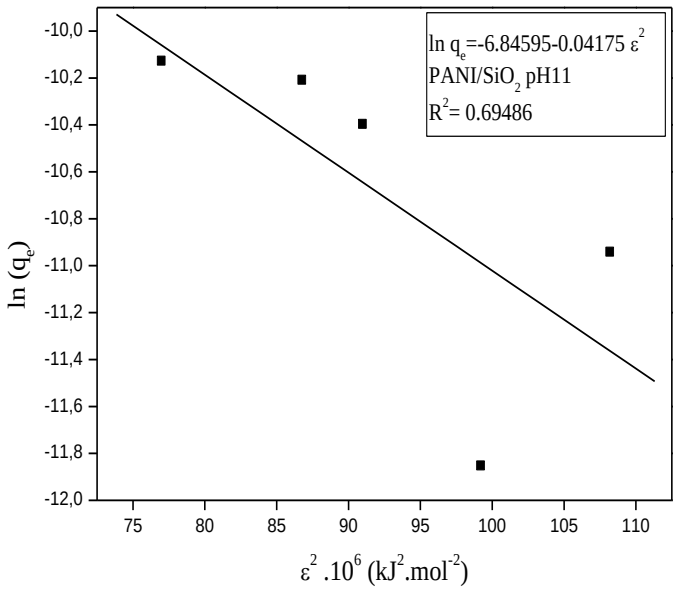

d)

Figure II.10: Dubinin-Kaganer-Radushkevich isotherm plot for MB adsorption by **(a) (b)** PANI and **(c) (d)** PANI/SiO_2 composite in acidic and basic mediums.

Low R^2 values demonstrate that DKR isotherm have low agreement with the experimental data. The calculated adsorption energy values ranging from 2.24 to 5.32 < 8 $kJ.mol^{-1}$, indicates that the adsorption of MB onto PANI and PANI/SiO_2 surfaces are physical in nature **[32, 33]**.

A comparison of the efficacy of the synthesized materials on the adsorption process is provided in Table II.2.

Table II.2: Adsorption isotherms parameters of MB on PANI and PANI/SiO_2 composite at pH 2 and 11

Isotherm		PANI (pH2)	PANI (pH11)	PANI/SiO_2 (pH2)	PANI/SiO_2 (pH11)
Langmuir	K_L (L g^{-1})	0.57597	0.09081	1.77328	0.20906
	q_m (mg g^{-1})	7.89889	13.86385	1.30303	31.42677
	R_L	$0 < R_L < 1$	$0 < R_L < 1$	$0 < R_L < 1$	$0 < R_L < 1$
	R^2	0.88845	0.17234	0.91575	0.3616
Freundlic	k_f (L g^{-1})	3.56744	3.92062	0.67684	6.14691
	n_f	3.55252	6.6212	3.92572	1.60462
	R^2	0.80783	0.08493	0.58776	0.69909
Dubinin-K-R	q_m (mg g^{-1})	20.09799	0.0205	$1.424 .10^{-5}$	0.00106
	B	-0.01766	-0.09925	-0.02045	-0.04175
	R^2	0.74661	0.85615	0.60007	0.69486
	E_{ads} (kJ/mol)	5.32	2.24	4.94	3.46

The validity of the models was verified by the good correlation with the exprimental data assessed by correlation coefficients R^2 values. The equilibrium adsorption isotherms data of the two adsorbents (Table II.2) demonstrate that Freundlich and Dubinin–Radushkevich isotherms have low agreement with the experimental data, whereas Langmuir model has produced the best agreement but not in all cases (In case of PANI and PANI/SiO_2 at pH 2).

II.5.5 Thermodynamic study

Thermodynamic parameters, such as E_a (activation energy), ΔG (Gibb free energy change), ΔH (enthalpy change) and ΔS (entropy change) are useful to explain the nature of adsorption. The E_a is calculated from the Arrhenius equation, shown below:

$$k = A.\ exp^{(-Ea/RT)} \qquad \text{(II.10)}$$

where T is the absolute temperature, A is the Arrhenius constant and k is the frequency constant **[26]**. The ΔG is calculated by the following equation **[19]**:

$$\Delta G = -\ RT \ln \frac{q_e}{C_e} \qquad \text{(II.11)}$$

The ΔH and ΔS are calculated from the Van't Hoff equation by plotting ln q_e/Ce vs. 1/T, as indicated below.

$$\ln \frac{q_e}{C_e} = \ln k = \frac{\Delta S^0}{R} - \frac{\Delta H^0}{RT} \qquad \text{(II.12)}$$

where T is the temperature. Values of ΔH^0 and ΔS^0 (Table II.3) were calculated from the slope and intercept of Van't Hoff plots of ln K versus 1/T **[34]**. (Figure II.11).

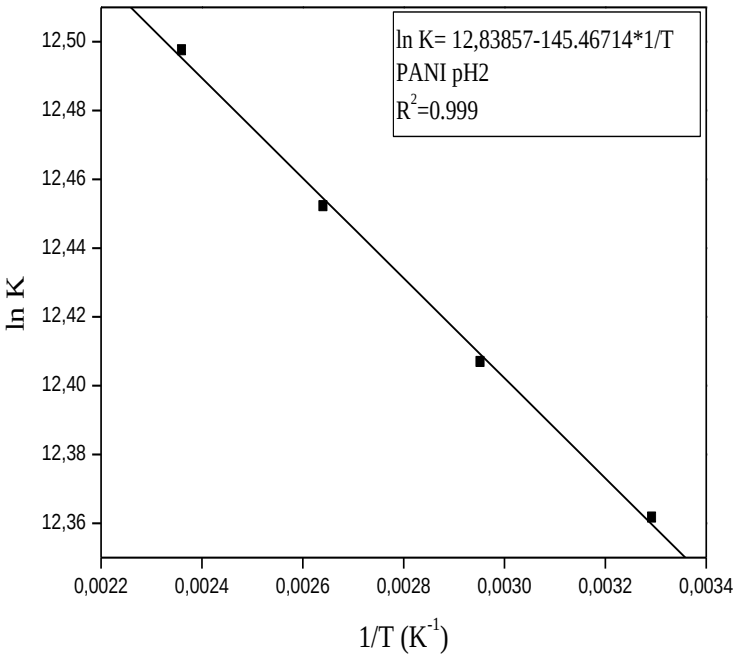
ln K= 12,83857-145.46714*1/T
PANI pH2
R2=0.999
12,50
12,48
12,46
12,44
12,42
12,40
12,38
12,36
ln K
0,0022
0,0024
0,0026
0,0028
0,0030
0,0032
0,0034
1/T (K-1)

a)

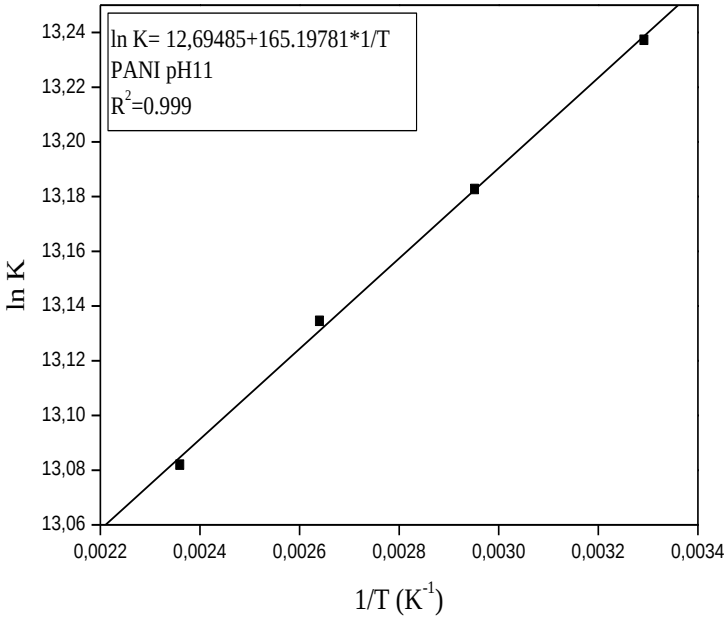
ln K= 12,69485+165.19781*1/T
PANI pH11
R2=0.999
13,24
13,22
13,20
13,18
13,16
13,14
13,12
13,10
13,08
13,06
ln K
0,0022
0,0024
0,0026
0,0028
0,0030
0,0032
0,0034
1/T (K-1)

b)

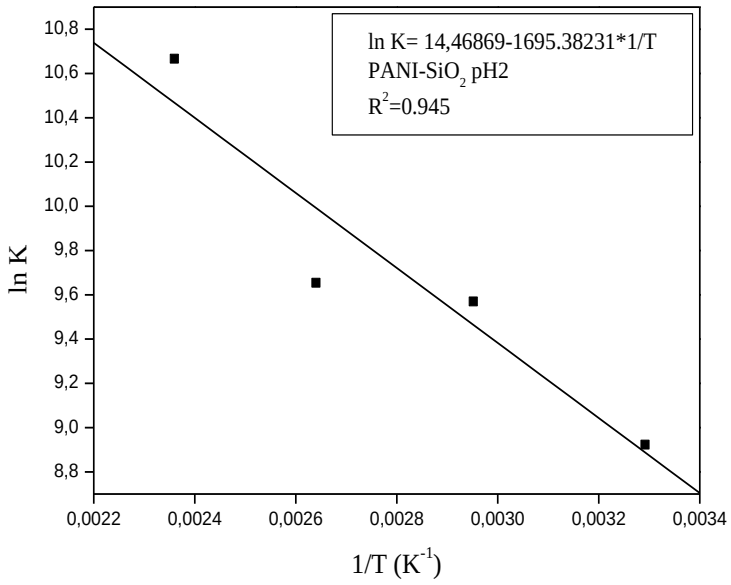

c)

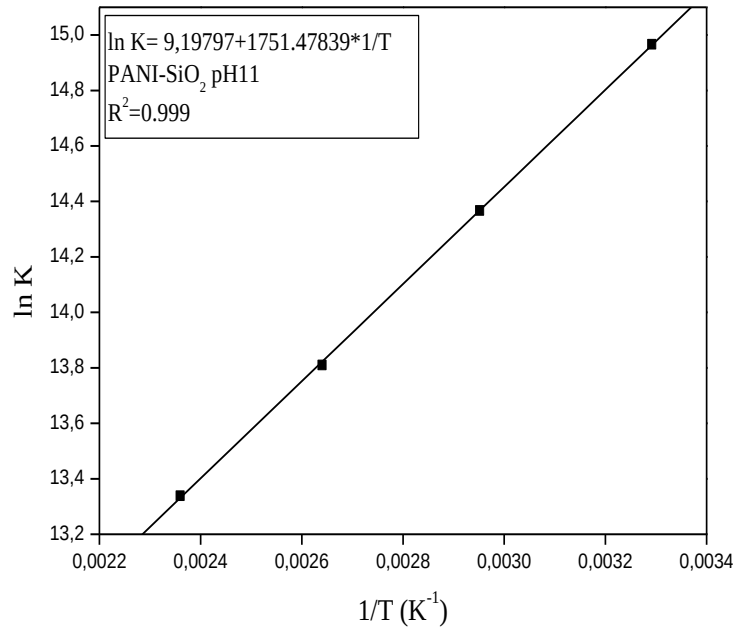

d)

Figure II.11: Determination of standard enthalpy change for the adsorption of MB by (a) (b) PANI and (c) (d) PANI/SiO_2 composite in acidic and basic mediums

Figure II.11 shows the Van't Hoff diagram, obtained by plotting ln k vs. 1/T after adsorption of MB. The enthalpy change value is useful to explain the adsorption phenomenon. Rehman et al **[35]**. described the criteria for physisorption and chemisorption between adsorbate and

adsorbent in relation with enthalpy change (ΔH°): 4–10 kJ.mol^{-1} (physical adsorption), 2–40 kJ.mol^{-1} (Hydrogen bonding forces) and > 40 kJ.mol^{-1} (chemical adsorption) **[36]**. The enthalpy variation values in the present work, as illustrated in Table II.3, are -1.21 and +1.37 kJ.mol^{-1} for the adsorption of MB on PANI (at pH 2 and 11), -14.1 and +14,56 kJ.mol^{-1} for the PANI/SiO_2 composite, these values with their negative sign confirm the physical and exothermic process at acidic pH, and endothermic process at alkaline pH, respectively. The ΔG° values are also useful to explain the adsorption phenomenon. When ΔG° is between -20 - 0 kJ.mol^{-1} show physisorption and -400 to -80 kJ.mol^{-1} show chemisorption **[37, 38]**. In this part, ΔG° values decreases with increasing temperatures in the ranges 30-45°C. For Methylene Blue adsorption on the pure PANI and PANI/SiO_2 composite, the values of ΔG° varies from - 31.22 to - 46.10 kJ.mol^{-1} and - 22.54 to - 47 kJ.mol^{-1}, respectively. This result confirms that MB adsorption onto PANI and its derivatives is spontaneous and physical in nature.

Table II.3: Thermodynamic parameters of MB adsorption onto PANI and PANI/SiO_2 composite

	T (°C)	**Δ*H*° (kJ mol^{-1})**	**Δ*S*° (kJ mol^{-1} K^{-1})**	**Δ*G*° (kJ mol^{-1})**
	30	-1.21	0.106	-31.22 < 0
PANI	35			-34.95 < 0
pH 2	40			-39.22 < 0
	45			-44.03 < 0
	30	1.37	0.105	-33.43 < 0
PANI	35			-37.13 < 0
pH11	40			-41.36 < 0
	45			-46.10 < 0
	30	-14.1	0.12	-22.54 < 0
PANI-SiO_2	35			-26.95 < 0
pH 2	40			-30.40 < 0
	45			-37.58 < 0
	30	14.56	0.076	-37.80 < 0
PANI-SiO_2	35			-40.47 < 0
pH 11	40			-43.50 < 0
	45			-47.00 < 0

The ΔG^0 values are more negative indicating that adsorption is more spontaneous. The positive value of ΔS^0 reveals the increased randomness at the dye and doped PANI and PANI/SiO_2 interfaces during the adsorption process.

References

[1] Wallace GG, Spinks GM, Kane-Maguire LAP, et al. Conductive electroactive polymers: intelligent polymer systems. London: Taylor & Francis Group, 2009, 47-64.

[2] Walton DJ, Davis FJ and Langley PJ. The synthesis of conducting polymers based on heterocyclic compounds. In: Davis FJ (ed) Polymer chemistry: a practical approach. New York: Oxford University Press, 2004, 178-180.

[3] Macdiarmid AG. Polyaniline and polypyrrole: where are we headed?. Synth Met 1997, 84: 27-34.

[4] Do Nascimento GM. In: Almeida LCP (ed) Conducting polymers: synthesis, properties and applications. New York: Nova Publishers, 2013, 160-161.

[5] Wang J, Deng B, Chen H, et al. Removal of Aqueous Hg(II) by polyaniline: sorption characteristics and mechanisms. Environ Sci Technol 2009, 43: 5223-5228.

[6] Macdiarmid AG, Chiang JC, Richter AF, et al. Polyaniline: a new concept in conducting polymers. Synth Met 1987, 18: 285-290.

[7] Boevazh A and Sergeyev VG. Polyaniline: synthesis, properties, and application. Polym Sci Ser C 2014, 56: 144-153.

[8] Ayad M, El-Hefnawy G and Zaghlol S. Facile synthesis of polyaniline nanoparticles; its adsorption behavior. Chem Eng J 2013, 217: 460-465.

[9] El-Sharkaway EA, Kamel RM, El-Sherbiny IM, et al. Removal of methylene blue from aqueous solutions using polyaniline/graphene oxide or polyaniline/reduced graphene oxide composites. Environ Technol 2020, 41: 2854-2862.

[10] Trchová M and Stejskal J. Polyaniline: the infrared spectroscopy of conducting polymer nanotubes. Pure Appl Chem 2011, 83: 1803-1817.

[11] Tokarský J, Mamulová-Kutláková K, Neuwirthová L, et al. Texture and electrical conductivity of pellets pressed from PANI and PANI/Montmorillonite intercalate. Acta Geodyn Geomater 2013; 10: 371-377.

[12] Liu P. Preparation and characterization of conducting polyaniline/silica nanosheet composites. Curr Opin Solid State Mater Sci 2008, 12: 9-13.

[13] Zengin H and Erkan B. Synthesis and characterization of polyaniline/silicon dioxide composites and preparation of conductive films. Polym. Adv. Technol. 2010, 21 216-223.

[14] Ayad MM, Abu El-Nasr A and Stejskal J. Kinetics and isotherm studies of methylene blue adsorption onto polyaniline nanotubes base/silica composite. J Ind Eng Chem 2012; 18: 1964-1969.

[15] Gu H, Guo J, Zhang X, et al. Giant magnetoresistive phosphoric acid doped polyaniline-silica nanocomposites. J Phys Chem C 2013; 117: 6426-6436.

[16] Karthik R and Meenakshi S. Removal of hexavalent chromium ions using polyaniline/silica gel composite. J Water Process Eng 2014; 1: 37-45.

[17] Kumar N, Bahl T and Kumar R. Study of the methylene blue adsorption mechanism using ZrO_2/ Polyaniline nanocomposite. Nano Express 2020; 1: 1-10.

[18] Worch E. Adsorption technology in water treatment fundamentals, processes and modeling. Berlin: Walter de Gruyter, 2012, p.100-159.

[19] Humelnicu D, Soroaga LV, Arsene C, et al. Adsorptive performance of soy bran and mustard husk towards arsenic (V) ions from synthetic aqueous solutions. Acta Chim Slov 2019; 66: 326-336.

[20] Dada AO, Adekola FA and Odebunmi EO. Kinetics, mechanism, isotherm and thermodynamic studies of liquid-phase adsorption of Pb^{2+} onto wood activated carbon supported zerovalent iron (WAC-ZVI) nanocomposite. Cogent Chem 2017; 3: 1-20.

[21] Maruthapandi M, Kumar VB, Luong JHT, et al. Kinetics, isotherm, and thermodynamic studies of methylene blue adsorption on polyaniline and polypyrrole macro-nanoparticles synthesized by C-Dot-initiated polymerization. ACS Omega 2018; 3: 7196-7203.

[22] Bouzid S, Khenifi A, Bennabou KA, et al. Removal of orange II by phosphonium-modified Algerian bentonites. Chem Eng Commun 2015; 202: 520-533.

[23] Karaer H and Uzun I. Adsorption of basic dyestuffs from aqueous solution by modified chitosan. Desalin Water Treat 2013; 51: 2294-2305.

[24] Mu B, Tang J, Zhang L, et al. Preparation, characterization and application on dye adsorption of a well-defined two-dimensional superparamagnetic clay/polyaniline/Fe_3O_4 nanocomposite. Appl Clay Sci 2016; 132: 7-16.

[25] Mahanta D, Madras G, Radhakrishnan S, et al. Adsorption of sulfonated dyes by polyaniline emeraldine salt and its kinetics. J Phys Chem B 2008; 112: 10153-10157.

[26] Aljeboree AM, Alshirifi AN and Alkaim AF. Kinetics and equilibrium study for the adsorption of textile dyes on coconut shell activated carbon. Arabian J Chem 2017; 10: S3381-S3393.

[27] Majhi D and Patra BN. Preferential and enhanced adsorption of dyes on alum doped nanopolyaniline. J Chem Eng Data 2018; 63: 3427-3437.

[28] Kim HG, He F and An B. The Application of alginate coated iron hydroxide for the removal of Cu(II) and phosphate. Appl Sci 2019; 9: 1-13.

[29] Kumar R, Ansari SA, Barakat MA, et al. A polyaniline@MoS2-based organic–inorganic nanohybrid for the removal of Congo red: adsorption kinetic, thermodynamic and isotherm studies. New J Chem 2018; 42: 18802-18809.

[30] Majumdar S, Saikia U and Mahanta D. Polyaniline-coated filter papers: cost effective hybrid materials for adsorption of dyes. J Chem Eng Data 2015; 60: 3382-3391.

[31] Dickcha B and Ackmez M. Adsorption of reactive red 158 dye by chemically treated cocos nucifera L. shell powder. New York: Springer, 2011, p.1-3.

[32] Ozudogru Y, Bekci ZM, Buyukates Y, et al. Heavy metals uptake from aqueous solutions using marine algae (Colpomenia sinuosa): kinetics and isotherms. Chem Ecol 2012; 28: 469-480.

[33] Baseri JR, Palanisamy PN and Sivakumar P. Application of polyaniline nanocomposite for the adsorption of acid dye from aqueous solutions. E-J Chem 2012; 9: 1266-1275.

[34] Amer WA, Omran MM, Rehab AF, et al. Acid green crystal-based in situ synthesis of polyaniline hollow nanotubes for the adsorption of anionic and cationic dyes. RSC Adv 2018; 8: 22536-22545.

[35] Rehman MS, Kim I, Rashid N, et al. Adsorption of brilliant green on biochar prepared from lignocellulosic bioethanol plant. Clean: Soil Air Water 2016; 44: 55-62.

[36] Rafiqi FA and Majid K. Sequestration of methylene blue (MB) dyes from aqueous solution using polyaniline and polyaniline–nitroprusside composite. J Mater Sci 2017; 52: 6506-6524.

[37] Patra BN and Majhi D. Reduced graphene oxide-polyaniline hybrid: preparation, characterization and its applications for ammonia gas sensing. J Phys Chem B 2015; 119: 8154-8164.

[38] Li J, Huang Y and Shao D. Conjugated polymer-based composites for water purification. In: Saini P (ed) Fundamentals of conjugated polymer blends, copolymers and composites: synthesis, properties and applications. New Jersey: Scrivener Publishing, 2015, pp589-590.

Chapter three

Theoretical calculation

III. Theoretical calculation (modeling approach)

III.1 Molecular modeling software:

Molecular modeling software generally includes the following modules:

1- Construction, visualization and manipulation of molecules.

2- Calculations.

3- Saving structures and managing files.

4- Study of molecular properties **[1]**.

III.1.1 Construction, visualization and manipulation:

a- The construction of molecules can be done using several methods:

- From pre-existing fragments (Chem 3D): these are associated by substitution, the structure is then developed by successive modifications of the initial skeleton (Type of bond, type of atom, stereochemistry).

- From a structure drawn in two dimensions (Hyperchem): the transformation into a three-dimensional structure is then obtained by global adjustment of the parameters, the random stereochemistry can then be modified.

- From geometric data (coordinates of atoms from an Rx structure) or from current databases (e.g. Cambridge Structural Data Base, Brookhaven Protein Bank)

b- 3D visualization of molecules constitutes an important part of stereochemistry. We can visualize molecules using a laptop thanks to programs allowing the molecule to be moved in 3D and the main parameters to be displayed: interatomic distances, angles between bonds, VDW radii, etc.

c- Manipulating molecules on the screen:

1- Move the entire molecule.

2- Move an atom or a group of atoms.

3- Cut a molecule.

4- Combine several molecules **[2]**.

III.1.2 Calculations

The calculation methods used respond more or less well to these two types of concerns:

- Molecular Mechanics (MM) based on classical mechanics calculations to calculate the steric energy of the system.
- Quantum Mechanics (QM) based on the resolution of a differential equation based solely on the electronic coordinates of the system (Schrödinger equation). The principle of these calculations is to express molecular orbitals as combinations of atomic orbitals. The Huckel method and the Hartree-Fock method (semi-empirical calculations) involve different approximations corresponding to different methods. The density functional method (DFT) calculates the energy of the system from the density and no longer from molecular orbitals. The latter method requires fewer calculations for similar results **[3]**.

III.1.3 Saving structures

Structures are saved in the form of a matrix containing the coordinates of the atoms and a bond table for:

- Their subsequent use in the same software

- The use of these data in other programs **[4]**

III.1.4 Studies of molecular properties:

From Molecular Mechanics calculations: - geometry measurements: valence angles, bond lengths, dihedral angles, etc. - characterization of asymmetric centers - analysis of the different components of steric energy (elongation energy, twisting, etc.)

From Quantum Mechanics calculations:
- Analysis of energy calculation
- Molecular orbitals
- Electrostatic potential
- Spectral characteristics (IR, UV) **[5]**

III.2 Software presentation

For molecular modelling, certain software are used such as:
- ChemSketch: 2D and 3D formula editor, geometric optimization by molecular mechanics using the ChemBasis programming language)
- RasMol: Molecule viewer
- Chime: Same principle as RasMol, with additional options such as lipophilic potential.
- Mopac: Semi-empirical quantum calculations

- Open Babel: Molecular coordinate file converter
- Tinker: Very complete set of programs for molecular mechanics and dynamics
- PovChem: Allows you to create 3D images of molecules using the ray tracing technique using Pov-Ray software **[6]**.

III.3 The choice of methods

For large molecules (>1000 atoms): proteins or polymers, current computing capabilities do not allow quantum chemistry to be carried out on the entire molecule → Molecular Mechanics (MM).
For the smallest molecules we can use quantum chemistry (QM)
• up to 1000 atoms: semi-empirical methods
• up to 100 atoms: DFT or ab-initio methods **[7]**

III.4 Semi-empirical methods

Semi-empirical methods are techniques for solving the Schrödinger equation of systems with several electrons using data adjusted to experimental results in order to simplify calculations. They are simplified methods that include a certain number of empirical parameters and consider only the electrons of the valence shell; the electrons of the inner layers are included in the nuclear core.

There are thus numerous semi-empirical methods which depend on the number of simplifications (neglected types of interactions) and parameter settings: CNDO, NNDO, MNDO, AM1, PM3, SAM1. The AM1 method, developed in 1985, is the most used and often gives very good results for a very short calculation time. PM3 is a variant of the AM1 model, PM3 differs from AM1 only in parameter values. These were established by comparing a large number and variety of experimental values with calculated molecular properties.

In this part of work, we used a semi-empirical method: PM3 **[8-10]**.

III.5 Calculated Properties

The software is capable of predicting many properties of molecules, reactions including:
- Energies and structures of molecules, energies and structures of transition states, bonding or reaction energies.
- Molecular orbitals, atomic charges, dipole moments, ionization potential, electrostatic potential, etc.
- Parameters of NMR spectra.

- Vibration frequencies, IR, UV spectra, etc **[11]**.

III.6 Software used

III.6.1 Chem-Office ultra software:

ChemOffice ultra brings together chem3D ultra, ChemDraw Ultra, chemFinder ultra, etc. Chem 3D ultra is a pro-software (product-software) for molecular modeling and visualization with a new graphical interface. It allows molecular mechanics to be carried out with MM_2 for the optimization of geometry and molecular dynamics, semi-empirical calculations (AM1, PM3, MNDO, etc.) with interfaces to programs: GAMESS, Gaussian and MOPAC.

It optimizes the geometry of transition states and evaluates certain physical properties (dipoles, charges, densities, etc.) **[12]**

III.6.2 Hyperchem software

Hyperchem is molecular modeling software developed by Autodesk, INC, and distributed by Hypercube INC (Ontario, Canada). It is sophisticated molecular modeling software that is known for its quality, flexibility, and ease of use.

Uniting 3D visualization and animation, hyperChem can perform molecular mechanics and molecular dynamics calculations. It also offers the possibility of making semi-empirical calculations (AM1, PM3, CNDO, etc.) **[13]**

III.7 Mulliken analysis

III.7.1 Mulliken atomic charges:

In 1955, Mulliken proposed a first approach for the calculation of partial charges. The approach he proposed at the time stood out for its numerical and conceptual simplicity and remains one of the most used today. The Mulliken charge carried by atom (i) is defined as the difference between the electronic population of the isolated atom (Z_i) and that of the atom within the molecule. The latter is defined as the sum of the electrons located in the atomic orbitals centered on i and half of the electrons located in the molecular orbitals constructed from atomic orbitals centered on (i).

Its mathematical formulation is therefore:

$$q_i = Z_i - [\sum_{\mu \in i} (DS)_{\mu\mu} + \frac{1}{2} \sum_{v \neq \mu} (DS)_{\mu v}] \qquad \text{(III.1)}$$

III.7.2 Molecular Electrostatic Potential (MESP)

Molecular surface electrostatic potential MESP is a graph of the electrostatic potential mapped onto the isoelectronic density surface and which simultaneously displays molecular shape, size and electrostatic potential values. Molecular electrostatic potential (MESP) mapping is very useful in the study of molecular structure in relation to physicochemical properties **[9, 14]**. In this study, the electrostatic surface potentials are presented by different colors (Figure III.9 (a,b)). The red colored parts represent the regions of negative electrostatic potential while the green colored parts represent the regions of positive electrostatic potential. A part of the molecule, which has a negative electrostatic potential is sensitive to electrophilic attacks, the positive is linked to nucleophilic reactivity.

III.7.3 Calculation of Mulliken atomic charges and electrostatic potential distribution

The possible interactions between MB dye and PANI, PANI-SiO_2 sorbent sites were considered through theoretical calculation of electronic charges and electrostatic potential distribution in methylene blue using HyperChem v8 software **[15]**. The geometry optimization of the MB, Mulliken atomic charges and electrostatic potential were assessed by the semi empirical PM_3 method derived from the Hartree-Fock theory **[16]**.

Figures III.1 and III.2 show the calculated Mulliken atomic charges of MB at pH 2 and 11. For MB molecules in acidic medium pH = 2, the totality of the positive charges were centered onto alkyl amine groups in both ends of the benzenic cycles (left and right sides $–N^+H(Me)_2$; $+0.976e^-$), in amine group –NH(+ 0.38 e^-) and sulfur atom S (+ 0.35 e^-) in the central ring, in the benzenic cycles with sulfur and nitrogen atoms (+0.108 e^-). It is interesting to note that, alkyl amine groups $–N^+H(Me)_2$ in both sides are the most positively charged. Also, the charge in –NH amine group is higher than in sulfur atom (Figure III.1). However, in alkaline medium at pH=11, the charges of sulfur atom in the centred ring ($+0.097e^-$) and alkyl amine groups – $N(Me)_2$; $+0.02e^-$) at the ends of MB molecule are highly reduced. The benzenic cycles adjacent to the central ring having sulfur and nitrogen heteroatoms are completely charged negatively (-1.043 e^-) (Figure III.2).

The chemical reactivity of materials is better perceptive by the electric potential surface (EPS). It is useful to detect favorable interaction sites in molecules. Figures III-1 and III-2 illustrate the PM3 calculated 3D mapped isosurface of the electrostatic potential surrounding the MB dye in acidic and basic solution (pH=2 and pH=11). Methylene blue molecule in acidic pH close to 2, shows an electrostatic potential characterized by the red colors indicating negative potential regions (0.370-0.0 esu), followed by green colors, which denote strong

positive potential regions (0.0-1.304). In alkaline medium, MB dye shows negative potential regions (red colors; -0.334-0.0 esu), followed by, strong positive potential regions (green colors; 0.0-0.500). Positively and/or negatively charged molecules tend to interact with the sorbent sites where the electrostatic potential is strongly negative and positive, respectively.

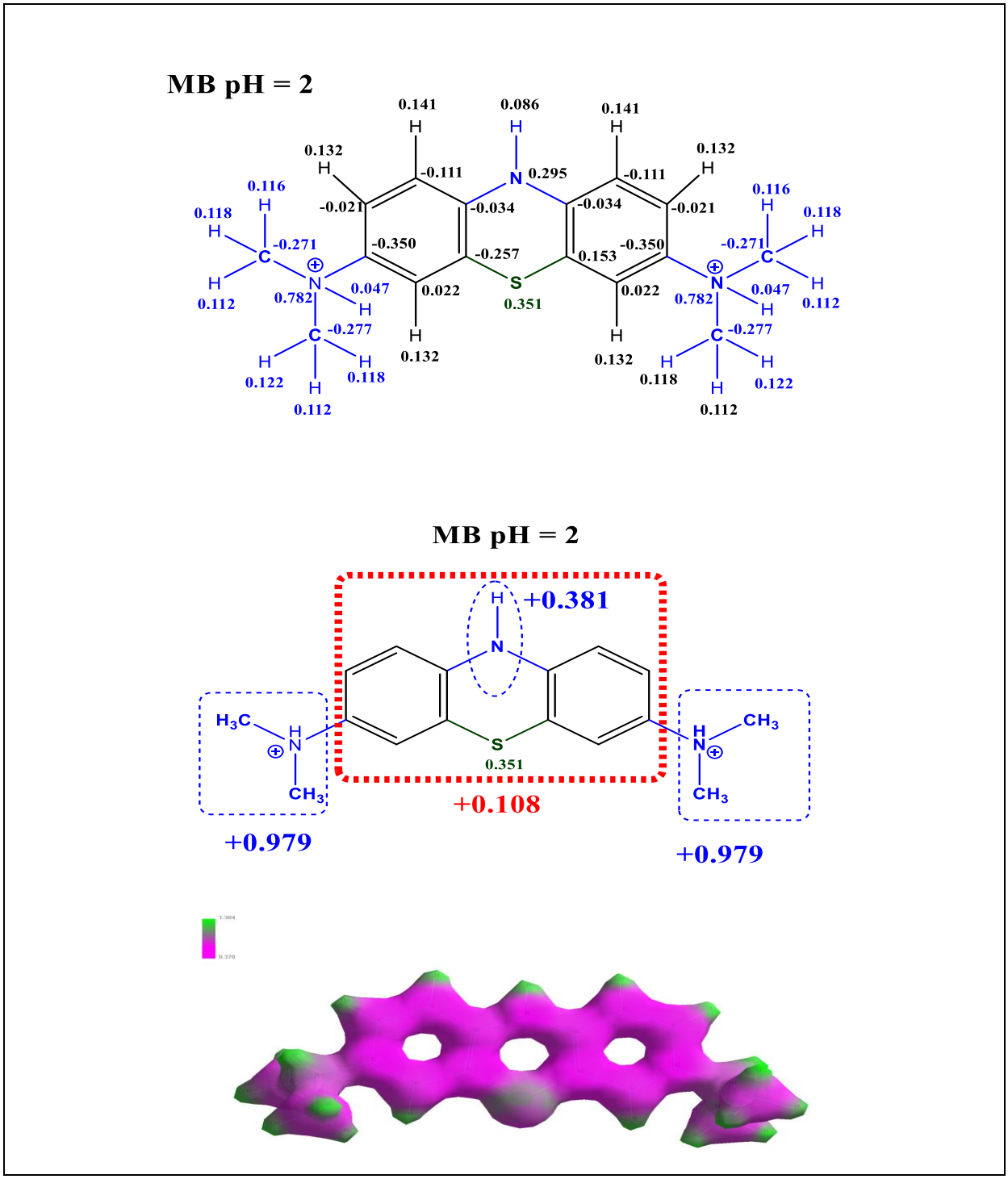

Figure III.1: Semi-empirical PM3 calculated Mulliken atomic charges and (3D) mapped isosurface surrouding the MB molecule at pH = 2

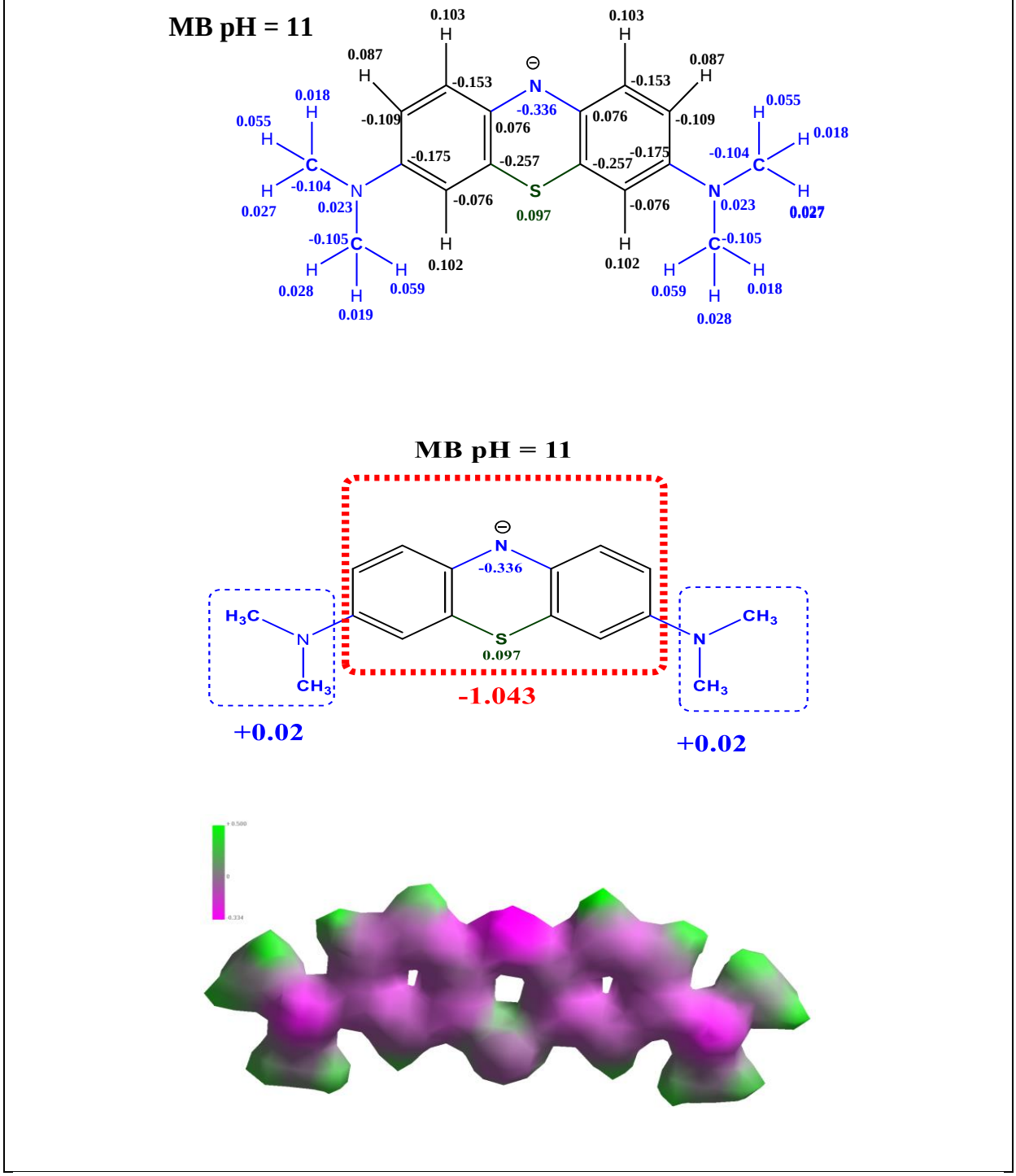

Figure III.2: Semi-empirical PM3 calculated Mulliken atomic charges and (3D) mapped isosurface surrouding the MB molecule at pH=11

III.7.4 Adsorption mechanism

Before talking about the MB adsorption mechanism onto PANI and PANI-SiO_2, the following points needs to be taken in consideration to explain the nature of adsorption process:

1- Species to be considered in a system with MB in aqueous solution as function of pH are schematized below. As can be seen in Figure III.3, MB possess three basic sites represented by the nitrogen atoms in the middle ring and in alkyl amine groups, the pKa values reported respectively are close to pKa_1=2.6, pKa_2=11.2 and pKa_3=11.2 **[17]**, this indicates that the nitrogen atom in the middle ring is the least basic. The calculated isoelectric point (IEP) of MB molecule was 8.33 (calculated as the average pKa values). From the speciation forms in figure III.3, MB dye can adopt three chemical forms, the tri-protonated form as MBH_3^{2+} in very acidic medium (pKa < 2.6) where the ends alkylamine groups ($-NH(CH_3)^+_2$) are both charged positively. For 2.6 < pKa < 8.33, methylene blue is in the mono protonated (MBH) and di-protonated MBH_2^+ forms. However, for pKa values greater than 8.33 the nitrogen atom in the central cycle of MB molecule is completely deprotonated, the MB dye become negatively charged (MB^-).

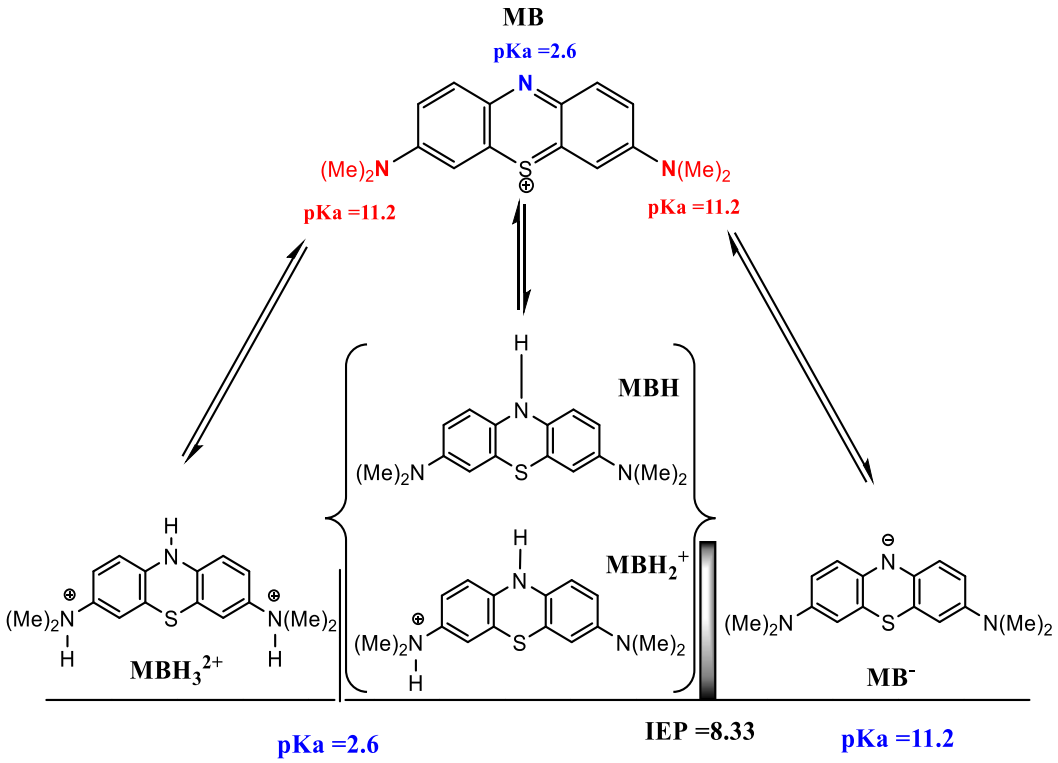

Speciation of MB forms in water

2- The proposed mechanisms of adsorption of methylene blue onto PANI and PANI-SiO_2 in the different cases (pH 2 and 11) are shown in figures from figure III.4 to figure III.7. All theoretical calculations were done according to semi-empirical PM3 calculated Mulliken atomic charges using HyperChem v8 software.

a) MB onto PANI

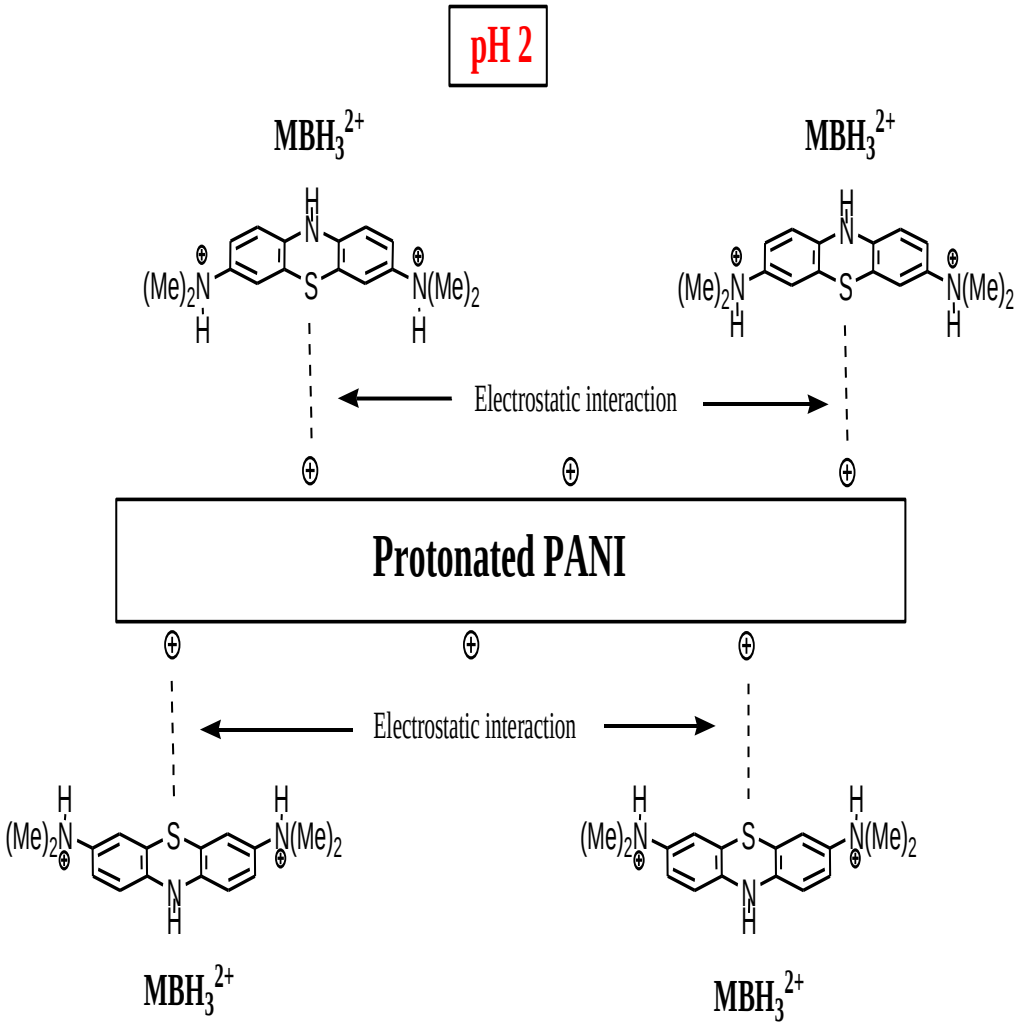

Figure III.4: The proposed mechanisms of adsorption of methylene blue onto PANI at pH 2

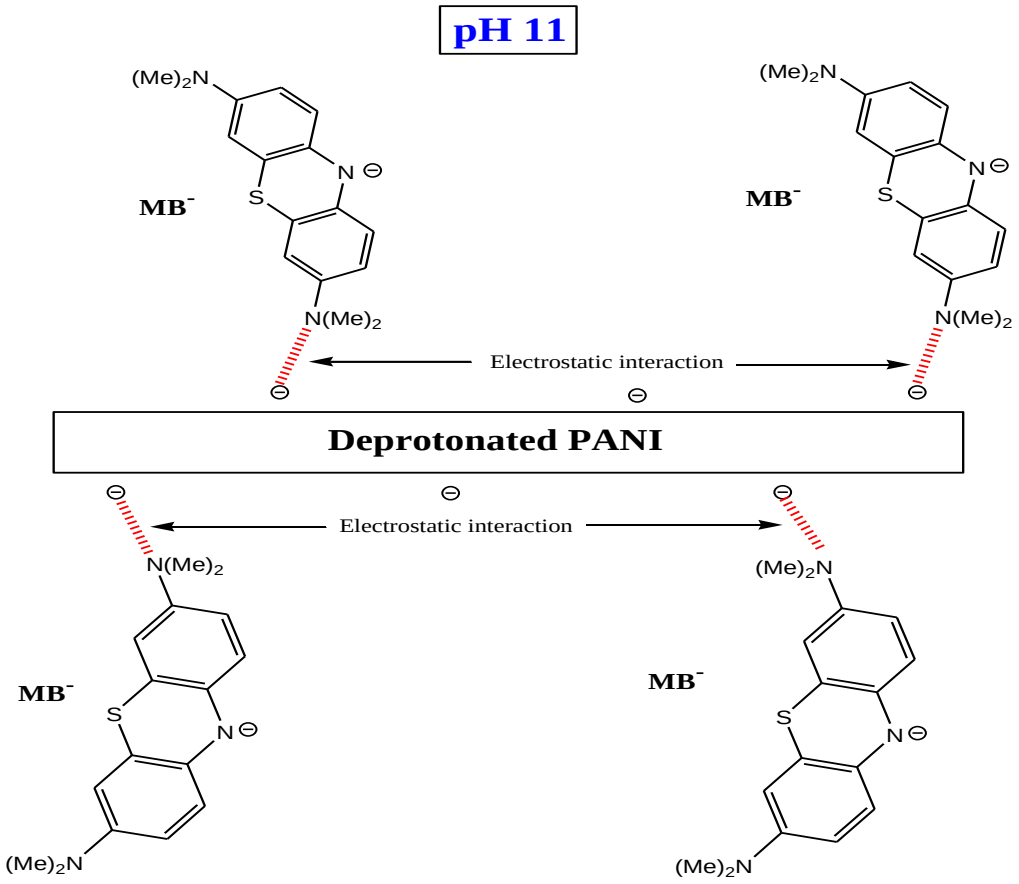

Figure III.5: The proposed mechanisms of adsorption of methylene blue onto PANI at pH 11

b) MB onto PANI-SiO_2

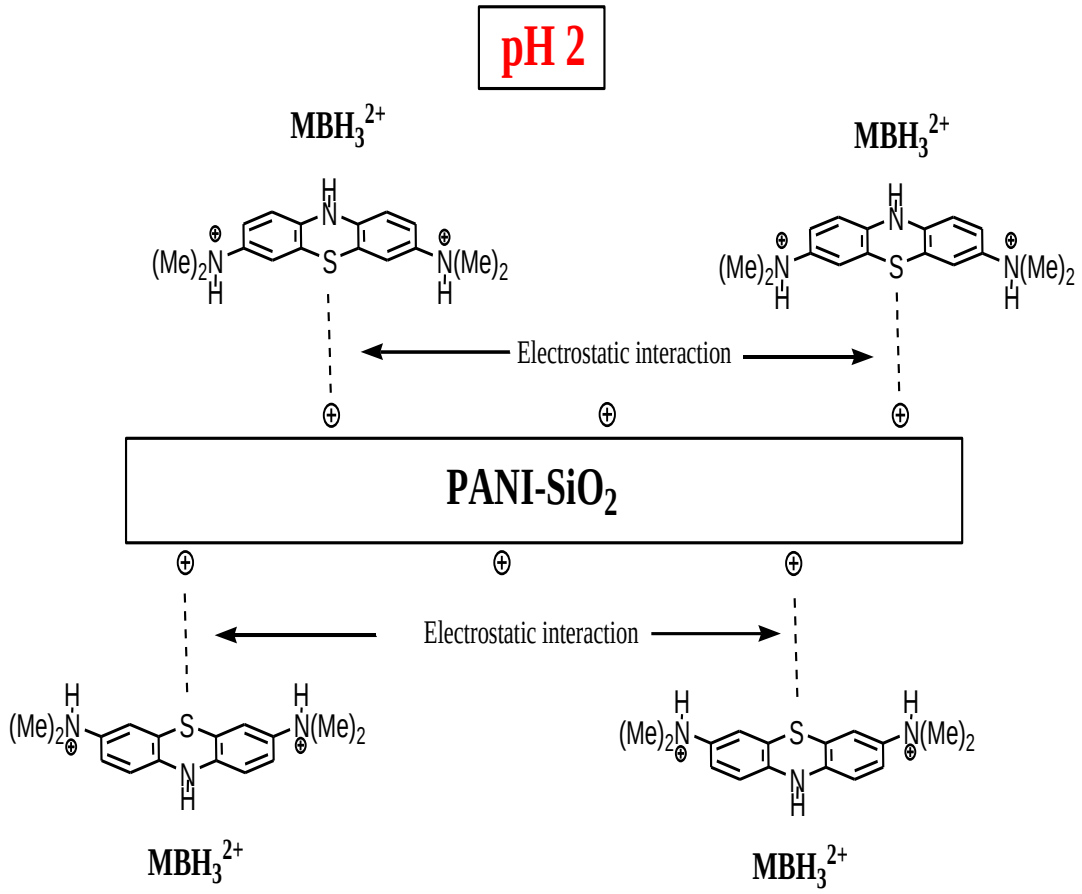

Figure III.6: Proposed mechanisms of adsorption of methylene blue onto PANI-SiO_2 at pH 2

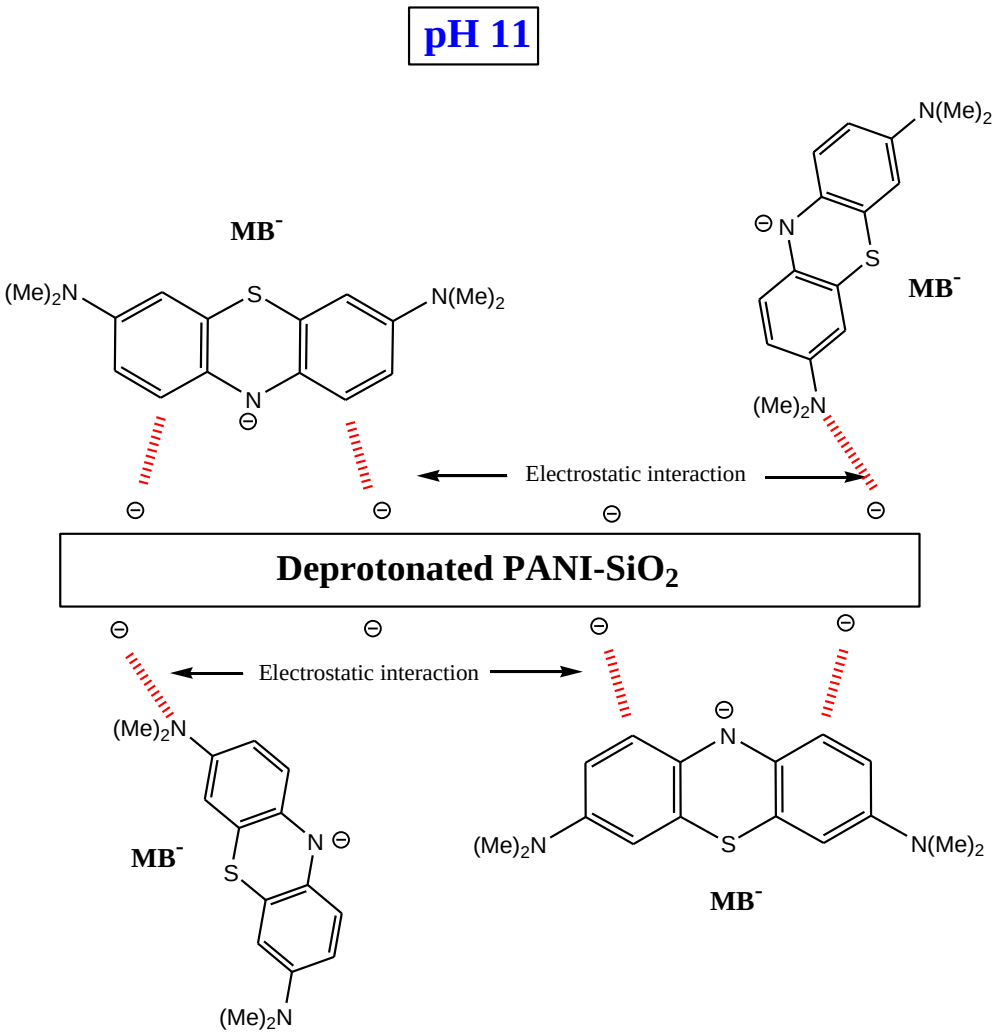

Figure III.7: Proposed mechanisms of adsorption of methylene blue onto PANI-SiO_2 at pH 11

The last proposed mechanisms are also argued by recording the FTIR spectrum of both dye loaded PANI and PANI-SiO_2.

The PANI FTIR spectrums showed in Figure (III.8(a)) where the different absorption bands represent the characteristic bands of the PANI. Peak at 798 cm^{-1} attributed to the out-of-plane bending of C-H in benzenoid ring, 1234 cm^{-1} and 1116 cm^{-1} correspond to C-H and C-N stretching vibration of the quinoid rings, 1295 cm^{-1} correspond to C-N stretching vibration of the benzenoid unit, 1460 cm^{-1} and 1598 cm-1 correspond to C=C stretching vibration of benzenoid and quinoid rings, 2933 cm^{-1}: protonated imine $–NH^{+}–$ 3443 cm^{-1} secondary amine –NH–. Else, for PANI MB loaded (after adsorption), it can be seen that the intensity of the peaks 1460 cm^{-1} and 1598 cm^{-1} corresponding to C=C stretching vibration of benzenoid and quinoid rings decrease due to the weak interactions between the PANI and the dye molecules.

However, in PANI-SiO_2 (Figure III.8(b)), the peak at 1650 cm^{-1} belong to bending motions of absorbed H_2O on SiO_2, and the peaks show slight displacement, which could be due to weak interactions such as Van Der Waals forces and the hydrogen bond between PANI and SiO_2. Also, for both adsorbents and after adsorption, appearance of the peak around 1045 cm^{-1} corresponding to C-S stretching vibration which indicates the occurrence of adsorption.

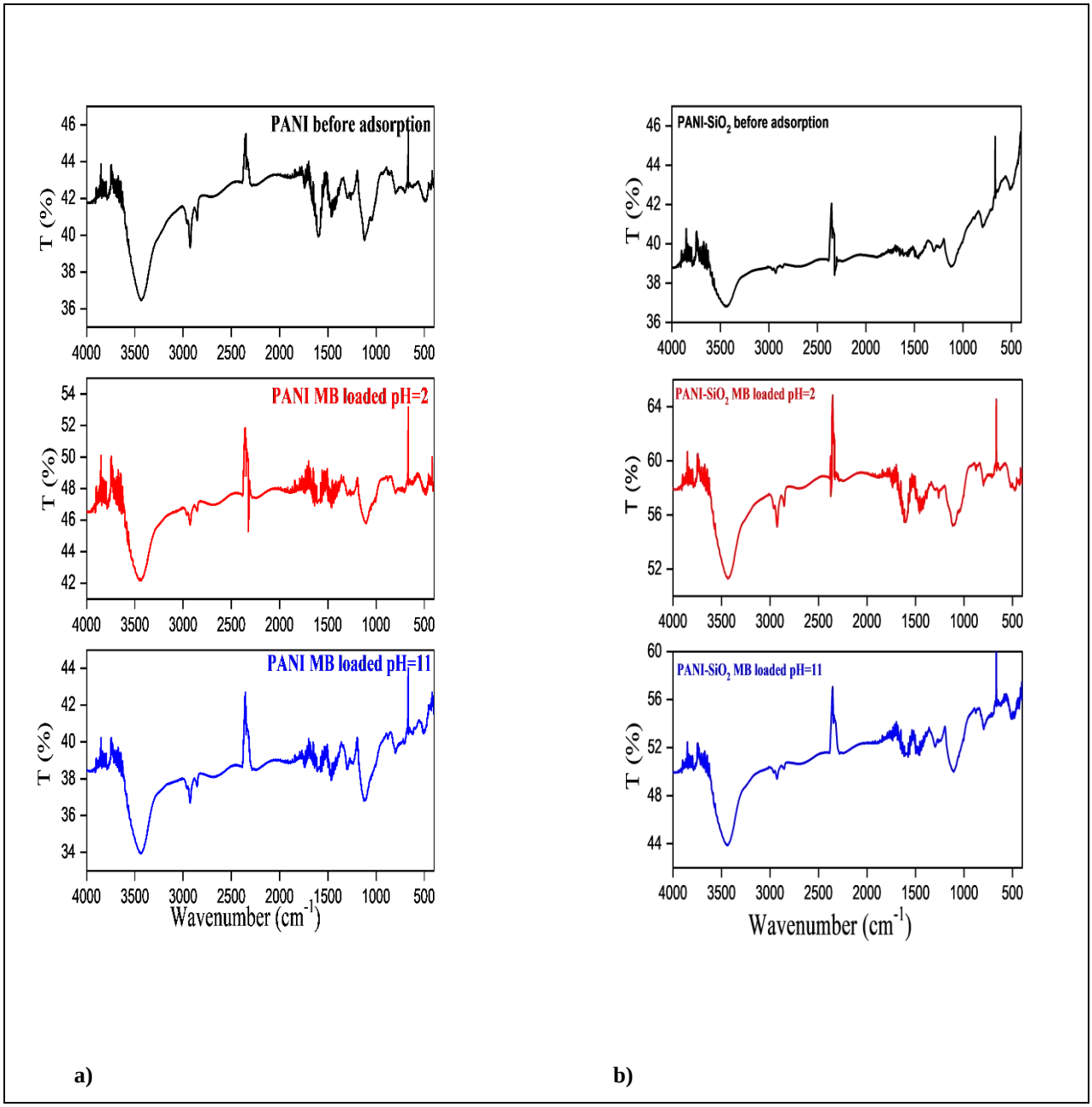

Figure III.8: FTIR spectra of (a) pure PANI (b) PANI-SiO_2 composite before and after adsorption

References:

[1] Vidal B. Chimie quantique de l'atome à la théorie de Huckel. Masson. 1993.

[2] Leforestier C. Introduction à la chimie quantique cours et exercices corrigés. DUNOD, 2005.

[3] Chaquin P. Pratique de la chimie theorique. LCT-UPMC, 2000.

[4] Rivail J. L. Eléments de chimie quantique à l'usage des chimistes. CNRS, 1999.

[5] David C. Young Cytoclonal Pharmaceutics Inc. Computational Chemistry: A Practical Guide for Applying Techniques to Real-World Problems Copyright. John Wiley & Sons, Inc. 2001.

[6] Silvi B. and Fourati N. Molecular Physics: An International Journal at the Interface Between Chemistry and Physics 1984, 52, 415-430.

[7] Stewart J. J. P., Optimization of parameters for semiempirical methods V: Modification of NDDO approximations and application to 70 elements. J Mol Model. 2007, 13: 1173–1213.

[8] Cancès E., Le Bris C. Maday Y., Méthodes math matiques en chimie quantique. Une introduction. Springer, Berlin, 2006.

[9] Koch, W.; Holthausen, M.C. A Chemist's guide to Density Functional Theory, Oxford University Press, New-York, 1989.

[10] Jensen, F. Introduction to computational chemistry. J. Wiley & Sons Ltd. 1999.

[11] Mueller M. Fundamentals of Quantum Chemistry: Molecular Spectroscopy and Modern Electronic Structure Computations, Kluwer Academic/Plenum Publishers, New York, 2001.

[12] Van Damme S., Bultinck P. and Fias S.. Electrostatic Potentials from Self-Consistent Hirshfeld Atomic Charges. *J. Chem. Theory Comput.* 2009, *5*, 334–340.

[13] David C. Young. Computational chemistry: A Practical Guide for Applying Techniques to Real-World Problems. by John Wiley & Sons, New York, 2001.

[14] Rogers D. W., Computational chemistry using the PC. John Wiley and sons, New Jersey, 2003.

[15] HyperChem (TM) Professionnal 8.0, Hypercube, Inc., 1115 NW 4th Street, Gainesville, Florida 32601, USA.

[16] Stewart JJP. Optimization of parameters for semi-empirical methods. J Comput Chem 1989; 10: 209-220.

[17] Sabnis RW. Handbook of Biological Dyes and Stains: Synthesis and Industrial Applications. New Jersey: John Wiley & Sons, 2010, p.293.

General Conclusions

In the present study, PANI and PANI/SiO_2 composite were successfully synthesized and used as adsorbents for removal of MB (cationic dye) from aqueous solutions in acidic and alkaline mediums. The adsorption of MB was studied as a function of contact time, initial MB concentration and sorbent dosing. A high amount of dye (6.97 $mg.g^{-1}$) was adsorbed on PANI/SiO_2 composite in comparison to that adsorbed with pure PANI (5.2 $mg.g^{-1}$). By comparing the effect of the medium (acidic or alkaline), the PANI homopolymer and the PANI/SiO_2 composite exhibit high adsorption efficiencies in the alkaline medium compared to those in the acidic medium. Therefore, the adsorption capacity increased with the increasing pH value. The pseudo second order is more adequate for the adsorption kinetics of MB by PANI and PANI/SiO_2 composite in acidic and basic mediums. From the intraparticle diffusion results, the MB molecules are scattered in adsorbent particles and then propagated in polymeric micropores. The Langmuir isothermal model fitted more closely to the data of MB adsorption in this study. The negative sign of ΔH values confirm the physical and exothermic process at acidic pH, and endothermic one at alkaline pH. The ΔG variation confirms that the process of adsorption between MB and both adsorbents used in this study is physical and spontaneous. Theoretical calculation of electronic charges and electrostatic potential distribution in methylene blue using HyperChem v8 software were used to propose a mechanism of adsorption between MB and the two adsorbents (PANI and PANI/SiO_2).

Abstract

Conducting Polymeric composites have attracted great attention over the last years because of their potential uses in chemical, electronic and optical devices, and as catalysts as well as in adsorption processes. Chemical synthesis of polyaniline (PANI) and polyaniline-SiO_2 composite and their adsorptive performance were reported in the present work. These materials were prepared and evaluated for their methylene blue (MB) dye adsorption characteristics from aqueous solution. Adsorption equilibrium kinetic and thermodynamic experiments of MB onto PANI and PANI/SiO_2 were studied. The effects of initial dye concentration, contact time and temperature on the adsorption capacity of PANI and PANI/SiO_2 for MB have been investigated. The pseudo-first order and pseudo-second order kinetic models were used to describe the kinetic data. It was found that adsorption kinetics followed the pseudo-second order at all of the studied temperatures. The Langmuir, Freundlich and Dubinin Raduschkevich adsorption models were used for the mathematical description and the HyperChem v8 software was exploited to propose a possible mechanism of the adsorption process.

Keywords: Polyaniline, polyaniline composite, adsorption, methylene blue dye, Langmuir isotherm.

Résumé

Les composites polymères conducteurs ont attiré une grande attention ces dernières années en raison de leurs utilisations potentielles dans les dispositifs chimiques, électroniques et optiques, ainsi que comme catalyseurs ainsi que dans les processus d'adsorption. La synthèse chimique de la polyaniline (PANI) et du composite polyaniline-SiO_2 et leurs performances d'adsorption ont été rapportées dans le présent travail. Ces matériaux ont été préparés et évalués pour leurs caractéristiques d'adsorption du colorant bleu de méthylène (MB) à partir d'une solution aqueuse. Des expériences cinétiques et thermodynamiques d'équilibre d'adsorption du MB sur PANI et PANI/SiO_2 ont été étudiées. Les effets de la concentration initiale du colorant, du temps de contact et de la température sur la capacité d'adsorption du PANI et PANI/SiO_2 pour le MB ont été étudiés. Les modèles cinétiques de pseudo-premier ordre et de pseudo-second ordre ont été utilisés pour décrire les données cinétiques. Il a été constaté que la cinétique d'adsorption suivait le pseudo-second ordre à toutes les températures étudiées. Les modèles d'adsorption de Langmuir, Freundlich et Dubinin Raduschkevich ont été utilisés pour la description mathématique et le logiciel HyperChem v8 a été exploité pour proposer un mécanisme possible du processus d'adsorption.

Mots clés : Polyaniline, composite polyaniline, adsorption, colorant bleu de méthylène, isotherme de Langmuir.

ملخص

لقد اجتذبت المركبات البوليمرية الناقلة للكهرباء اهتمامًا كبيرًا خلال السنوات الماضية بسبب استخداماتها المحتملة في الأجهزة الكيميائية والإلكترونية والبصرية، وكمحفزات وكذلك في عمليات الامتزاز. تم في هذا العمل الإبلاغ عن التركيب الكيميائي للبوليانيلين (PANI)ومركب البوليانيلين-SiO_2وأدائهما الامتزازي. تم تحضير هذه المواد وتقييمها لخصائص امتزاز صبغة أزرق الميثيلين (MB) من المحلول المائي. تمت دراسة تجارب التوازن الحركي والديناميكي الحراري لـ MB على PANI و$PANI/SiO_2$. تم دراسة تأثيرات تركيز الصبغة الأولي ووقت التلامس ودرجة الحرارة على قدرة الامتزاز لـ PANI و $PANI/SiO_2$ لـ MB. تم استخدام النماذج الحركية من الدرجة الأولى والنماذج الحركية من الدرجة الثانية لوصف البيانات الحركية. وقد وجد أن حركية الامتزاز تتبع الرتبة الثانية في جميع درجات الحرارة المدروسة. تم استخدام نماذج الامتزاز Langmuir وFreundlich و Dubinin Raduschkevich للوصف الرياضي وتم استغلال برنامج HyperChem v8 لاقتراح آلية محتملة لعملية الامتزاز.

الكلمات المفتاحية: البولي أنيلين، مركب البولي أنيلين، الامتزاز، صبغة الميثيلين الزرقاء، نموذج الامتزاز لانجمير.